A study of adipogenic development in the skin dermis

SARAH LOUISE MORRIS

A study of adipogenic development in the skin dermis

Sarah L. Morris

Supervisor: Prof. Colin Jahoda

Thesis submitted for the degree of Master of Science
School of Biological and Biomedical Sciences
Durham University

2013

Abstract

With the rise of obesity, the process of fat development, adipogenesis, is increasingly important to understand. In particular, several studies have indicated differences in the developmental origins and properties of different adipose depots. This thesis is concerned with adipogenesis in the recently identified adipose tissue depot in the lower dermis of the skin, divided from the underlying subcutaneous fat by the *panniculus carnosus* muscle layer in rodents. The study was aimed at developing new experimental tools, and providing new insights into the timing of adipose tissue development in this depot in mice. Experiments also explored the process of mitotic clonal expansion, and miRNAs in adipogenesis.

Essential to the study of adipogenesis in developing skin is the establishment of model systems that reflect events *in vivo* and that are capable of being manipulated experimentally. Two models: a substrate organ culture system and a 3D cell aggregate spherical model were developed and refined. These were then used for investigation into the timing of adipogenesis in the lower dermis. Staining of C/EBPα transcription factor and lipids in spherical cell culture revealed that cells between the ages of E14.5 and E18.5 were committed to undergo adipogenesis. This early timing of events was further suggested by collagen IV staining of mouse back skin showing distinct differences in expression between the upper and lower dermis at E14.5.

The first stage of adipogenesis *in vitro*, mitotic clonal expansion, was also explored. Experiments showed important differences between the uniform sequence of events of adipogenesis *in vitro* and the range of scenarios in 3D systems suggesting clonal expansion might not be necessary. Finally, a preliminary study on the role of miRNAs in skin adipogenesis was conducted using qPCR. This yielded some interesting initial trends which can be further investigated in future studies.

Table of Contents

List of figures and tables

Chapter 5

List of Appendices

List of abbreviations

ADD1	adipocyte determination and differentiation-dependent factor
BAT	brown adipose tissue
BMP	bone morphogenic protein
BrdU	5-bromo-2'-deoxyuridine
cAMP	cyclic adenosine mono phosphate
cDNA	complementary deoxyribonucleic acid
C/EBP	CCAAT/enhancer binding protein
CHOP	C/EBP homologous protein
Chr	chromosome
CUP	C/EBP undifferentiated protein
DAPI	4',6'-diamidino-2-phenylindole
DAT	dermal adipose tissue
DEPC	diethylpyrocarbonate
DEX	dexamethasone
dH_2O	deionised water
DNA	deoxyribonucleic acid
DS	donkey serum
E	embryonic day
E2F	E2 transcription factor
EdU	5-ethynyl-2’-deoxyuridine
EGF	epidermal growth factor
EGFR	epidermal growth factor receptor
ERK	extracellular signal related kinase
EPAC	exchange proteins directly-activated by cAMP
FA	fatty acid
FABP4	fatty acid binding protein
FBS	fetal bovine serum
FGF	fibroblast growth factor
Fu	fungizone
GLUT	glucose transporter
Gpc	glypican

GS	goat serum
GSK	glycogen synthase kinase
H&E	Hematoxylin and Eosin
HCl	hydrochloric acid
HDAC	histone deacetylase
HFD	high fat diet
HMGA2	high motility group AT-hook 2
I	IGF-1 (see below)
IGF	insulin-like growth factor
KGF	keratinocyte growth factor
KLF	kruppel-like factor
MAPK	mitogen activated protein kinase
MCE	mitotic clonal expansion
MEM	Minimum Essential Medium
miRNA	micro ribonucleic acid
mRNA	messenger ribonucleic acid
MIX	methylisobutylxanthine
MSC	mesenchymal stem cell
OC	organ culture
O/N	overnight
ORO	Oil Red O
PBS	phosphate buffered saline
PEPCK	phosphoenolpyruvate carboxykinase
PFA	paraformaldehyde
PGC	PPAR co-activator protein
PKA	protein kinase A
PPAR	peroxidase proliferated activated receptor
Pref	preadipocyte factor
P/S	penicillin/streptomycin
PTN	pleiotrophin
qPCR	quantitative polymerase chain reaction
RBP	retinol binding protein
RNA	ribonucleic acid
RT	room temperature

RXR	retinoid X receptor
SAT	subcutaneous adipose tissue
snRNA	small nuclear ribonucleic acid
snoRNA	small nucleolar ribonucleic acid
SREBP	sterol regulatory element binding protein
S-V	stromal vascular
SVF	stromal vascular fraction
Tbx	T-box
TG/TAG	triglyceride
TGF	transforming growth factor
TNF	tumour necrosis factor
UCP-1	uncoupling protein
UTR	3’-untranslated region
VAT	visceral adipose tissue
WAT	white adipose tissue
2D	two dimensional
3D	three dimensional

This thesis has not been submitted or accepted for any other degree. Work on the establishment of model systems in chapter 3 (Sections 3.2.1 - 3.2.3) was carried out in conjunction with Miss Olivia Davies. All other sections of this thesis are the result entirely of my own work.

Acknowledgements

I would firstly like to thank Professor Colin Jahoda for giving me the opportunity to complete this project. Everything I have learnt during the past year has given me the inspiration and tools I will need for my future scientific career. I would also like to thank all of the members of Prof. Jahoda's research group for their invaluable assistance during the year particularly in making available their scientific expertise. In particular, I would like to thank Olivia Davies for all the discussion of results which kept my project moving forwards. I would also like to acknowledge the staff of the LSSU facility at Durham University for providing animals for my work with endless patience.

Chapter 1

Introduction

Obesity, and related diseases such as type II diabetes and cardiovascular disease, are a growing problem for medical services around the world. The study of fat development both during development and throughout life is therefore increasingly important. Adipose tissue is spread around the body in a number of different fat ‘depots’ and is thought to have different developmental origins depending on its position in the body (Billon et al., 2008). This observation has led to mounting interest in determining whether different fat depots have functional differences (Lafontan and Berlan, 2003; Gesta et al., 2006; Billon et al., 2008). The work presented in this thesis focuses on the white adipose tissue depot in the lower dermis of the skin.

1.1 Skin

Skin is the largest organ in the body and arguably one of the most important as it forms the primary barrier against the harsh external environment. The barrier function provides protection in both directions: against pathogens trying to enter the body but also against loss of water and nutrients from the body (Proksch et al., 2008). As well as its barrier function, the skin is also important for sensation, thermoregulation, and storage of lipids and water (Chuong et al., 2002). Adult mammalian skin is comprised of two major layers: the epidermis and dermis separated by a basement membrane, and also contains a number of skin appendages, such as hair follicles, and sebaceous glands. Below the dermis is the hypodermis or subcutis (McGrath et al., 2008). Each layer is described in more detail below. The structure of the skin varies between body locations and species. At the most fundamental level it can either be hairy, the most widespread, or glabrous (non-hairy) skin but there are also variations in thickness, the length of hair follicles, and density of component cells (Kanitakis, 2002). Importantly, in humans, in most areas the dermis is continuous with underlying hypodermis or subcutis whereas in small rodents these layers are separated by the panniculus carnosus muscle layer (Kanitakis, 2002; Godjonsson, 2007).

1.1.1 Epidermis

The uppermost layer of the skin, the epidermis, can, in turn, be subdivided into four levels (Figure 1.1). The primary cell type throughout all of the layers is the keratinocyte, but the epidermis also contains melanocytes, Langerhans cells, Merkel cells, and inflammatory cells.

The progenitor population of keratinocytes is found in the *stratum basale*, next to the basement membrane. The cells become more differentiated and specialised as they migrate upwards towards the skin surface before they become differentiated corneocytes in the *stratum corneum* and are eventually shed. Figure 1 shows the structure of the epidermis and illustrates the changing shape of keratinocytes as they move upwards (Wickett and Visscher, 2006).

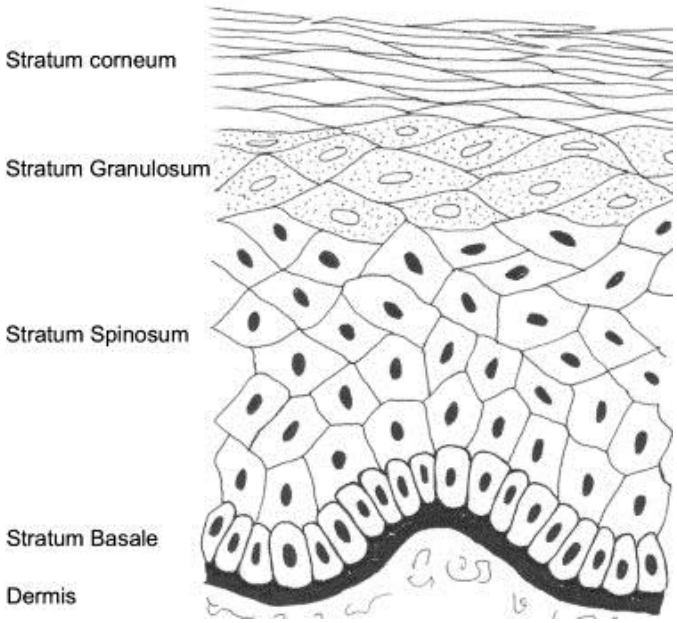

Figure 1.1: Schematic representation of the layers of the epidermis (reproduced from Wickett and Visscher, 2006)

Epidermal progenitor cells residing on top of the basement membrane divide to replenish the cells being shed from the epidermis (Levy et al., 2005).The basal cells enlarge as they move up into the *stratum spinosum* before beginning to flatten. Inside spinous cells, a dense network of keratin filaments is being formed and arranged into thin bundles. Envelope proteins,

such as involucrin, are also being produced and deposited on the inner surface of the plasma membrane (Fuchs, 1990).

In the upper spinous layer, and moving into the granular layer, organelles begin to be broken down. Vesicles, originating from the Golgi apparatus, enriched in lipids, enzymes, and structural proteins, become defined as the epidermal lamellar bodies, the contents of which are then secreted into intercellular spaces (Proksch et al., 2008). By the time keratinocytes reach the *stratum corneum*, they have lost their nucleus and cell organelles and gained an insoluble cornified envelope within the plasma membrane. These corneocytes offer protection and are the basis of the barrier function of the skin (McGrath et al., 2008).

Two other cell types in the epidermis are melanocytes and Langerhans cells. Melanocytes are found in the basal layer of the epidermis alongside proliferating keratinocytes. They produce pigment granules, melanosomes, containing melanin, which are transferred into keratinocytes, offering protection from ultraviolet light. Langerhans cells are antigen-presenting cells; part of the immune system in the skin (Wickett and Visscher, 2006; McGrath, 2008).

1.1.2 Dermis and subcutis

The dermis can also be subdivided into two further layers known as the papillary (upper) and reticular (lower) dermis. The primary cell type of both layers is the fibroblast, and these cells secrete the molecules which make up the extracellular matrix. Differences in the composition and organisation of the extracellular matrix help to distinguish between the papillary and reticular dermis (Sorrell and Caplan, 2004; McGrath et al, 2008). Both layers contain collagen bundles made up of collagen I and III, but those in the papillary dermis are less well-organised than in the reticular dermis. The lower reticular dermis has less collagen III than the upper papillary dermis. Elastins and proteoglycans are also differentially expressed between the two layers (McGrath et al., 2008).

The hypodermis or subcutis is situated beneath the dermis and is primarily formed of lobules of adipocytes (Kanitakis, 2002). The adipocytes are separated by connective tissue and cells including fibroblasts and mast cells. In small rodents there is a thin striated muscle layer known as the panniculus carnosus located beneath dermis separating the hypodermis and preventing movement of cells between the layers (McGrath et al, 2008; Wojciechowicz et al., 2013). In humans, this layer mainly does not exist meaning the dermis and hypodermis are continuous with each other, with some hair follicles even extending beyond the dermis into the underlying subcutis (Calonje et al., 2011). Although subcutaneous adipose tissue is one of the major depots for fat, there are also white adipocytes in the lower (reticular) dermis which begin to accumulate fat from embryonic day 18 onwards (Wojciechowicz et al., 2013).

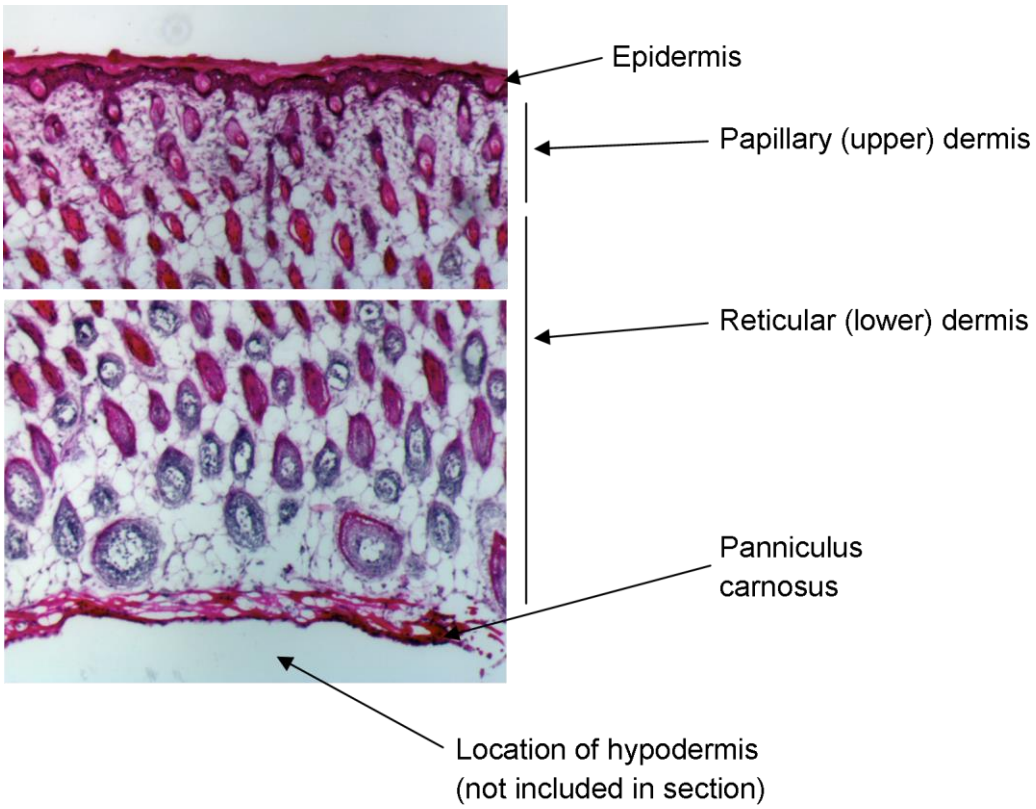

Figure 1.2: Hematoxylin & Eosin staining showing structure of 7 day new-born mouse back skin. Large white lipid-filled adipocytes are visible throughout the reticular (lower) dermis interspersed between hair follicles.

1.1.3 Hair follicles

Hair follicles and the hairs that they produce are an important part of the skin's protective function as they act in a thermoregulatory role and as barriers. Follicles are complex structures formed from developing skin through local interactions between the epidermis and dermis. In mice, the first wave of hair follicle development starts at embryonic day 14.5 (E14.5). An initial signal from the dermis results in the epidermis thickening at regular intervals forming 'placodes'. Underlying dermal cells then cluster into a 'dermal condensation'. The cells in the placode proliferate and grow down into dermis surrounding the cells of the dermal condensate which ultimately become the dermal papilla in the bulb of the hair follicle. Further proliferation and migration of the epidermal cells facilitate the formation of the inner root sheath and hair shaft. In mice, the epidermal placodes begin to grow down between E14.5 and E15, and continue to elongate until approximately E18.5 (Miller, 2002).

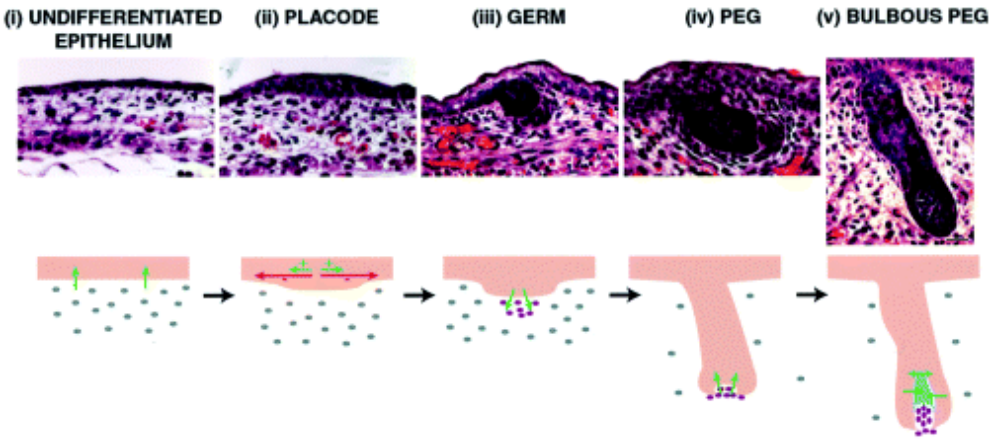

Figure 1.3: Diagram of stages of hair follicle morphogenesis (adapted from Miller, 2002)

Once the hair follicle structure has developed, they undergo turnover of hairs facilitated by the hair follicle cycle. The hair follicle cycle stages are anagen (growth), catagen (regression), and telogen (rest). A new hair is grown in each cycle during the anagen stage and usually remains anchored in the hair follicle until the telogen-anagen transition at the end of the cycle when it is lost by a process known as exogen (Alonso and Fuchs, 2006).

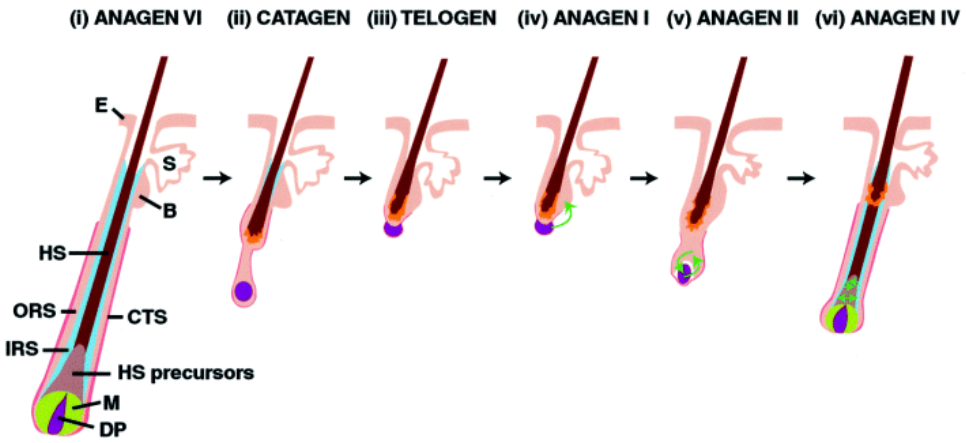

Figure 1.4: Schematic of the structures and stages of the hair follicle cycle. E, epidermis; S, sebaceous gland; B, bulge; HS, hair shaft; ORS, outer root sheath; IRS, inner root sheath; CTS, connective tissue sheath; M, matrix; DP, dermal papilla (reproduced from Miller, 2002)

1.2 The adipose organ

The adipose organ is composed of a number of adipose tissues which are located in various “depots” throughout the body particularly in the subcutaneous and visceral regions (Figure 1.5). In rodents and other small mammals, fat is mainly contained within two subcutaneous depots (posterior and anterior) and a number of visceral depots in the thorax (mediastinic) and abdomen (epididymal, mesenteric, omental, parametrial, perirenal, perivaric, pervesical, retroperitoneal) around the internal organs (Cinti, 2007).

Adipocytes only account for approximately 50% of the cells in adipose depots as there are also vascular elements, preadipocytes, fibroblasts, mast cells, macrophages, nervous elements, and mesenchymal cells. Mammals have two types of adipocyte: white and brown, which are spread throughout these depots although in differing amounts determined by genetic and environmental factors (Rosen and MacDougald, 2006; Cinti, 2007). The terminology "white" or "brown" adipose tissue is based on a physical difference in colour reflecting either a predominance of white or brown adipocytes (Cinti 2001; 2007). White adipocytes are also found in other locations such as the skin, thymus, lymph nodes, bone marrow, parotid, parathyroid, pancreas, and other tissues (Cinti, 2007; Wojciechowicz et al., 2013).

A unique feature of adipose tissues compared to other organs is its ability to change size to quickly adapt the nutritional availability. It does this through hypertrophy (cell size increase), hyperplasia (cell number increase), release of lipids, and cell death (Sun et al,. 2011). Although there is evidence to suggest that the total number of fat cells remains constant after adolescence, there is a small turnover of approximately 10% throughout life (Spalding et al., 2008). Adipose tissue stem cells are mesenchymal-like stem cells which can be isolated from the stromal-vascular fraction (SVF) (Zuk et al., 2001). There is also evidence that there is a population of committed progenitor adipocytes, still dividing, which are able to dedifferentiate (Kajita et al., 2013).

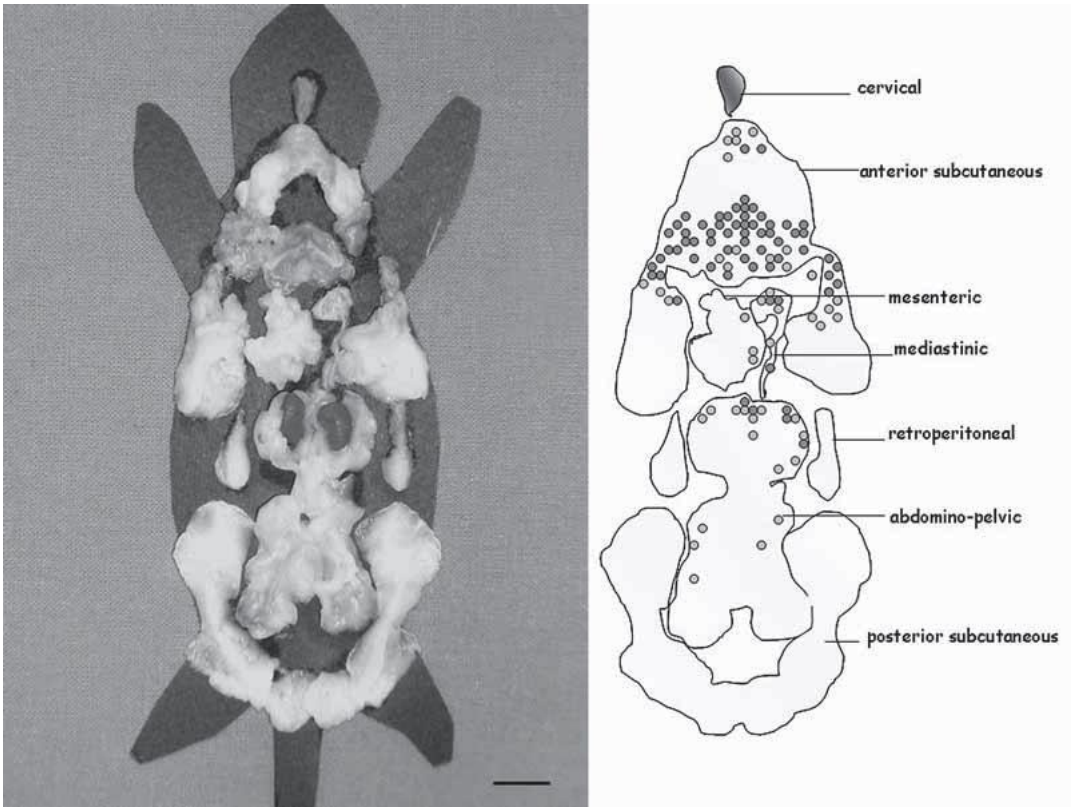

Figure 1.5: Diagram of the location and relative size of fat depots in mice (reproduced from Cinti, 2007)

1.2.1 Developmental origin of adipose tissue

There is growing evidence that adipocytes in different depots show differing properties and developmental gene expression depending on their

location and origin. Most adipocytes are mesodermal in origin differentiating from mesenchymal progenitor cells which become committed to the adipogenic lineage. A subset of adipocytes around the salivary glands and ear, however, are thought to be derived from neuroectoderm developing from neural crest cells (Billon et al., 2007).

The mass of adipose tissue stored in each location, and in particular the size of individual adipocytes, can have an impact on obesity-related diseases as more visceral fat leads to a higher risk of insulin-resistance and cardiovascular disease (Gesta et al., 2006; Arner et al., 2010). Large adipocytes especially in abdominal subcutaneous fat, rather than many small adipocytes, lead to an increased risk of type II diabetes (Weyer et al., 2000). The depot specific differences displayed by adipocytes provide an important argument for studying adipogenesis *in vivo* as opposed to using *in vitro* cell-line models where preadipocytes generally show the same properties and gene expression.

1.2.2 White adipose tissue (WAT)

1.2.2.1 White adipocytes

WAT is primarily made up of white adipocytes although it does also contain some brown adipocytes. As stated above white adipocytes are found in both of the subcutaneous depots, the visceral depots, and in small numbers in other tissues. The morphology of white adipocytes depends on their location however they range in size from 30-40 μm to 150-160 μm and have a spheroid shape. Within white adipocytes, most of the cellular space is occupied by a single lipid filled vacuole forcing organelles to inhabit the small border of cytoplasm around the edge. They are also surrounded by an external lamina and have pinocytotic vesicles, a feature common between white and brown adipocytes (Cinti, 2001; Cinti, 2007). They only have a small number of mitochondria compared to brown adipocytes and these are much smaller and contain fewer cristae (Cinti, 2007; Rogers et al., 2012).

During their development, white adipocytes contain several fat droplets (although one is often predominant) which join together to form the

characteristic unilocular cell (Cinti, 2007). The preadipocytes, which, in rodents, are morphologically identical to connective tissue fibroblasts, are closely associated with the walls of capillaries. In humans, fibronectin is expressed in the external lamina of white preadipocytes. This expression disappears by the time adipocytes are fully differentiated and the lamina instead becomes immunoreactive for laminin, collagen IV, and heparan sulphate (Hausman and Campion, 1982; Cinti, 2007).

1.2.2.2 Functions of WAT

A major function of WAT is to store and release energy in the form of lipids. The stored fatty acids (as triglycerides) allow the body to have a constant supply of energy between meals and during longer fasting periods. Energy storage was once thought to be the only function of white adipocytes however there is now a large body of evidence to show that it also has important roles in regulating physiological and pathological processes such as immunity and inflammation. It is also part of the endocrine system producing hormones, known as adipokines, such as leptin (Trayhurn and Beattie, 2001; Cinti, 2007).

1.2.2.3.1 Lipid and glucose metabolism

Lipid metabolism includes the processes of fatty acid (FA) synthesis, lipogenesis, and lipolysis. Most of the triglycerides (TG/TAG) stored in white adipocytes come from the diet, however there is also some synthesis of fatty acids, a process known as lipogenesis (Large et al., 2004). After food consumption, long chain fatty acids are transported into adipocytes and combined with glycerol 3-phosphate in a metabolic pathway resulting in TAG. Proteins such as fatty acid transport protein (FATP) and fatty acid binding protein (FABP) are positioned in the plasma membrane in order to transport FAs into adipocytes. FAs are also synthesised in the liver and adipocytes from non-lipid substrates, mainly glucose (Large et al., 2004; Lafontan and Langin, 2009).

The opposite mechanism by which energy is released during a period of fasting is lipolysis. This is a step-wise process which releases three

molecules of free fatty acid and one of glycerol. The initiation of lipolysis is predominantly the result of hormone stimulation, such as insulin or catecholamines. It is tightly controlled through autocrine and paracrine signalling to ensure a steady supply of free fatty acids to tissues which utilise them (Large et al., 2004; Lafontan and Langin, 2009).

Glucose is taken up into adipocytes in response to insulin signalling through a tightly regulated mechanism. Glucose transporters (GLUTs) are present in the plasma membrane to facilitate this process; the principal member of the family being GLUT4. Defective expression of GLUT4 has been linked to both obesity and type II diabetes (Dalen et al., 2003). Glucose is rapidly taken up into cells from the blood following dietary intake to prevent hyperglycaemia and toxicity to peripheral organs (Huang and Czech, 2007). When the energy from glycolysis is not required, excess glucose can be stored as glycogen in the liver and muscles, or in triacylglycerides in adipose tissue. During times of starvation, glucose can be released from these same tissues (Large et al., 2004).

1.2.2.3.2 Endocrine function

WAT expresses a large number of secretory factors which fall under three categories: growth factors, hormones, and adipokines. The first of these groups: the growth factors, include proteins such as insulin-like growth factor 1 (IGF-1) which are involved in proliferation and differentiation of the adipose depots where they are expressed (Poulos et al., 2009). Adipokines, cytokines expressed by adipocytes, include factors such as interleukin 6, retinol binding protein 4, tumour necrosis factor α (TNFα), and transforming growth factors (TGF). These act as signalling molecules and help, amongst other roles, to regulate energy homeostasis, insulin sensitivity and the inflammatory response (Poulos et al., 2009; Kwon and Pessin, 2013).

The hormones expressed by adipocytes are the factors, along with some adipokines, which identify adipose tissue as being part of the endocrine system. The first hormone discovered was leptin (Zhang et al., 1994) and it was this discovery which changed the traditional view of WAT as simply a

location for energy storage. Leptin, resistin, and adiponectin are the three hormones which have been identified as being expressed by adipocytes. Between them, they have diverse roles in regulating growth, metabolism, behaviour, and the inflammatory response (Poulos et al., 2009).

Leptin acts in a paracrine manner to fulfil a number of functions; primarily acting at the hypothalamus to regulate appetite and food consumption, but it also improves insulin sensitivity in a number of organs and possibly enhances angiogenesis (Ronti et al., 2006). Leptin receptor expression is widespread allowing the hormone to directly and indirectly influence physiological processes (Fruhbeck, 2000). Expression of leptin and insulin sensitivity of the adipocytes is affected by insulin deprivation in porcine stromal-vascular (S-V) cells, whereby low insulin levels result in more insulin-sensitive adipocytes (Chen et al., 1999). The functions of the other hormones are less well researched however resistin has been shown to have a role inflammation through proinflammatory cytokines (Pang and Le, 2006). Adiponectin is also linked to insulin sensitivity (Poulos et al., 2009).

1.2.3 Brown adipose tissue (BAT)

Brown adipocytes, the principal constituent of BAT, differ from white adipocytes in their structure, function, and location (Cinti, 2001; Cinti 2007). Brown adipose tissue is principally found in the regions of subcutaneous fat particularly the anterior subcutaneous depot in lean mice. All of these regions are highly vascularised and innervated as brown adipocytes are closely associated with both capillaries and noradrenergic nerves (Cinti, 2007).

Brown adipocytes also differ in their shape and size from white adipocytes. They have an ellipsoid shape and are smaller with a minimum size of 15-20 μm and a maximum diameter of only 40-50 μm. They do not contain one large lipid droplet but instead are multilocular cells with many smaller lipid filled vacuoles. They also contain a very high number of large mitochondria which are crossed with many cristae. These mitochondria express uncoupling protein-1 (UCP-1), a protein unique to brown adipocytes.

This protein is responsible for the brown adipocytes function of non-shivering thermogenesis in extreme cold conditions (Cinti, 2007).

1.2.3.1 Lipolysis and heat dissipation in BAT

Brown adipocytes use stored fatty acids to produce heat UCP-1. It has been found that the thermogenic properties of BAT are completely dependent on this protein and homologs of the gene (UCP-2 & -3) are unable to fulfil the same role (Matthias et al., 2000). The process of non-shivering thermogenesis in brown adipose tissue starts with lipolysis of stored triglycerides into long-chain fatty acids (Nicholls and Locke, 1984). UCP-1 resides in the mitochondrial membrane acting as an H+ pump, causing dissipation of the proton electrochemical gradient and thus generating heat. The mechanism by which it does this is not completely understood although there is a definite requirement for long-chain fatty acids for the process to occur (Nicholls and Locke, 1984; Breen et al., 2006).

1.2.4 Dermal, hair follicle-associated, and subcutaneous fat

Subcutaneous adipose tissue (SAT) is one of the major depots for white adipose tissue in rodents, pigs and humans. In rodents subcutaneous fat is stored in anterior and posterior depots (Cinti, 2007). These are separated from the WAT in the lower dermis of the skin by a muscle layer called the panniculus carnosus. This is not the case in larger animals or in humans where the depots are continuous. Porcine SAT can be subdivided into inner, middle, and outer layers through different stromal composition. The outer SAT is located in the hypodermis and in "lobules" around the base of hair follicles (Hausman and Martin, 1982). Hausman and Kauffman, 1986a, found that differentiation of porcine SAT proceeded from the inner to the outer layer with adipocytes appearing in the inner layer from 60 days fetal development but not until 75 embryonic days in the outer layer. Cells developed in clusters where the number and size of clusters increased with age. Hair follicle associated adipocytes appeared to follow a different developmental pattern to other outer adipocytes as the cell clusters were larger at an earlier age compared to the rest of the outer layer (Hausman and

Kauffman, 1986a). Preadipocytes were similarly arranged in clusters in rat adipocyte development (Hausman and Campion, 1984).

In humans, subcutaneous fat is continuous throughout the body and, similarly to porcine SAT, is split into several layers (Hausman and Hausman, 2007). It varies in thickness however is thickest in the abdomen in both women and men, a common feature of primates (Pond, 2007). There are also adipocytes in the lower dermis however these are not separated from underlying subcutaneous fat by a muscle layer as they are in rodents (Schmidt and Horsley, 2012). Previously, the adipocytes in the lower dermis of rodents had also been classified as part of the subcutaneous depot (Klein et al., 2007). Recent evidence, however, shows that in mice these depots are completely distinct from each other and do not mix at any point during development. It has also been shown that the dermal layer of WAT does not need the underlying subcutaneous depot to develop (Wojciechowicz et al., 2013).

Schmidt and Horsley also explored hair follicle associated adipocytes in mice (termed intradermal fat) and similarly concluded that it is distinct from the underlying SAT. They determined that it only started developing postnatally which contradicts Wojciechowicz et al. who first observed fat droplets at E18.5 days. Regardless of the exact timing, the distinction of this layer from subcutaneous adipose tissue is important. It is particularly important in relation to the growing evidence that the distribution of fat in the various depots has important consequences for development of health problems related to obesity (Gesta et al., 2006). It is unknown whether human dermal and subcutaneous fat are as developmentally distinct as in rodents, however it is clear that two separate layers do exist.

1.2.5 Obesity and related disorders

Changes in diet and exercise have made obesity a problem around the world. It results from an imbalance between food intake and requirement for calories and is also linked to the ratio between white and brown adipose tissue. In early-onset obesity, the increase of adipose tissue has been shown

to be due to both hypertrophy and hyperplasia of adipocytes. In most cases of adult obesity however it is more due to the increase in size of existing adipocytes; although there is some evidence that there is a maximum size for an adipocyte. The biggest problem with obesity is the associated health problems which it introduces including type II diabetes, dyslipedemias, and cardiovascular disease. It even increases the risk of Alzheimer's disease and some cancers. These metabolic disorders are brought about due to increased insulin resistance and adipose tissues' role as part of the endocrine system (Gesta et al., 2007).

Differences between adipose depots become important in obesity as there is evidence that an increase in intra-abdominal or visceral fat puts patients at a higher risk of metabolic disease than subcutaneous fat around the thighs and hips. The distribution of fat between these depots does shift towards the abdomen with age even in lean subjects (Gesta et al., 2006). In addition, it has been shown that the size of individual adipocytes within depots is important rather than just the overall mass (Arner et al., 2010). In the abdominal subcutaneous depot, it has been found that large adipocytes increase the risk of type II diabetes, even without a subject necessarily being obese (Weyer et al., 2000). There is not a simple relationship between adipocyte size, obesity, and metabolic disease as there are large variations between individuals. It has also been shown that developmental genes can also have a function in fat differentiation as a number of the genes are differentially expressed between depots. Glypican and T-box 15, in particular, indicate a higher risk of metabolic disease when more highly expressed in subcutaneous fat (Gesta et al., 2006).

There is some debate about the extent of hyperplasia in increasing adipose tissue volume; in adult humans it was found that weight gain or loss did not significantly affect the number of adipocytes (Spalding et al., 2008). In mice, however, there is evidence that a high fat diet (HFD) causes hyperplasia; although there is a difference in the potential for *de novo* adipogenesis between depots with much less in subcutaneous fat than gonadal depots (Wang et al., 2013).

Although the increase of adiposity in obesity increases the overall risk of associated diseases, there is some suggestion that subcutaneous fat depots may even be protective compared to high levels of visceral adipose tissue (VAT). Several experiments have shown that increased subcutaneous fat without an increase in visceral fat leads to improvement in insulin sensitivity and a lower risk of impaired glucose metabolism (Miyazaki et al., 2002; Snijder et al., 2005). There is even evidence that transplantation of subcutaneous fat into visceral depots can reduce the overall adipose tissue mass (Tran et al., 2008). This is a confused and controversial area of research, however, as another study found that the protective effects of subcutaneous adipose tissue were only seen in subjects with high levels of VAT (Porter et al., 2009).

A potential therapeutic method for treating obesity by increasing the amount BAT has been suggested. It is thought that the ratio of brown:white adipose tissue is important for maintaining homeostasis of adipose tissue endocrine functions. BAT does decrease in humans with age however recent evidence has shown that it does not disappear completely and it is thought that stimulating production of BAT may help with symptoms of obesity. In rodents it has been found that ablation of BAT could lead to obesity, diabetes and hyperlipidemia (Gesta et al., 2007).

1.3 Adipogenesis

The tightly controlled process of differentiation by which mature adipocytes are formed is known as adipogenesis. It is generally thought of in two-stages: the commitment of stem cells to the adipogenic line (preadipocytes) and the terminal differentiation of these cells into mature lipid-containing fat cells (adipocytes) (Tang and Lane, 2012). Most of the work on establishing the stages and signalling in this process has been done in cell culture particularly studying the terminal differentiation of preadipocytes into mature adipocytes. The 3T3 cell line, originally isolated from whole embryos between 17 and 19 days in age, is the most commonly used *in vitro* model used to conduct experiments.

The 3T3-L1 cell line is an established pre-adipocyte sub-clone of 3T3 mouse fibroblast cells which can be induced by an 'adipogenic medium' (see section 1.3.1) to form mature adipocytes containing lipid droplets (Green et al., 1974). *In vitro* investigation has given a number of insights into the process of adipogenesis however cell culture is known to have a number of limitations and so research is now moving towards finding *in vivo*-like methods for the study of adipogenesis.

Adipogenesis studies have also been carried out on human mesenchymal stem cells derived from a variety of locations including adipose tissue derived. The adult human stem cells are able to differentiate down the adipogenic lineage in response to hormonal or mechanical stimuli (Young et al., 2013). Preadipocytes derived from variable fat depots show differences in their lipid accumulation potential, however, with subcutaneous preadipocytes having the great potential for differentiation (Tchkonia et al., 2002). It has also been found that human dermal fibroblasts, which express mesenchymal stem cell-like markers, are able to differentiate into adipocytes in culture, although in a delayed timespan compared to adipose tissue derived stem cells (Jaager and Neuman, 2011). It is important to note that differences have been seen between murine and human adipogenesis particularly at the epigenomic level (Mikkelson et al., 2010).

In addition to *in vitro* work, farm animals such as pigs have also been used for investigation into the formation of adipose tissue (Poulos et al., 2009). Research has also been carried out in mouse models making use of transgenic techniques to manipulate the mouse genome and observe the results (Valet et al., 2002).

1.3.1 Adipogenesis *in vitro*

The cells used most commonly for the in vitro investigations into adipogenesis are the 3T3 cell lines: 3T3-L1 and 3T3-F442a. In the most frequent differentiation protocol, cells are allowed to grow until they reach confluence and become growth arrested. Differentiation of the cells is then stimulated through hormonal induction, although spontaneous differentiation can occur. The most common method of induction is using insulin, or IGF-1, dexamethosone, and methylisobutylxanthine (Tang and Lane, 2012). At this point the cells re-enter the cell cycle for one to two rounds of cell division, a process known as mitotic clonal expansion (discussed more in chapter 4). Following this the cells exit the cell cycle for the last time and continue to terminal differentiation through the expression of adipocyte-specific genes leading to fat accumulation and acquirement of endocrine functions (Fernyhough et al., 2007).

Adipogenesis *in vitro* progresses through a transcription factor cascade involving members of the CCAAT/enhancer-binding protein (C/EBP) family and peroxidise proliferated activated receptor gamma (PPARγ), as well as other transcription factors. In 3T3 cells it has been found that C/EBPβ and δ, along with members of the Kruppel-like transcription factor (KLF) family are expressed within the first hour after induction (Rosen et al., 2000; Wu and Wang, 2013). These act to activate PPARγ and C/EBPα expression which are often termed the "key transcription factors" for adipogenesis and, once expressed, are able to transactivate each other's expression (Fernyhough et al., 2007).

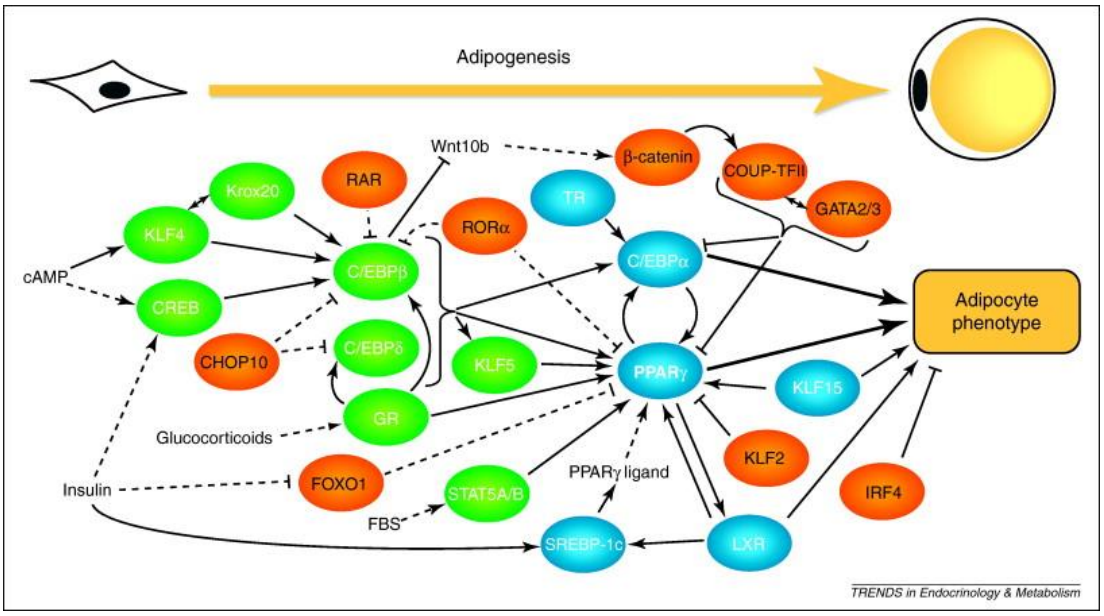

Figure 1.6: Diagrammatic representation of the transcriptional cascade leading to differentiation of preadipocytes into mature adipocytes (Siersbæk et al., 2012)

1.3.2 Adipogenesis *in vivo*

There have been far fewer studies of adipogenesis *in vivo* largely due to the fact that knockout animals are in general not viable, particularly animals which are null for the central transcription factors. To bypass this problem, information has been gained by using conditional knockouts or chimeric animals. These loss-of-function experiments have provided some compelling evidence for the presence and requirement for certain genes *in vivo* (Tanaka et al., 1997; Wang et al., 2006; Lee et al., 2013). A full picture of the process *in vivo*, though, is still proving to be out of reach.

Interestingly, *in vivo* studies have found that the transcription factor cascade discovered in cell line studies may be activated in a different order (Asaki et al., 2004). C/EBPα, in particular, may be expressed earlier than previously thought based on cell line models (Hausman, 2000; Asaki et al., 2004). In cultures of porcine, rodent, and human primary S-V cells C/EBPα, β and δ, and PPARγ mRNA expression could be detected before cells had reached confluence and before hormonal induction. Additionally C/EBP proteins were observed to peak at the same time or not display peaks in expression at all. In porcine foetal tissue, the order of expression was completely reversed as C/EBPα and PPARγ proteins were detected before

C/EBPβ and C/EBPδ (Manchado et al., 1994). Many more questions, therefore, remain as to whether adipogenesis studies *in vitro* accurately reflect the differentiation process *in vivo*, and indeed whether different fat depots *in vivo* develop under the same molecular controls as each other.

Adipogenesis, angiogenesis, and hair follicle development are thought to be closely linked *in vivo*. There is comprehensive research that adipogenesis and angiogenesis, in particular, are related in a spatiotemporal fashion. Injection of preadipocytes, such as 3T3-F442A cells, subcutaneously into mice leads to neovascularisation by angiogenesis of the fat as it continues to develop (Fukumura et al., 2003; Neels et al., 2004). Studies have shown that the preadipocytes are able to induce vessel formation during their development into mature white fat cells and the kinetics of angiogenesis matches the formation of lipid-filled vacuoles in the cells (Fukumura et al., 2003; Neels et al., 2004). Additionally adipogenic/ angiogenic clusters of cells have been shown to segregate from surrounding cells (Nishimura et al., 2007).

The link between hair follicle development and adipogenesis is less established however it has been hypothesised to exist on a number of occasions. Lipid filled cells have been found around the base of hair follicles in pigs, rodents, and humans (Hausman and Martin, 1982; Schmidt and Horsley, 2012; Wojciechowicz et al., 2013). In mice, the white adipose tissue depot in the lower dermis has been shown to vary in thickness with the hair follicle cycle, with the layer decreasing in size concurrently with follicle regression (Wojciechowicz et al., 2013).

1.3.3 Molecular control of adipogenesis

1.3.3.1 CCAAT/enhancer binding proteins

The C/EBP family of transcription factors have been extensively investigated for their role in adipogenesis and have been shown to be of the utmost importance to the progression of differentiation. *In vitro*, C/EBPβ/δ are activated almost immediately, within 4 hr, in direct response to hormonal induction, however their DNA binding activity is only gained after a lag of approximately 14 h (Cao et al., 1991; Tang and Lane, 2000). At the outset of differentiation, C/EBP homologous protein (CHOP-10) heterodimerises with C/EBPβ to prevent the latter from acquiring DNA binding activity (Tang and Lane, 2000). Simultaneous to downregulation of CHOP-10, from approximately 8 hr after induction, C/EBPβ is sequentially phosphorylated by mitogen activated protein kinase (MAPK) and glycogen synthase kinase (GSK3β) allowing it to bind to, and start transcription of target genes (Tang and Lane, 2000; Tang et al, 2005).

In addition to information obtained through cell culture studies, C/EBPβ and δ have been demonstrated to be required for adipogenesis *in vivo*. Double knockout mice for these genes were not viable much beyond birth displaying significant reductions in lipid accumulation throughout different adipose tissue depots (Tanaka et al., 1997). Despite their importance in adipogenesis, the C/EBP family are not specific to adipose tissue, also being expressed in the liver, lungs and intestine (Tontonoz et al., 1995). In adipose tissue, however, the family members do have distinct functions as it was demonstrated that although C/EBPβ could replace C/EBPα to restore liver function, the same was not possible for normal fat development.

C/EBPα is one of the central transcription factors in adipogenesis although descriptions of the extent of its role have differed between studies. In 3T3 cells, C/EBPα expression has been described as being seen anywhere between the second and fifth day of culture (Cao et al., 1991; Jiang and Lane, 2000). Most reports agree that C/EBPα acts in a pathway with PPARγ although research has shown that C/EBPα can be sufficient to

induce differentiation of 3T3-L1 preadipocytes (Lin and Lane, 1994). Further investigation however showed that C/EBPα was not able to induced differentiation in a PPARγ-/- fibroblastic cell line (Rosen et al., 2001).

C/EBPα expression during adipogenesis is induced by C/EBPβ binding to the promoter region. Before this can occur however, repressor units have to be dislodged from the C/EBPα promoter. One of these is the C/EBP undifferentiated protein (CUP) which is downregulated after mitotic clonal expansion (Jiang and Lane, 2000). The other is HDAC1 (histone deacetylase 1) which has a repressive function on transcription through binding to the proximal promoter region of C/EBPα. C/EBPβ is able to bind the C/EBP regulatory unit but is unable to activate transcription until HDAC1 is dislodged and degraded through a PPARγ dependent mechanism (Zuo et al., 2006).

Once activated, C/EBPα can maintain its own expression (Tang et al., 1999; Jiang and Lane, 2000). C/EBPα activates expression of genes such as leptin and adiponectin, and is important for promoting the full insulin sensitivity displayed by adipocytes (Rosen et al., 2001; Tang and Lane, 2012).

C/EBPα is anti-mitotic and is therefore thought to have a major role in halting the expansion phase and maintaining cells in growth arrest (Tang et al., 1999; Hamm et al., 2001; Tang et al., 2003). *In vitro*, terminal differentiation of adipocytes is brought about partly by C/EBPα repression of E2 transcription factor (E2F) resulting in the final arrest of cell proliferation. This requirement has also been shown to exist *in vivo*. Mice with E2F repression-defective C/EBPα alleles have continued cell proliferation and show severe defects in adipocyte differentiation (Porse et al., 2001).

There is also evidence that C/EBPβ is essential for the process of mitotic clonal expansion. A number of studies have found that a lack of C/EBPβ expression blocks adipogenic differentiation of 3T3-L1 cells through an inability to enter the S-phase of cell division (Tang et al., 2003; Zhang et

al., 2004). The crucial nature of C/EBPβ is thought to be due to its transcriptional activation of histone H4 (Zhang et al., 2011).

1.3.3.2 Peroxidase-proliferated activated receptors

There are three homologs in the PPAR family: α, β/δ, and γ. These homologous proteins are differentially expressed between different tissues. PPARγ is a key transcription factor for adipogenesis as it has a central role in the function of adipocyte genes such as FABP4 and PEPCK (phosphoenolpyruvate carboxykinase) (Fernyhough et al., 2007). There are four mRNA isoforms produced through differential promoter binding and alternative splicing although three of these all result in the same protein product. PPARγ2 is specifically expressed in adipose tissue and has been demonstrated to able to induce differentiation of PPARγ null fibroblasts (Rosen and McDougald, 2006).

PPARγ acts in concert with other nuclear factors as co-activators and co-repressors. These are able to bind and cause conformational changes to affect gene expression. In the absence of co-factor binding it is through that PPARγ can induce constitutive induction or repression of its target genes (Fernyhough et al., 2007). It has been shown that during adipogenesis PPARγ is required to heterodimerise with retinoid X receptor (RXR), another nuclear factor, for it to become transcriptionally active (Rosen et al., 2000). PPARγ is activated by C/EBPβ/δ as well as its expression being regulated by ERK/MAPK signalling (Clarke et al., 1997; Farmer, 2005). MAPK phosphorylates PPARγ to deplete its transcriptional activity (Tontonoz and Spiegelman, 2008). C/EBPα and PPARγ together activate the adipocyte specific genes which result in lipid accumulation and the other functions of adipose tissue such as hormone signalling (Tang and Lane, 2012).

PPARγ has also been demonstrated to be needed for adipogenesis *in vivo*. In chimeric mice containing both cells with and without expression of PPARγ, the PPARγ null cells are not found incorporated into adipose tissue. However it was also found that PPARγ is not enough to induce adipogenesis *in vivo* outside of an adipogenic niche (Rosen et al., 1999; Ban et al., 2008).

1.3.3.3 Kruppel-like factors

Kruppel-like factors (KLFs) are a family of zinc-finger transcription factors. There are both factors which promote (KLFs 15, 5, 4, 6, 9) and inhibit (KLFs 2, 3, 7) adipogenesis being expressed in white and brown adipocytes. KLF15 is upregulated during adipogenesis and in 3T3-L1 cells is found to have maximal expression on day 6 after induction although the mRNA first appears after 4 days (Uchida et al., 2000). It is thought to regulate GLUT4, a key transcription factor for glucose metabolism. KLFs 4, 5, and 6 are all expressed very quickly after induction of adipogenesis within the first 30 min or 1 h. As such they are involved in the regulation of other transcription factors earlier in adipogenic differentiation programme, including C/EBPβ and δ and PPARγ2. KLF5 expression by contrast is induced by C/EBPβ and δ (Oishi et al., 2005).

The inhibitory members of the KLF family are, as expected, expressed most highly before adipogenesis begins and are downregulated during the differentiation process. They inhibit the key transcription factors and also inhibit the expression of adipokines (Wu and Wang, 2013). *In vivo*, KLF2 is most highly expressed in the lung but *in vitro* it has been shown to have the potential to downregulate the expression of PPARγ, C/EBPα, and adipocyte differentiation and determination factor 1 (ADD1)/sterol regulatory element-binding transcription factor 1 (SREBP1c) completely blocking preadipocyte differentiation (Anderson et al., 1995; Bannerjee et al., 2003).

1.3.3.4 Other factors involved in adipogenesis

ADD1 is another important transcription factor involved in adipocyte development and also cholesterol homeostasis (where it is known as SREBP1). It is a member of the basic-helix-loop-helix family of transcription factors which have the ability to bind to two distinct DNA sequences. *In vitro* experiments in preadipocytes showed that expression of dominant-negative form of ADD1 is sufficient to block adipogenesis (Kim and Spiegelman, 1996). It is suggested that ADD1/SREBP1 could have a role in activation of

PPARγ and it is also believed to regulate expression of the hormone, adiponectin (Kim and Spiegelman, 1996; Seo et al., 2004).

Extracellular factors and signalling pathways have been identified which are thought to activate or inhibit the transcription factors described above. These include the Wnt and bone morphogenic protein (BMP) signalling pathways amongst others (Bost et al., 2002; Date et al., 2004; Bowers et al., 2008). These two pathways are particularly thought to be involved in the lineage commitment stage of adipocyte differentiation although neither pathway has a completely elucidated role. The Wnt pathway can act by either a "canonical" or "non-canonical" mechanism. It is thought that the canonical pathway is able to induce undifferentiated precursor cells to enter the adipogenic lineage, although Wnt10b has been shown to block later adipocyte differentiation by blocking expression of key transcription factors (Tang and Lane, 2012). BMP2 and 4, and retinoblastoma protein signalling have all also been implicated in adipocyte commitment.

Preadipocyte factor 1 (Pref-1) is recognised as a marker for preadipocytes as it is downregulated in adipogenesis in 3T3-L1 cells and is inhibitory if overexpressed. It also has a negative effect on adipogenesis *in vivo* (Sul et al., 2000; Wang et al., 2006). Mice overexpressing Pref-1 have a lower fat content and show lower expression of adipocyte-secreted factors. If there is a lack of Pref-1, mice show faster fat deposition (Wang et al., 2006).

1.3.4 miRNAs in adipogenesis

MicroRNAs are endogenous small, non-coding pieces of RNA about 20-25 nucleotides in length. They were originally discovered in C. elegans but are now known to exist in plants, vertebrates and invertebrates (Lee et al., 1993; Rana, 2007; Romao et al., 2011). They are found in the parts of the genome previously classified as ‘junk’ DNA, most commonly in introns of genes and but some have also been identified in intergenic DNA. A few are even found within exons. Those found within introns and exons of genes mainly appear to be enclosed with the gene which they regulate so that they are transcribed at the same time (Rana, 2007; Ramao et al., 2011).

In vertebrates, miRNAs are found differentially expressed in different organs throughout the body and have been described in a diverse range of developmental and metabolic roles (Esau et al., 2004; Lin et al., 2009). MiRNAs function by binding to the 3' untranslated region of their target mRNA. They prevent translation of the mRNA into protein either by suppression of translation or, less commonly, degradation of the mRNA (Rana, 2007; Romao et al., 2007).

A number of miRNAs have been identified which appear to have either an activating or inhibitory role in adipogenesis. MiRNAs have commonly been identified by microarrays of adipogenic cell lines or primary cultured cells and then further investigated in cell culture. Very little work has yet been done on establishing their role *in vivo* (Ramao et al., 2011). There is a very long list of miRNAs which have been found to be either up- or down-regulated during adipogenesis however only a small number of these have been further investigated (Esau et al., 2004; Kajimoto et al., 2006). Research has also been done on identifying the target(s) of the miRNAs. Amongst those found are the master adipogenic regulators, C/EBPα and PPARγ, as well as other members of signalling pathways thought to be involved in adipogenesis such as the Wnt pathway (Kennell et al., 2008; Lin et al., 2009).

MiRNAs can be either up- or down-regulated during adipogenesis and this, combined with expression studies in cell culture, has led them to being classified as either pro- or anti-adipogenic. The miR-27 gene family is one of the most widely investigated. The members of the family are miR-27a and miR-27b, both of which are anti-adipogenic. Microarray data shows them to be downregulated during adipogenesis, and overexpression in cell culture of 3T3-L1 preadipocytes inhibits their differentiation into mature adipocytes (Lin et al., 2009). Overexpression of miR-27 also inhibited the adipogenic differentiation of OP9 cells, a multipotent mesenchymal cell line, when they were treated with adipogenic stimulants (Lin et al., 2009). By monitoring the mRNA levels, Lin et al., 2009, found that the miR-27 gene family significant inhibits the transcriptional induction of PPARγ within a day of adipogenic

stimulation and both PPARγ and C/EBPα within two days of adipogenic stimulation. Kim S.Y. et al., 2010, also specifically investigated miR-27a and similarly found it to be anti-adipogenic through suppression of PPARγ expression.

MiR-143 and the miR-17-92 cluster (miR-17-5p, miR-17-3p, miR-18, miR-19a, miR-20, miR-19b, and miR-92-1) are two of the gene families found to be pro-adipogenic (Esau et al., 2004; Wang et al., 2007). MiR-143 has mainly been investigated in primary human adipocytes; however it has also been shown to be upregulated on microarrays of 3T3-L1 cells during adipogenesis. Inhibition of miR-143 stops adipogenic differentiation however overexpression is not enough to stimulate adipogenesis without another adipogenic stimulant. Investigation of protein levels identified ERK5 as a potential target of miR-143 (Esau et al., 2004). As listed above, the miR-17-92 cluster is comprised of seven separate miRNA genes. In 3T3-L1 adipogenesis the cluster has been found to be significantly upregulated during the mitotic clonal expansion stage and they are thought to promote adipogenesis through negative regulation of Rb2/p130 which is involved in cell proliferation (Wang et al., 2007). MiR-378 has also been shown to enhance adipogenesis *in vitro*. Interestingly, the gene encoding miR-378 is located in the first intron of PPARγ co-activator protein (PGC1α) which is important in brown adipocyte differentiation (Gerin et al., 2010).

1.4 Thesis aims

The work in this master's thesis aimed to investigate the similarities and differences between the established *in vitro* adipogenesis pathway and the process *in vivo*, specifically looking at white adipose tissue in the lower dermis of the skin. Microarray work performed by the Jahoda lab on developing skin fat has indicated that there are molecular and cellular differences between what is seen in culture and development of adipose tissue *in vivo*. This project firstly aimed to establish an effective model system for the study of adipogenesis in the lower dermis exploring a substrate organ culture method, and three-dimensional cell culture of dermal cells. Beyond and around the establishment of model systems, the work in this thesis goes on to explore three related areas of adipogenesis. 1) The timing of adipogenesis in the lower dermis, 2) mitotic clonal expansion as a precursor to adipogenic differentiation, 3) miRNAs in the skin during adipogenesis.

Detailed methods for all of the work in this thesis are described in chapter 2. The first model system established was a substrate organ culture system of mouse back skin, however the unreliable results obtained from this method when older embryonic skin was being used led to a second model being developed. Both the substrate organ culture and the three-dimensional cell culture models are presented in chapter 3. The original hypothesis for the timing of adipogenesis was that cells in the lower dermis began to differentiate into adipocytes from approximately 16 embryonic days onwards. During the establishment of the 3D cell culture model it became apparent that this process started earlier than previously supposed. Work in chapter 3 investigated this further particularly through immunofluorescent staining of C/EBPα and ORO staining of lipid droplets.

Work in chapter 4 aimed to test the hypothesis that the mitotic clonal expansion stage seen *in vitro* is in fact an artefact of hormonal induction. The primary method used was DNA replication labelling with EdU in whole skin pieces and 3D cell culture. The organ culture system was used to get a snapshot of the cell proliferation at three embryonic time points. The skin was taken from embryonic mice and incubated for a short timescale. The uptake

of EdU into cells which had undergone DNA replication was visualised through fluorescent staining.

Chapter 5 explored the role of miRNAs in adipogenesis. MiRNAs linked to adipogenesis were identified through literatures searches and bioinformatic analysis of microarray data. Five of the identified miRNAs were investigated in mouse back skin with quantitative PCR.

Chapter 6 served to draw together all of the areas explored in this thesis with final points of discussion. It also suggested future directions for research based on interesting questions which have arisen from the results in this thesis.

Chapter 2

Methods

2.1 Housing, breeding and feeding conditions of mice.

Mice (FVB) from the Durham University Life Sciences Support Unit and Charles Rivers Laboratories were bred and maintained at a temperature of 21^{o}C, with 55% humidity and kept on a 12 hour light/dark cycle. All animals were watered and fed ad libitum.

The baseline age of embryos used for experiments was established through analysis of vaginal plugs. Breeding pairs were kept together overnight and the presence of a vaginal plug in the morning indicated a successful mating, at which point embryos were considered to have undergone 0.5 days of gestation. Mice were sacrificed using carbon dioxide.

2.2 Two- and three-dimensional primary cell culture

2.2.1 Preparation of dermal cells from whole skin

Skin specimens were cut from the dorsal lateral back skin of embryonic day 14 through to embryonic day 18 mice (E14 - E18) and carefully separated from underlying muscle and subcutaneous fat. Specimens were gathered in 1 ml of standard medium consisting of 1x Minimum Essential Media (MEM; Gibco) with antibiotics (100 µl/ml Penicillin/Streptomycin (P/S) and 2 µl/ml Fungazione (Fn)). The skin was then washed twice in sterile 1x Earle's solution, followed by incubation in 1 ml Trypsin/Pancreatin working solution (5% trypsin, 6% pancreatin in 1x Earle's solution (1:1:2 ratio)) at 4^{o}C for 40-90 min depending on the embryonic age. The dermis was separated from the epidermis using watchmaker's forceps and gathered in 1 ml cold 1x Earle's solution. Dermal specimens were transferred to 1 ml warm working solution of DNase I/collagenase II and incubated at 37^{o}C and 5% CO_2 for 15 min. The dermis was disrupted into a single cell suspension by repeated pipetting. If the dermis remained aggregated, the solution was incubated for a further 5 min. The single cell suspension was filtered through a 70µm sterile cell strainer (Fischer) which was then centrifuged at 3000 rpm for 5 minutes at room temperature (RT). The cell pellet was resuspended in growth medium which was made from standard medium with the addition of 10% Fetal Bovine Serum (FBS; Gibco).

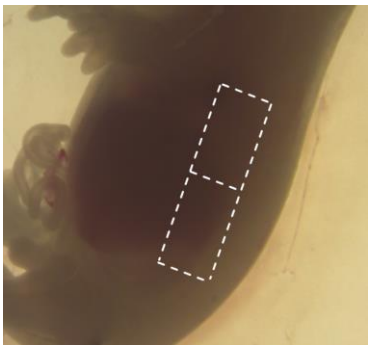

Figure 2.1: Location of removal of skin pieces for separation of dermis and epidermis. Skin was taken from the dorsal lateral back area on each side of the mouse embryo. The long strip was cut into two smaller pieces for more efficient separation of dermis and epidermis.

The number of cells in 1 ml of medium was calculated by counting on a haemocytometer, taking an average from two separate sets of 10 squares. This number was divided by 10 to calculate the number of cells in 1 µl of single cell suspension before determining how much standard growth medium needed to be added to obtain the required density for plating or droplets (see below for densities).

2.2.2 Two-dimensional culture

Cells were plated into 6-well plates at a density of 24,000 cells/well in growth medium. The plates were incubated at 37^{o}C/5% CO_2 for 4-8 days depending on the original developmental age of the skin, then fixed in calcium formal in preparation for Oil Red O analysis.

2.2.3 Three-dimensional spheroid culture of dermal cells

The cell suspension was diluted to 600 cells/µl and pipetted in 10 µl drops of growth medium on a petri dish lid which was suspended over a dish of sterile deionised water (dH_2O) and incubated at 37^{o}C/5% CO_2. The cells aggregated in the drop to form a sphere. For direct comparison to 2D cell cultures, spheres were transferred to 6-well plates in 0.2 ml of growth medium per plate and allowed to adhere (described in section 2.1.4 below). Alternatively, for immunofluorescence and lipid analysis, spheres were transferred to Tissue-Tek® O.C.T.™ Compound (Sakura) after 2, 3, 4, 6 or 8 days depending on the embryonic age from which the cells were derived. Approximately 10 spheres were collected in a block, snap-frozen in liquid

nitrogen and stored at -80^{o}C. Sections were cut on a cryostat (Leica CM3050) at 7µm for immunofluorescence analysis and 10µm for analysis of lipids by Oil Red O staining (see section 2.4 below).

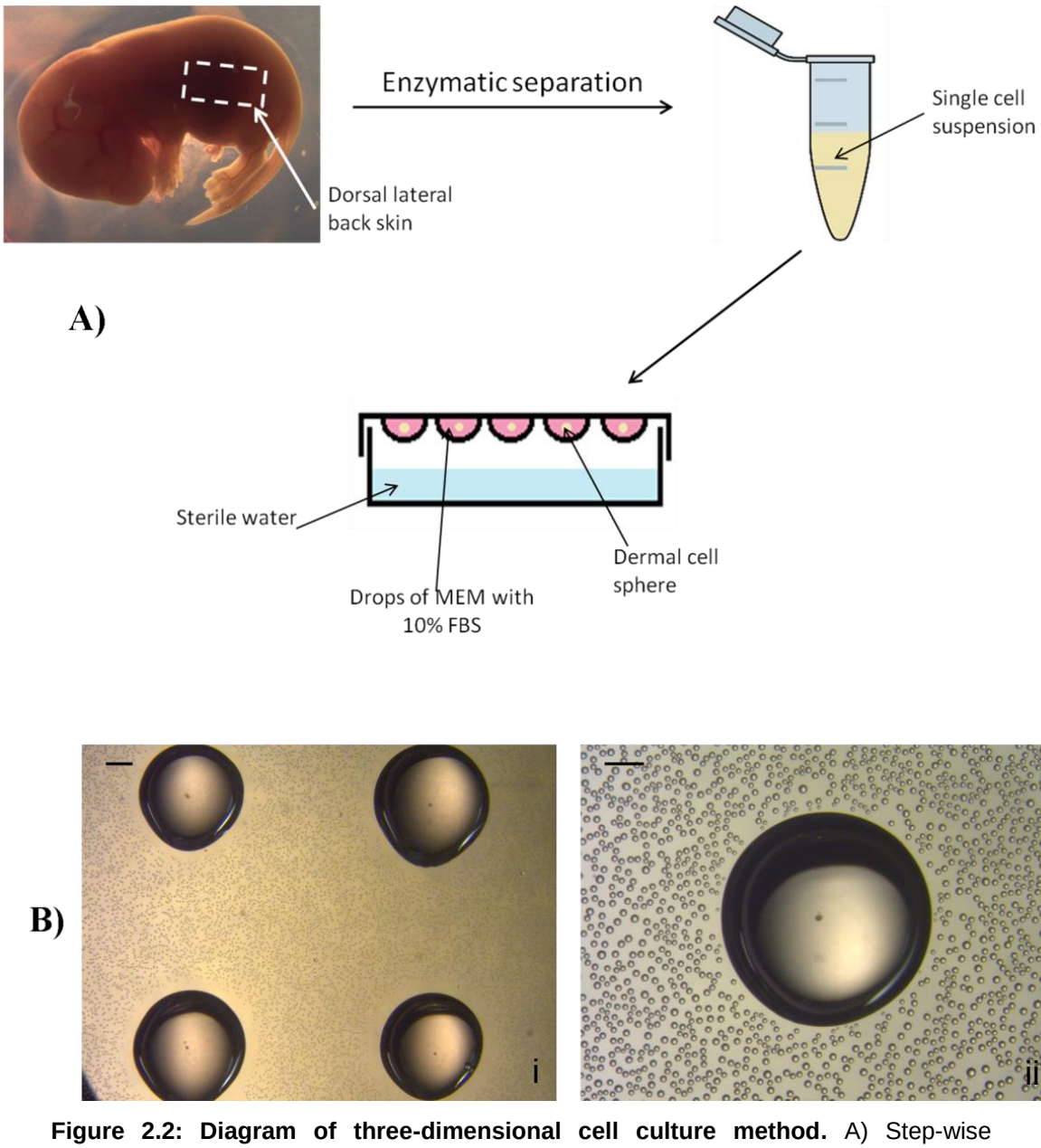

Figure 2.2: Diagram of three-dimensional cell culture method. A) Step-wise progression of removal from the dorsal lateral back skin to make dermal cell spheres. Enzymatic separation of epidermis and dermis and tissue dissociation was achieved in 5% trypsin / 6% pancreatin solution followed by collagenase II / DNase I. 10 µl drops of single cell suspension were suspended over sterile water. B) Microscope pictures of spheres suspended over sterile water. Scale i) 1 mm, ii) 100µm

2.2.4 Transfer of 3D spheres to 2D culture

After 2-6 days, depending on the original developmental age of the skin, four spheres were transferred from the 3D hanging drop cultures into each well of a 6-well plate using an automatic pipette. Approximately 200 µl of growth medium was carefully added over the spheres ensuring they remained in the centre of the well. The spheres were left in 2D culture for 48 hr, then fixed in calcium formal for Oil Red O analysis.

2.3 Substrate organ culture technique

Rectangular pieces of back skin, approximately 2.5 x 3 mm, were cut from E14-14.5, and E16-16.5 mouse embryos. Samples, approximately 6 to 10 each experiment, were carefully detached from underlying muscle and transferred onto Nucleopore membrane filters (Whatman) previously coated in 3.5 mg/ml type I collagen from rat tail (Sigma). The filters were floated on either 2 ml of standard medium or the same medium with the addition of 0 or 2% FBS.

After incubation at 37^{o}C, 5% CO_2 for either 72 or 96 hr, samples were transferred to Tissue-Tek® O.C.T.™ Compound (Sakura), snap frozen in liquid nitrogen, and stored at -80^{o}C. Alternatively, skin was fixed in 4% paraformaldehyde overnight before being processed, through successive dehydration, and embedded in wax. Sections were cut on a microtome (Leica RM2125 RTS) at 8 µm and left to attach for at least 2 hr.

2.4 Modified hematoxylin & eosin staining of organ cultured skin

Frozen sections were cut at a thickness of 7 µm on a cryostat (Leica CM 3050) and attached to SuperFrost®Plus slides (Thermo Scientific). Sections were air-dried for up to 2 hr at room temperature. Back skin sections were washed in distilled water for 5 min followed by 5 min staining in Shandon Gill haematoxylin (Thermo Scientific). Sections were rinsed in tap water several times and then washed thoroughly in tap water for 5 min. Excess haematoxylin was removed by 1% acid ethanol (1% conc. hydrochloric acid in 70% ethanol) followed by two washes in tap water (1 min each). Next, sections were counterstained with eosin (Thermo Scientific) for

30 sec. The sections underwent sequential dehydration in 75% ethanol (3 x 1 min), 100% ethanol (2 x 2 min) and Histoclear (2 x 2 min) (National Diagnostics) and mounted in DPX (Agar Scientific).

2.5 Oil Red O staining

2.5.1 2D cells

Cells were washed in three times in PBS (5 min each) followed by fixation in calcium formal (40% formaldehyde (Sigma) and 1% calcium chloride) for 10 min. They were then washed in 60% isopropanol for 5 min and stained with oil red O (ORO) working solution for 15 min (3 parts of ORO stock : 2 parts dH_2O). Cells were rinsed again in 60% isopropanol and PBS before being mounted and coverslipped with glycergel (DakoCytomation). Alternatively, cells were stored in PBS at 4^oC for oil red O extraction and quantification (section 2.4.1.1 below). Photos were taken on a Zeiss Axiovert 10 microscope.

2.5.1.1 Oil red O extraction and quantification

ORO stained cells were allowed to air-dry completely prior to addition of 1 ml 100% isopropanol. The stain was extracted for 10 min at RT with gentle shaking. Absorbances were read at a wavelength of 510 nm on a NanoDrop 1000 spectrophotometer.

2.5.2 Back skin and 3D sphere sections

Back skin or 3D sphere sections were cut at 10 µm on the cryostat and left to air-dry for approximately 1 hr 30 min. For ORO lipid staining, the sections were firstly washed three times (5 min each) in PBS (Phosphate Buffered Saline), then fixed for 1 hr at RT in calcium formal: 4% paraformaldehyde (Sigma) and 1% calcium chloride. Next, sections were incubated in 60% isopropanol for 15 min, followed by 15 min staining in ORO working solution: 3 parts ORO (Sigma; saturated in 100% isopropanol) to 2 parts dH_2O. Sections were briefly rinsed in 60% isopropanol and washed in dH_2O. Nuclei were counterstained by dipping in Shandon Gill's haematoxylin (Thermo Scientific) and slides were mounted in Glycergel (DakoCytomation).

2.6 Immunofluorescence staining

Cryostat sections were cut at 7 µm and allowed to air-dry for approx. 90 minutes. FABP4 staining was either carried out on frozen sections or wax embedded skin sections cut at 8 µm. For each of the following antibodies, negative controls of staining without secondary antibody were carried out for each separate sample. Staining followed the same method as those described in sections 2.6.1 - 2.6.3 below with samples incubated in PBS containing 1% goat / donkey serum (G/DS) during the secondary antibody step. For pictures see Appendix V. Controls with no secondary antibody were also carried out to check for autofluorescence from samples.

1° antibody	Dilution	Supplier	2° antibody	Dilution	Supplier
C/EBPα	1:100 or 1:300	Santa Cruz	Goat anti-rabbit (AlexaFluor 488 or 594)	1:500	Life Technologies
Cyto-keratin	1:50	Zymed	Goat anti-mouse (AlexaFluor 488)	1:500	Life Technologies
FABP4	1:50	R&D Systems	Donkey anti-goat (AlexaFluor 594)	1:1000	Life Technologies

Table 2.1: Summary of primary and secondary antibodies used for immunofluorescent staining of mouse back skin and 3D cell culture sphere sections

2.6.1 C/EBPalpha

2.6.1.1 Back skin sections

Unfixed skin sections were washed in 1x PBS (3x 5 min) then blocked in 20% goat serum (GS) for 30 min at RT. Primary antibody was used at a 1:300 dilution (in 1% GS) and left on the sections to incubate overnight (O/N) at 4°C. Slides were washed three times in 1x PBS (5 min each) followed by incubation with secondary antibody (1:500) for 1 hr at RT. After three washes in 1x PBS (5 min each) slides were mounted in mowiol containing DAPI (Insight Biotechonology; 1:500).

2.6.1.2 3D sphere sections

Sections were fixed in 4% paraformaldehyde (PFA) solution for 15 min followed by permeabilisation in 0.5% Triton-X for 5 min. Following 3x 5min washes in 1x PBS sections were blocked in 20% GS for 30 min at RT. Next, primary antibody (1:100) incubation was carried out at RT for 90 min.

Sections were washed again and incubated with secondary antibody (1:500) for 90 min at RT. After a final three washes, slides were mounted in mowiol containing DAPI.

2.6.2 Cyto-keratin

Sections of 3D spheres were fixed in ice-cold for 15 min followed by 5 min in ice-cold methanol. Sections were then washed in 1x PBS for 3x 5 min and blocked for 30-60 min in 10-20% goat serum. Primary antibody incubation (1:50; Zymed) was carried out overnight at 4^{o}C. Sections were washed three times in 1x PBS (5 min each) followed by incubation with secondary antibody (1:500) for 1 hr at RT. After three washes in 1x PBS (5 min each) slides were mounted in mowiol containing DAPI.

2.6.3 FABP4

2.6.3.1 Frozen sections

Organ cultured skin sections were fixed in ice-cold acetone for 10 min and then briefly washed in 1x PBS. Sections were blocked in 10% DS for 1 hr and then incubated with FABP4 1^{o} antibody for 90 min at RT or O/N at 4^{o}C. Following three washes in PBS, sections were incubated with Donkey anti-Goat secondary antibody for 1 hr at RT. After a final three washes, sections were mounted in mowiol containing DAPI.

2.6.3.2 Wax-embedded sections

Sections were first rehydrated a succession of xylene, 100% ethanol, 95% ethanol, 70% ethanol, and dH_2O. They were then boiled in 10 mM Tris-citrate for 20 min and briefly washed in 1x PBS. Staining was continued as for frozen sections, starting from the blocking step.

2.7 5-ethynyl-2´-deoxyuridine (EdU) incorporation

2.7.1 Back skin

Back skin from mice embryos at E14-14.5, E15-15.5, and E16-16.5 was prepared and placed on type I collagen-coated filters as described in section 2.3. Filters were floated on 2 ml of standard medium with the addition of 2% FBS, and 1.5 µg/ml EdU (Invitrogen). Following a 2 hour

incubation period ('pulse') skin was transferred to Tissue-Tek® O.C.T.™ Compound (Sakura), snap frozen in liquid nitrogen, and stored at -80^{o}C.

Alternatively, following the 2 hr incubation with EdU, the medium was changed to 2 ml of standard medium (with 1 % FBS) and the skin was cultured for a further 72 or 96 hr before freezing. Frozen specimens were cut on a cryostat (Leica CM3050S) and sections (7 µm) were attached to SuperFrost®Plus slides (ThermoScientific).

2.7.2 3D cell culture

Dermal cells were obtained from E14.5 mice embryos and put into 3D cell culture using the method described in section 2.1. After three days in culture, spheres were transferred to a new 10µl drop of media containing 2.5 µg/ml EdU for a 4 hr 'pulse'. Spheres were then either transferred to a new drop of medium without EdU, for a further 1 or 6 days, or immediately snap frozen for analysis of proliferation. Alternatively spheres were cultured initially in medium containing 2.5 µg/ml EdU. After 48 hr these were either transferred to a new medium drop without EdU, or snap frozen for analysis.

2.8 EdU and immunofluorescence co-staining

EdU incorporation into DNA was visualised using the Click-iT® EdU Alexa Fluor® 488 Imaging Kit (Invitrogen) according to the manufacturer's instructions with modifications for skin sections. Sections were fixed in 4% paraformaldehyde (Sigma) for 15 minutes, rinsed in PBS, and permeabilised in 0.1% Triton X-100 (Sigma) for a further 15 min. Following a 5 min wash in PBS, sections were incubated in the dark with the reaction "cocktail" consisting of 1x Reaction buffer, 1x Reaction buffer additive, $CuSO_4$, and Alexa Fluor 488 azide, for 30 min at RT. Sections were washed three times in PBS (5 min each) and mounted in mowiol with DAPI (1:500). Alternatively, prior to mounting, sections were co-stained with either collagen IV or C/EBPα (see table below).

1° antibody	Supplier	Dilution	Blocking	1° antibody incubation	2° antibody
Collagen IV	AbD Serotec	1:50	-	O/N, 4°C	Goat anti-Rabbit; Alexa Fluor 594; Life Technologies
C/EBPα	Santa Cruz	1:50	20% GS, 30 min	90 min, RT	

Table 2.2: Summary of primary and secondary antibodies used for co-staining with EdU for the investigation of cell division in mouse back skin and dermal cell spheres

2.8.1 Cell counting and statistical analysis

Total number and EdU positive nuclei in E14.5, E15.5, and E16.5 back skin sections were counted on ImageJ using the "Image-based Tool for Counting Nuclei" plugin. Several images from two separate pieces of skin were used for each embryonic age. Two or three areas of interfollicular dermis were defined in each picture and divided into upper and lower dermis subdivisions using collagen IV staining (Figure 2.2). The plugin used for counting required images to be in greyscale therefore, once the subdivisions had been defined, the multi-colour images were split into separate channels for nuclei counting (Figure 2.3 and 2.4).

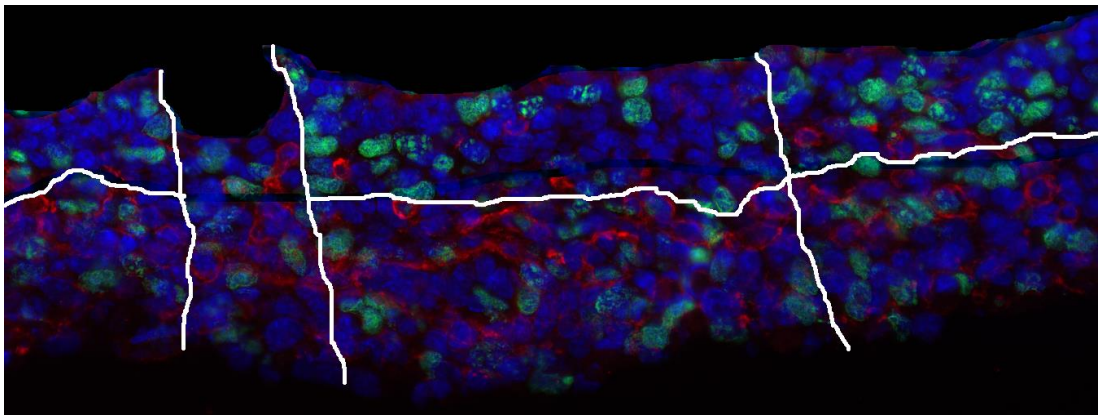

Figure 2.3: Example of dermis divided into smaller areas prior to total (blue) and EdU positive (green) nuclei counting. Dividing lines were added to each picture based on collagen IV staining prior to separating channels on ImageJ for counting (Figures 2.4 and 2.5, below). Hair follicles and the areas below were excluded.

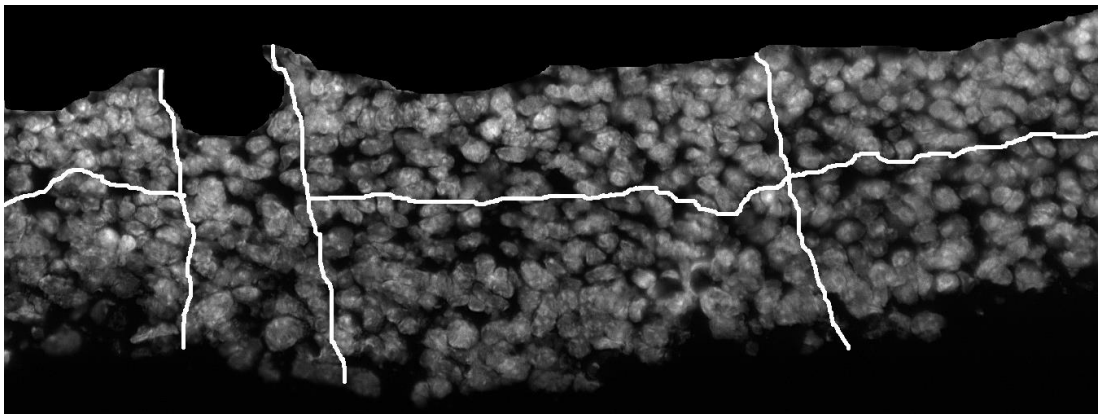

Figure 2.4: Greyscale image, divided into sections, of total nuclei. The total number of nuclei in each area was counted on ImageJ using the "Image-based Tool for Counting Nuclei" plugin

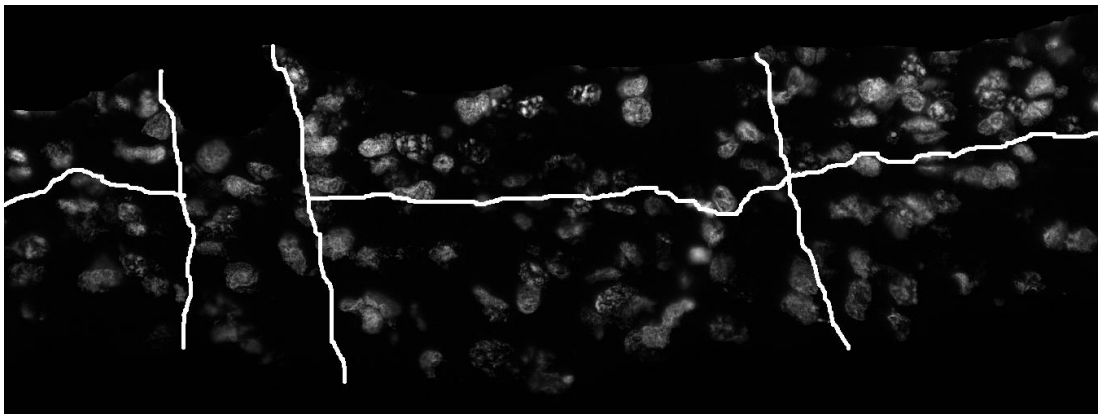

Figure 2.5: Greyscale image, divided into sections, of EdU positive nuclei. The number of EdU-positive nuclei in each area was counted on ImageJ using the "Image-based Tool for Counting Nuclei" plugin

It was assumed that the mean proportion of cells in the lower dermis subdivision was drawn from a beta distribution with mean, $\bar{p}$, and the mean proportion of cells in the upper dermis subdivision had mean $(1+\alpha)\bar{p}$. A likelihood ratio test was used to look for evidence that α differed from 0. Maximum likelihood estimates were found using solver in Microsoft Excel.

2.9 Bioinformatic analysis of microarray data

2.9.1 iGET FIRE

Complete gene lists exported from GeneSpring were prepared for FIRE analysis. Replicate raw values for each probe set ID were averaged and a ratio was created of the averages for the reference sample against

experiment sample. A log to the base two was taken of the ratio. These logs and the probe set IDs were inputted into the iGET website after selecting the "start with an information file with microarray prove IDs" option. Query parameters were set as “ebins” at 20 and “minr at either 1.5 or 5. Other parameters were maintained on the default settings.

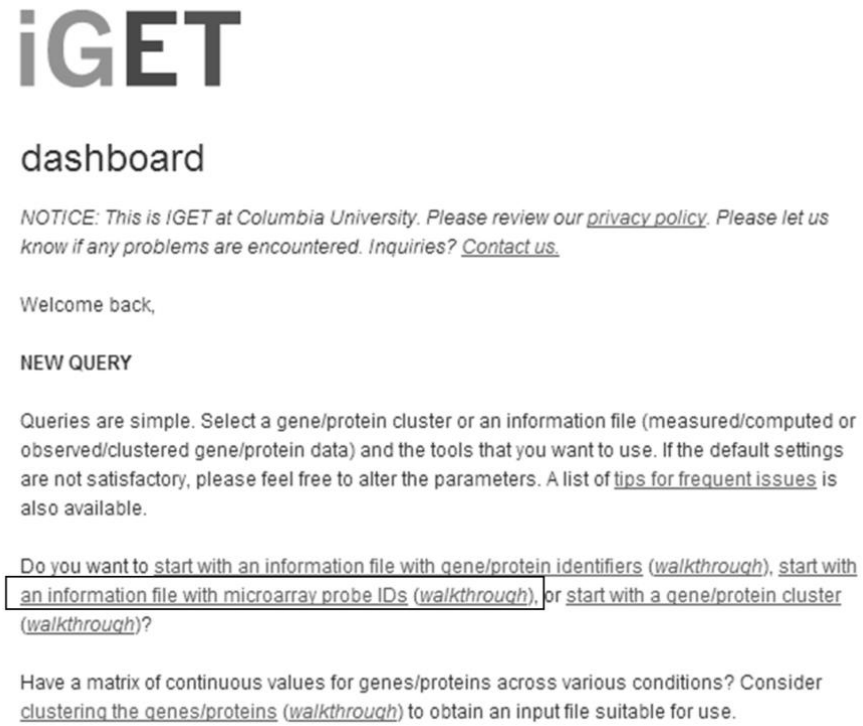

Figure 2.6: Screen capture of 'iGET dashboard' showing query selection

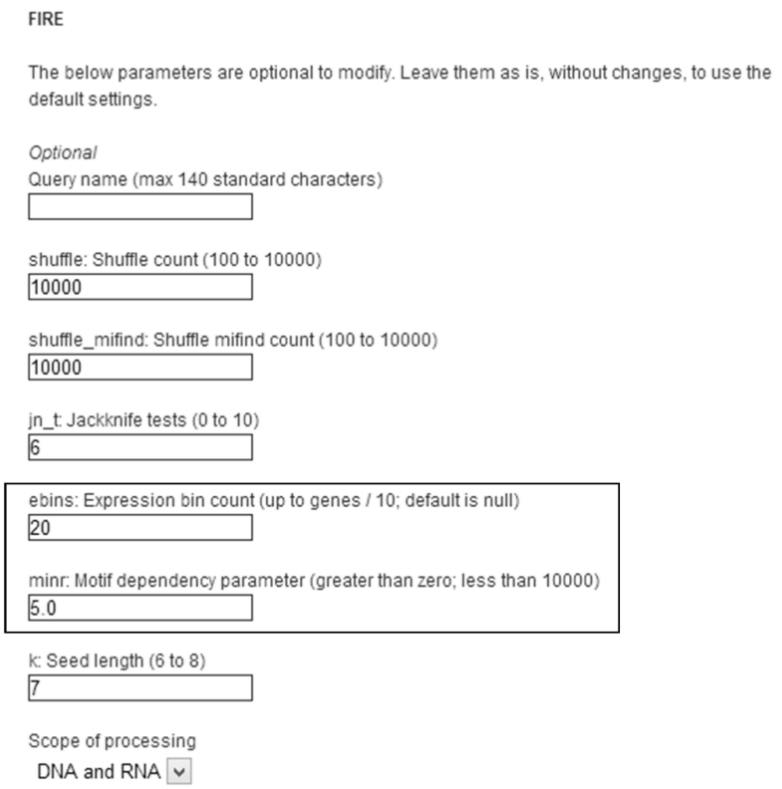

Figure 2.7: Screen capture of FIRE parameters

2.10 miRNA extraction

Total RNA content including small RNAs was extracted from mouse skin at embryonic days 14.5, 16.5, and 17.5 using the Qiagen miRNeasy kit. All work was carried out under RNase-free conditions by treating equipment with RNase-Zap or DEPC water. Briefly, skin was excised from the dorsal back area and separated using trypsin/pancreatin as described in section 2.1.1. Dermal and epidermal pieces were separately snap frozen in liquid nitrogen and disrupted into a powder before being transferred into 700 µl QIAzol Lysis Reagent. The solution was homogenised by repeated pipetting. The homogenate was left at RT for 5 min before the addition of 140 µl chloroform. The solution was mixed vigorously for 15 sec and then centrifuged at 12,000 x g for 15 min at 4^{o}C. The upper aqueous phase was transferred to a new RNase-free tube and 1.5 volumes of 100% ethanol was added. A spin column method of extraction was used going through several washes in Buffer RWT and Buffer RPE before the RNA was eluted into 30 µl RNase-free water. RNA concentration was calculated using a Nanodrop 1000 spectrophotometer.

2.11 Reverse transcription

cDNA synthesis was carried out using the miScript II RT (Qiagen) kit selectively converting mature miRNAs, snoRNAs, and snRNAs. A master mix was made up of 5x miScript HiSpec Buffer (4 µl per sample), 10x miScript Nucleics mix (2 µl per sample), and miScript Reverse Transcriptase mix (2 µl per sample). To 8 µl of this master mix, for each sample, 100 ng RNA was added and RNase-free water up to a total reaction volume of 20 µl. Samples were incubated at 37^{o}C for 1 hr, then heated to 95^{o}C for 5 min to inactivate the Reverse Transcriptase mix. Samples were immediately cooled on ice and stored at -20^{o}C.

2.12 Real-time, quantitative polymerase chain reaction for the detection of miRNAs

qPCR was carried out using the miScript SYBR Green PCR Kit (Qiagen) on a Rotorgene Q quantitative PCR machine.

Each individual PCR reaction contained 12.5 µl 2x QuantiTect SYBR Green PCR master mix, 2.5 µl 10x miScript Universal Primer, 2.5 µl 10x miScript Primer Assay, 5 ng cDNA, and 2.5 µl RNase-free water up to a total volume of 25 µl.

Step	**Time**	**Temperature**
PCR Initial activation step	15 min	95^{o}C
3-step cycling: 40 cycles		
Denaturation	15s	94^{o}C
Annealing	30s	55^{o}C
Extension	30s	70^{o}C

Table 2.3: Summary of qPCR stages

Chapter 3

The establishment of a 3D culture model for the study of dermal adipogenesis, and its utilisation for investigation of the timing of adipogenesis 'in vivo'.

3.1 Introduction

This chapter describes the establishment of two different *ex vivo* culture systems for the study of adipogenesis in the lower dermis. The two systems explored are: substrate organ culture of whole mouse skin and 3D cell culture of dermal cells. The model systems in this chapter were established in conjunction with Olivia Davies.

In 2D culture developing fat cells go through a number of stages as they change from preadipocytes to mature white adipocytes. The first visible change is the emergence of granularity within the cell. These granules then gradually materialize into very small fat droplets which continue to increase in size and group together until there is one large fat globule (Figure 3.1). Concurrently to accumulating fat droplets, the cells also change in morphology from an elongated fibroblastic shape, to a much smaller rounded cell (Figure 3.1).

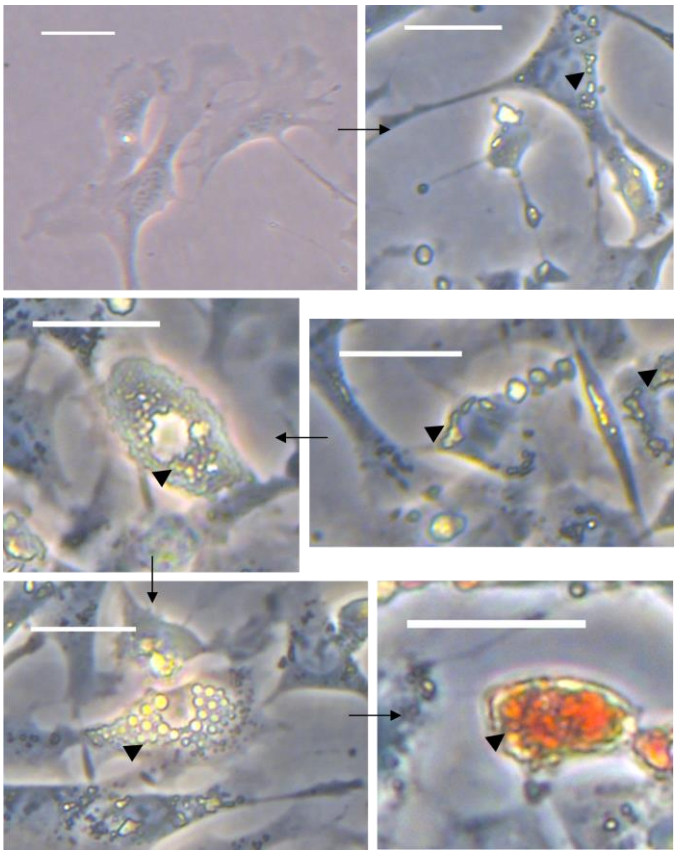

Figure 3.1: Sequential transformation of a mouse primary foetal fibroblast into a mature adipocyte (stained with Oil Red O). Small lipid droplets begin to accumulate in the cytoplasm (top right), gradually increasing in size and joining together into larger droplets

(middle row and bottom left). The droplets eventually merge into one large lipid globule which fills the cell (bottom right). Scale bars = 30 μm

Together with the widespread interest in adipogenesis has come the understanding that different adipose depots have different developmental origins and properties. It is perhaps surprising, therefore, that much of the information known about the timing of adipogenesis, and the cellular and molecular processes involved comes from work on cultured cell lines, in particular 3T3 cells (Tang and Lane, 2000; Gu et al., 2007; Hishida et al., 2009). Although this has provided valuable baseline information, there is increasing evidence that a) cell lines, and 2D culture in general, are not an accurate representation of differentiation *in vivo* and b) there may be site specific differences in adipose tissue biology.

2D culture results in cells that are geometrically very different to their counterparts in tissues, and it also deprives them of their natural surrounding matrix. Recent evidence has shown that these morphological changes have profound impacts on gene expression, an important factor when studying a developmental process (Tibbitt and Anseth, 2009). Fibroblasts in particular behave very differently in 2D culture with changes in the cytoskeleton and lamellipodia resulting in them flattening and spreading out over the culture dish (Birgersdotter et al., 2005). In addition to the changes seen in cells in 2D culture, there are also gene expression changes associated with establishing a cell line (Birgersdotter et al., 2005). These facts provide compelling evidence of the need for a model system for the study of adipogenesis in skin that is representative of *in vivo* events.

One method that has been used is spheroid or hanging drop cultures. Spheres of cells are formed through constant movement in a bioreactor or by culture of cells in a suspended droplet of medium: a 'hanging drop' (Genever et al., 2010; Higgins et al., 2010). Spheroid structures were originally observed in culture of tumour cells where they formed spontaneously when cells were cultured on non-adherent dishes (Wibe et al., 1984). The hanging drop method of creating spheres however, is a recent development (Higgins et al., 2010; Foty, 2011). In the Jahoda lab, spheroid culture has previously

been developed for the study of hair follicle dermal papilla cells (Higgins et al., 2010). Spheroid culture has also been utilised for study of mesenchymal stem cells (MSCs) to gain better knowledge of their differentiation potential and expression profile in an *in vivo*-like microenvironment (Genever et al., 2010). In addition, the much greater similarities between spheroid cell culture and *in vivo* tumours means that spheres are now being utilised for *in vitro* drug trials (Vorsmann et al., 2013).

Previous work has shown that in developing mouse skin, multilocular fat droplets are observed in the lower dermis, around the base of developing guard hairs, from E18.5 onwards (Figure 3.2b). Lipogenesis continues in postnatal mouse back skin, with the dermal adipose tissue layer expanding dramatically from postnatal day 1 to 4/5 days (Figure 3.2 c-d), during which time the adipocytes become fully developed containing one large fat globule (K. Wojciechowicz et al., 2013). Adipogenic markers can be observed even earlier than the first fat droplets: FABP4 is seen specifically in the lower dermis from E16.5 (Figure 3.2f). C/EBPα marks nuclei of committed adipogenic nuclei from E18.5 (Figure 3.2h) (K. Wojciechowicz et al., 2008; 2013).

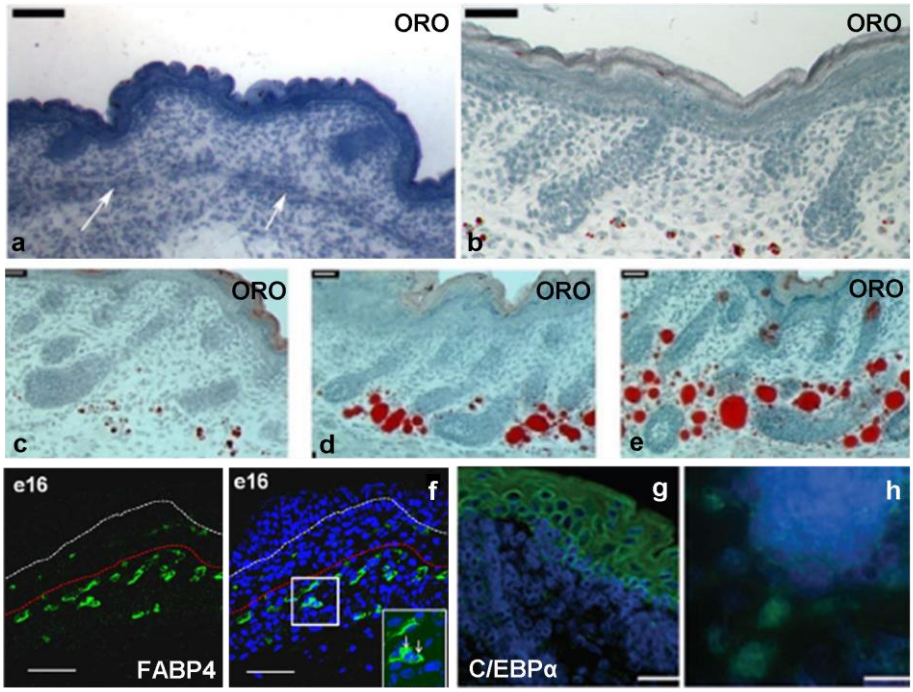

Figure 3.2: Sections of developing mouse back skin stained with ORO, FABP4, and C/EBPα. At E16 there are no fat droplets visible by ORO staining (a) but FABP4 expression is seen around cells in the lower dermis (f). C/EBPα (g, h) and ORO staining are seen in

E18.5-19 (b) back skin. Fat continues to accumulate as development continues at 0.5 dN (c), 1 dN (d), and 2 dN (e). Scale bars: a = 100 μm; b, f = 50 μm; c-e, g = 30 μm; h = 15 μm

The first aim of this chapter was to establish a reliable model system with which to investigate the molecular controls of adipogenesis in the developing skin dermis. An organ culture technique has previously been used in the Jahoda lab with E14 skin for the exploration of the roles of Epidermal Growth Factor (EGF) and Keratinocyte Growth Factor (KGF; also known as FGF7) in hair follicle development (Richardson et al., 2009). It was also used for the start of an investigation of the EGF pathway in adipogenesis with E16.5 skin (K. Wojciechowicz, 2011). This study showed that culture of E16.5 back skin for 3 days allowed adipogenesis to be examined through ORO of lipid droplets. Alternatively, before the appearance of fat droplets, skin could be analysed with staining for early markers such as C/EBPα or FABP4.

The initial part of in this chapter describes efforts to repeat and refine the E16 organ culture work of Wojciechowicz in order to study the influence of different molecular entities on adipogenesis. After a period of experimental work there was a realisation that a) the model was not working consistently and b) that we had been looking at relatively late processes in adipogenesis. A new aim of this study then became to try to investigate the timing of adipogenesis *in vivo*. We then took advantage of lab knowledge of manipulation of younger mouse skin to a) establish a new 3D culture model, and b) use this model to study cells from younger skin in an attempt to discover the point at which adipogenic commitment started. Having established that this was much earlier, the prospect of using the whole skin model at an earlier age (E14) was revived.

3.2 Results

3.2.1 Whole skin substrate organ culture

The aim of this chapter was to establish a reliable *ex vivo* culture system for the study of adipogenesis in the lower dermis of mouse skin, and in particular for studying the cellular and molecular basis of adipose tissue development. The first of these is a whole skin organ culture method. Whole skin pieces, carefully separated from the underlying subcutaneous fat and muscle, were cultured on type I coated collagen disks floating on medium (see section 2.3). Although this technique has the potential to be an effective *in vivo*-like model, the results with embryonic skin showed a large amount of variation making observations less reliable.

3.2.1.1 Organ culture of E16.5 mouse dorsal lateral back skin

Initially skin from E16.5 mouse dorsal lateral back skin was cultured for three days using MEM and 1% FBS serum. In total this organ culture regime was repeated four times (Table 3.1) and all repeats resulted in some healthy and other pathological pieces of skin, with the majority having both elements. Skin pieces which had remained healthy whilst in culture were relatively flat on the collagen filter and the skin remained tightly compacted (Figure 3.3a). The healthy and unhealthy areas of those skin pieces which had both could be distinguished from the outside before freezing. Healthy areas were more translucent under both bright and dark field microscopy than unhealthy areas. The unhealthy areas appeared darker or yellowed by bright or dark field microscopy, respectively. Developing hair follicles were more visible on the surface of healthy areas (Figure 3.3a, arrow).

Hematoxylin & Eosin (H&E) staining of healthy skin specimens showed regular hair follicles, tightly packed dermis and epidermis with layers of cornified epidermis above (Figure 3.3b and d). There was some oil red O (ORO) staining in these pieces of skin indicating fat development was more advanced than before the organ culture. In general, the fat cells were grouped together in one area of the dermis and only contained small lipid droplets (Figure 3.3c).

As well as skin specimens that had healthy and unhealthy areas some pieces had become entirely pathological as a result of culturing. These pieces, did not have any visible hair follicles, and lifted off the filter so that under dark field microscopy they had a dull, yellow/brown appearance (Figure 3.3e). H&E staining revealed separation between the epidermis and dermis or within the dermis (Figure 3.3f and h). In addition, these unhealthy specimens frequently tore during sectioning indicating weaknesses in the structure. The cornified layers of the epidermis frequently detached from the proliferating epidermis at a number of points along the length of the skin (Figure 3.3i). Hair follicles that had developed to a large extent before the skin was put into culture were still visible, but where the skin had split, they had shrivelled and shrunk or had completely disappeared. Pathological pieces of skin normally had fat droplets along their length, seen by ORO staining.

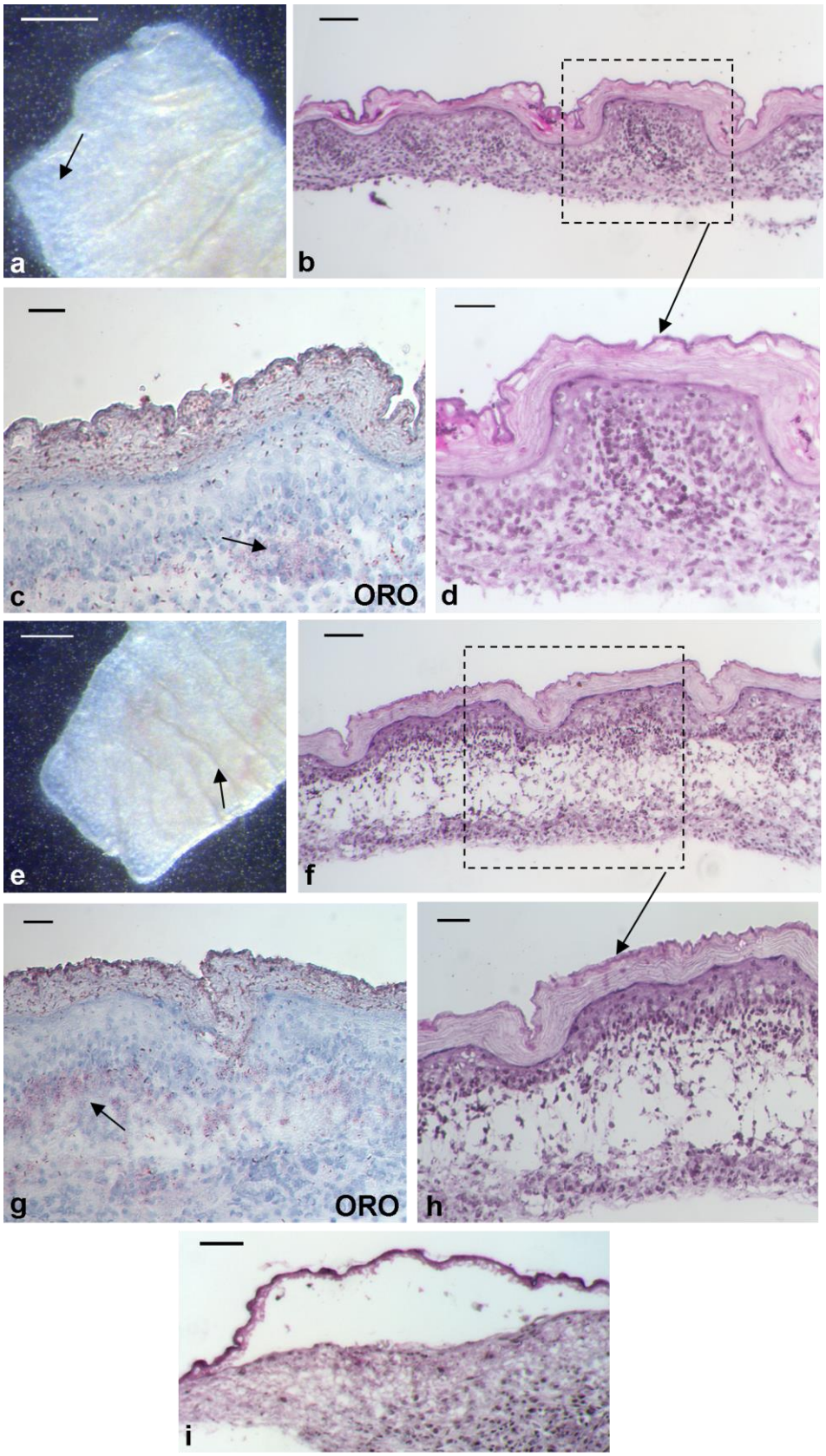

Figure 3.3: Whole skin organ culture of E16.5 mouse back skin is unreliable resulting in healthy and pathological skin after 3 days. Healthy areas of skin (a, arrow) have a white colour and clearly visible hair follicles. H&E staining of healthily cultured skin (b and d) shows a compact structure and hair follicles descending from the epidermis through the dermis. Lipid droplets, observed by ORO staining, are small and closely grouped together (c).

Pathological areas of skin (e, arrow) are a more yellow colour without visible hair follicles. H&E staining shows holes in the skin either within the dermis (f and h) or between the dermis and epidermis (i). Fat droplets seen close to splits in the skin are likely to be a stress response (g). Scale bars: a,e = 250μm; b,f = 65μm; c,d,g,h,i = 30μm

The initial culture system used Minimum Essential Media and 1% FBS. A number of changes to the media were tried in order to refine and increase the reliability of the model (Table 3.1 below). Adjustments included using MEM with either no serum, or 2% FBS (Figure 3.4), or using Williams' media (Figure 3.5). Williams' medium is more nutrient rich than MEM containing a wider range of inorganic salts, amino acids, vitamins, and other components.

Although some improvements were seen, the variability between different pieces of skin cultured under identical conditions remained too great for the model to be used experimentally. Skin cultured with Williams' media was, in general, more consistently healthy than that in MEM particularly when the media was not supplemented with serum, although there was still variability. This is highlighted in Figure 3.5 which shows example H&E staining of healthy and pathological specimens of skin for each William's media serum concentration.

Medium	**Serum percentage**	**Times repeated**
MEM	0%	2
	1%	4
	2%	2
William's	0%	1
	1%	1
	2%	1

Table 3.1: Summary of E16.5 organ culture repeats. Variables of media type (MEM or William's media) and Fetal Bovine Serum percentage (0%, 1%, or 2%) were explored as a way of introducing greater reliability into the results from the organ culture model.

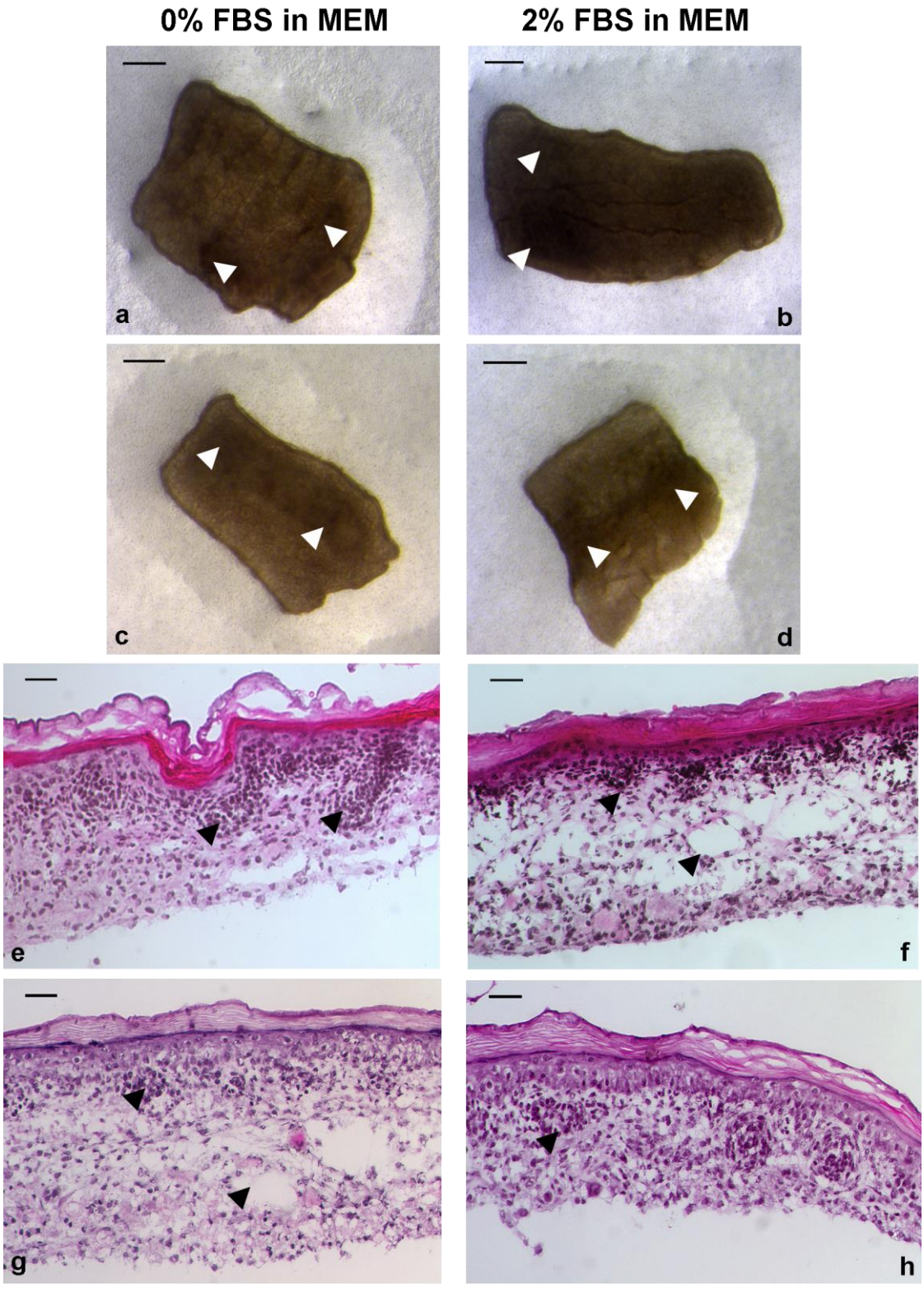

Figure 3.4: Variations in culture conditions for E16.5 organ culture did not result in greater reliability. Skin was cultured in MEM with 0% FBS (a, c, e, g) or containing 2% FBS (b, d, f, h). Macroscopic inspection did not necessarily reveal overall healthiness of the skin as pieces looked similar. Dark patches indicate areas which have become pathological (a-d). MEM without FBS generally resulted in healthier skin (e) however this was not always the case (g). MEM with 2% FBS resulted in unhealthy skin as shown by H&E staining where the hair follicles have shrunk (f) or are almost not visible (h). Scale bars: a-d = 250μm; e-h = 30μm

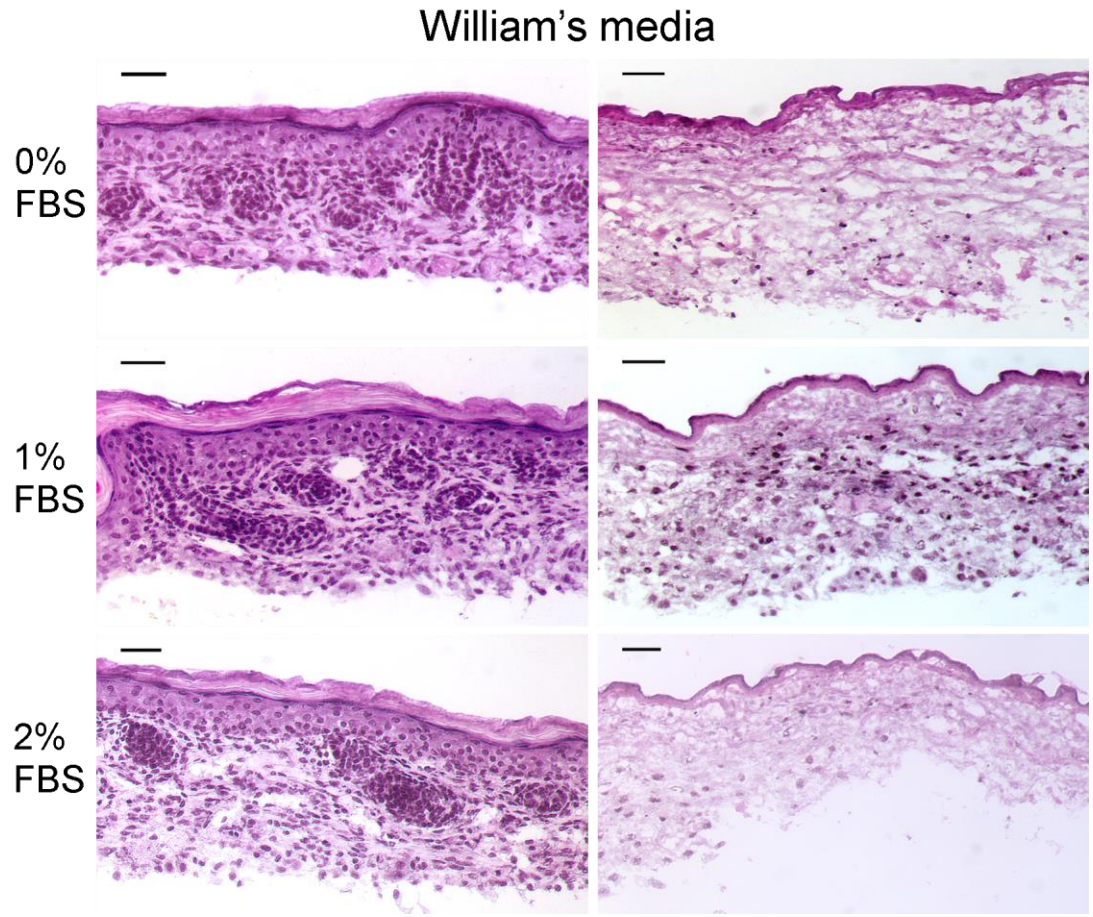

Figure 3.5: Culture of E16.5 mouse back skin with William's media gave variable results. Skin pieces cultured in William's media were often more healthy (left-hand column) than those cultured with MEM (Figures 3.3 and 3.4). However, the culture system was still unreliable as some specimens of skin became pathological with a loose structure and no hair follicles (right-hand column). Scale bars = 30μm

3.2.2 Three-dimensional (3D) dermal cell culture

The inconsistency seen in the organ culture model described above at E16.5 and older did not allow it to be used for its original purpose: the investigation of miRNAs in adipogenesis. Focus therefore shifted to establishing a second model system. This model was a 3D cell culture in which dermal cells, or a mix of cells from the whole skin, were grown as spheres in hanging drops of medium. A similar hanging drop technique was used by Han et al., 2011 for the study of murine epididymal adipose tissue development, although hanging drops were only maintained for three days before cells were transferred to 2D adherent culture. A 3D cell culture technique has advantages over traditional 2D adherent culture in allowing more cell-cell contact, and therefore more physiological conditions. It also allows cells to maintain a more natural morphology as they are not forced to flatten onto a surface.

Throughout the establishment of the culture systems, a secondary question concerned the timing of adipogenesis. This question was initially regarded as being important in deciding on the most appropriate ages to modulate the adipogenesis program through the addition and inhibition of miRNAs. A series of interesting and unexpected results however changed this to the primary project. As such, the following results are described with the question of when pre-adipocyte commitment occurs as the underlying subject of investigation.

3.2.2.1 Culture of dermal cells from embryonic days 17 and 18 (E17/18)

Previous work in the Jahoda lab showed that the earliest time-point fat droplets can be seen in lower dermal adipocytes is at embryonic day 18 (E18). Therefore it was decided to test the viability of the cell culture system initially from using cells from mouse embryos at 17 (E17.5) and 18 (E18.5) days gestation.

Both two and three-dimensional culture were set up to compare the development of adipocytes in each. At first dermal cells were plated into 6-well plates at a density of 6,000 cells per well and spheres were created at a

density of 6000 cells per drop or concentrated from the single cell suspension (approximately 50,000 cells per drop). To allow a direct comparison between the number of adipocytes seen in 2D and 3D cultures, spheres were transferred into 2D culture (one sphere per well) one day before both types were fixed to allow them to adhere and grow out into a single cell layer. Although this protocol did successfully allow development and analysis of fat cells, a number of changes were made for optimisation of the procedure.

Firstly, the density of cells used for 2D culture was changed. The low densities used originally, meant that during the time span of the experiment the cells were still widely dispersed throughout the culture dish preventing any cell-cell interactions. After several different densities were tried, it was decided to plate cells at the slightly higher density of 24,000 cells per well. This density gave cells enough space to spread and engage in cell-cell interactions without the requirement to split the cells during the experimental time span.

The other change made to the protocol was the transfer of spheres from 3D to 2D. Incubation of the spheres for 24 hours after transfer to 2D culture did not prove long enough for cells to grow out and adhere to the culture dish resulting in the majority being washed off and lost in subsequent analysis. This was changed so that transfer of the spheres was two days before fixation giving them 48 hours to adhere. Even with this change, very careful washing and staining was required to ensure the spheres remained stuck onto the culture dish.

The changes were successfully applied to the E18.5 cell culture. Analysis of the cultures by visual inspection and oil red O staining revealed fat development at both ages and in both types of culture. For all cultures, spherical 3D culture resulted in a much greater number of lipid-filled adipocytes than 2D culture alone. The smaller numbers of adipocytes amongst the 2D cultured cells were not well developed and in general only contained small lipid droplets. By contrast, when spheres were grown out into

2D, a large number of adipocytes were visible, although also not fully differentiated (Figures 3.6 A, B and 3.7a-d).

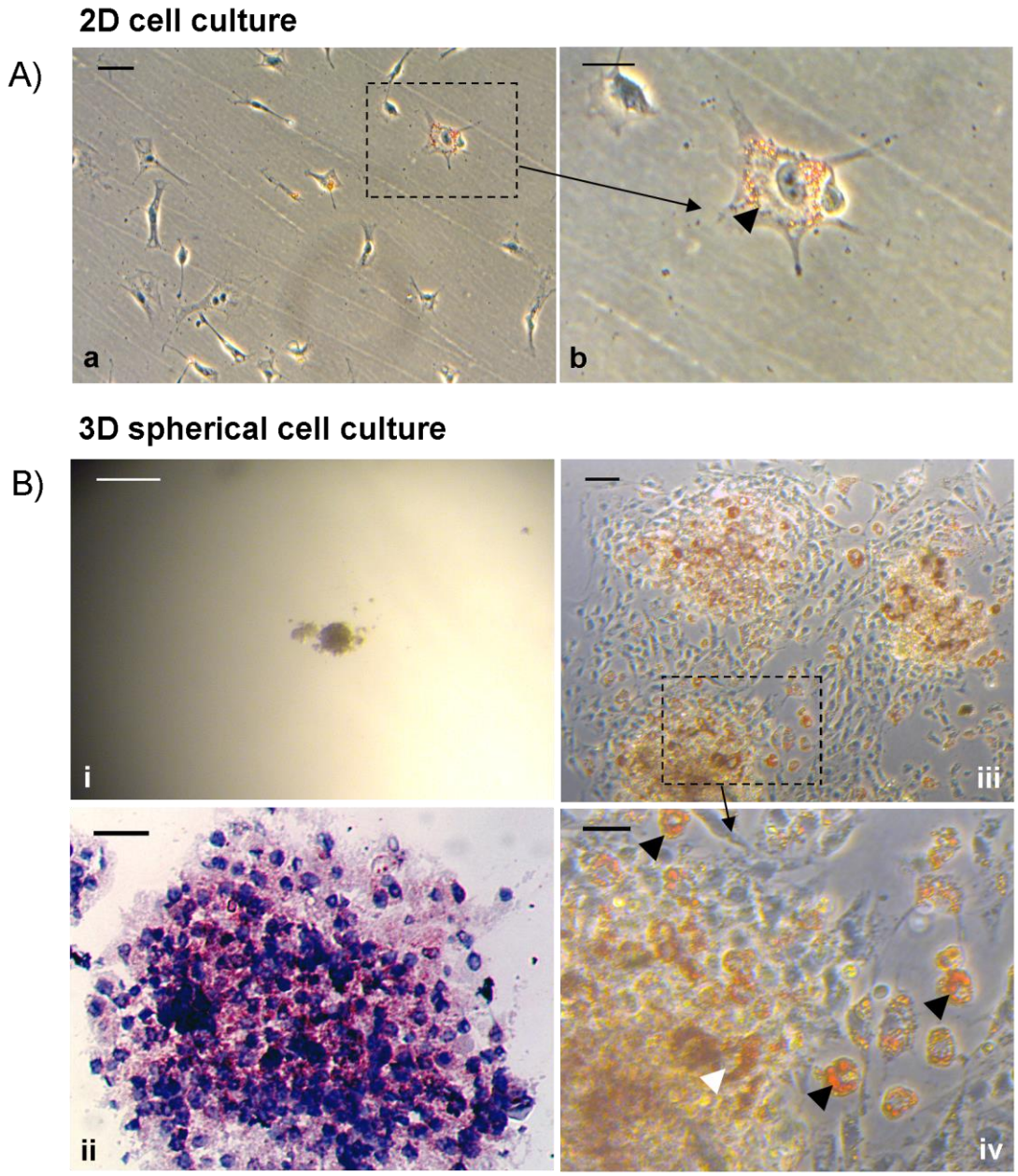

Figure 3.6: Lipid accumulation in 2D and 3D cell culture of E18.5 dermal cells. A) 2D cells seeded at a density of 6000 cells per well were cultured for 4 days before ORO staining (a). Differentiated cells accumulated small lipid droplets (b, arrowhead). B) (i) Example of a sphere suspended in medium. Spheres were either frozen down after 4 days and sectioned for staining (ii) or transferred to 2D after 2 days and allowed to grow out for 2 days (iii). Differentiated cells can be observed mainly in the centre of the sphere (ii). A much larger proportion of cells differentiate into adipocytes in the 3D model compared to 2D, and are also better developed with larger fat droplets (iv, black arrowheads). Cells containing fat droplets can also be observed within the sphere which have not grown out onto 2D in the time allowed (iv, white arrowhead). Scale bars: A) i= 60μm, ii= 30μm; B) i= 100μm, ii= 15μm, iii= 60μm, iv= 30μm

As well as being transferred into 2D culture, spheres were also snap-frozen in blocks for sectioning. Sections were used for ORO analysis; E17.5 sections were also stained for C/EBPα expression. ORO analysis of sphere sections from both E18 and E17 cultures showed that most of the adipocytes gather together in the centre of the sphere (Figures 3.6 B,ii and 3.5e). Although a large number of cells had differentiated and accumulated fat after 4 or 5 days of culture, the small droplets of lipid showed that differentiation was not complete. There was C/EBPα expression in E17.5 spheres after 5 days of culture but it was not nuclear (Figure 3.7g, h).

Dense groups of nuclei were observed in the spheres and it was hypothesised that these were due to epidermal contamination causing the two cell types to segregate into distinct areas. Cytokeratin staining confirmed the presence of epidermal cells in a large number of spheres (Figure 3.7f). Work undertaken to explore the effect of this contamination and remove the epidermal cells is described below.

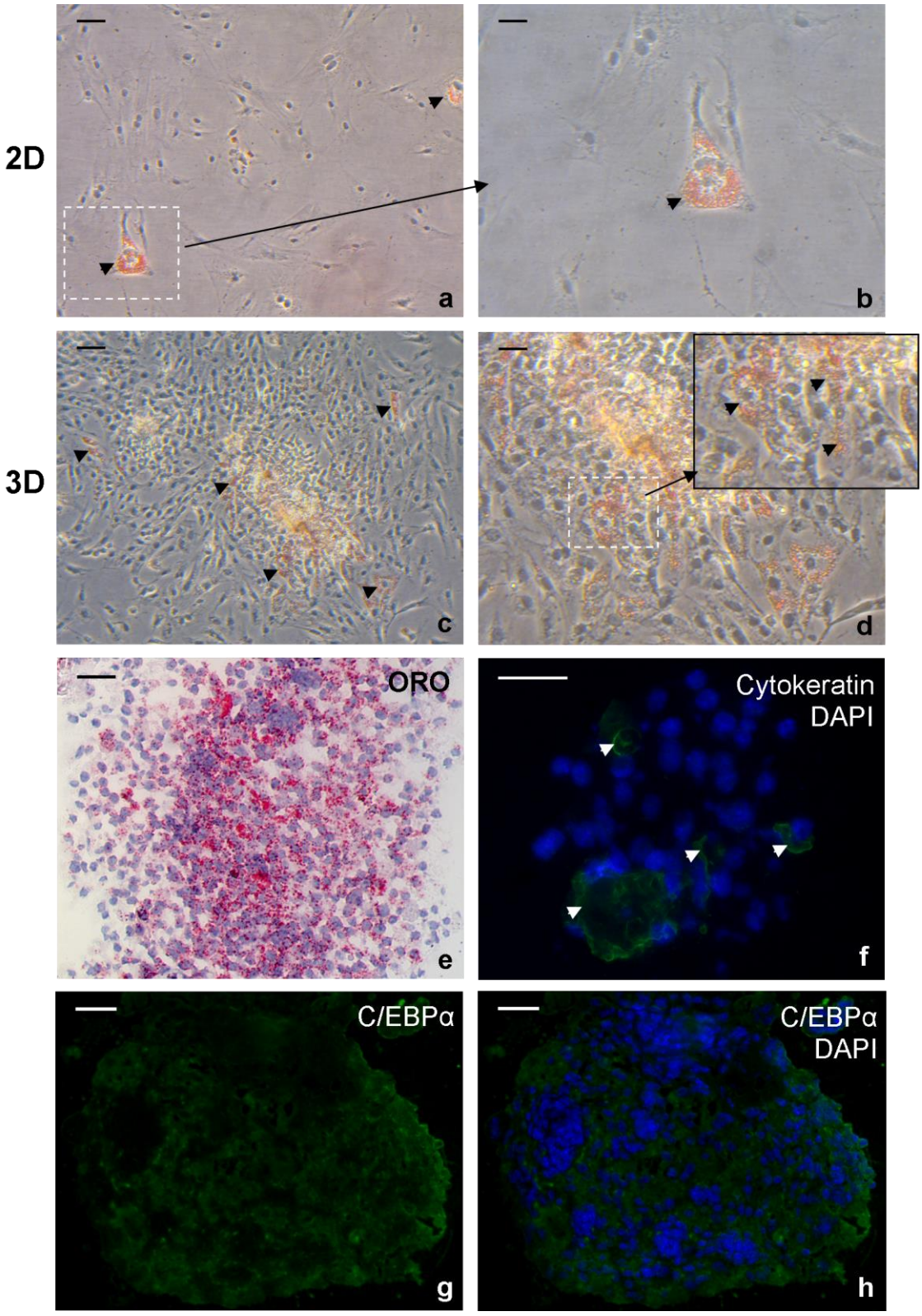

Figure 3.7: Lipid accumulation in 2D and 3D cell culture of E17.5 dermal cells. 2D (a,b) and 3D cell culture transferred to 2D (c,d) were ORO stained after 5 days. More staining was visible in 3D spheres (c,d) although the lipid droplets were small in both culture types. Some spheres were frozen after 5 days and sectioned (e) showing the majority of differentiated cells towards the centre of the sphere. Cytokeratin staining (f) revealed some epidermal contamination within the spheres. E17.5 dermal cell spheres did not have specific nuclear staining of C/EBPα after 5 days culture (g,h). Scale bars: a,c= 60μm; b,d= 30μm; e-h= 15μm

3.2.2.2 Three-dimensional culture of dermal cells from younger embryonic mouse skin

As dermal cells from E17 and E18 day embryos showed the capability to develop into adipocytes, it was decided to repeat the experiment with skin from younger embryos. Similar to dermal cells from older skin, E15.5 and E16.5 dermal cells showed the ability to follow the adipogenesis pathway and accumulate lipid droplets. They were cultured for a total of 6 or 7 days, respectively, so that they were analysed at the same "developmental time point" as E18.5 spheres, cultured for 4 days, and E17.5 spheres, analysed after 5 days (Figure 3.8).

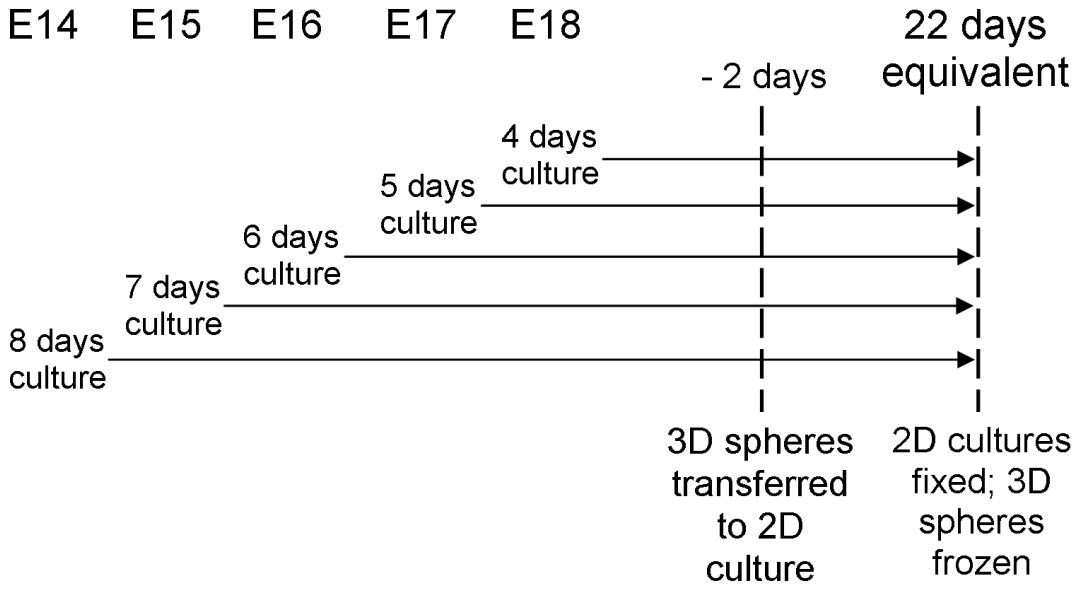

Figure 3.8: Dermal cell culture plan. Dermal cells isolated from mice of embryonic days 14-18 were cultured for a total of between 4 and 8 days to reach the developmental age equivalent of 22 days.

In E16.5 cell culture, ORO staining of cells initially maintained in 3D spheres then grown out in 2D showed approximately 25% (Figure 3.14) of the cells contained lipid droplets (Figure 3.9 d-f). Interestingly, although most of the droplets were small, some had started to join together to create the large, single lipid droplet that fills fully differentiated white adipocytes (Figure 3.9 e). The number of cells containing fat droplets was not uniform throughout the sphere. Sections through the sphere varied in the amount of staining visible from almost none to every cell containing fat droplets (Figure

3.11 c and d). The widest sections contained the most fat cells suggesting they were segregating from undifferentiated cells and gathering in the centre of the sphere (Figure 3.11 d).

2D cell culture of E16.5 dermal cells also resulted in development of adipocytes (Figure 3.9 a-c) although only approximately 4-5% of the cells contained any fat droplets (Figure 3.14). These cells varied from being early in differentiation, containing small granular fat droplets, to almost fully differentiated, with much larger fat globules (Figure 3.9 c).

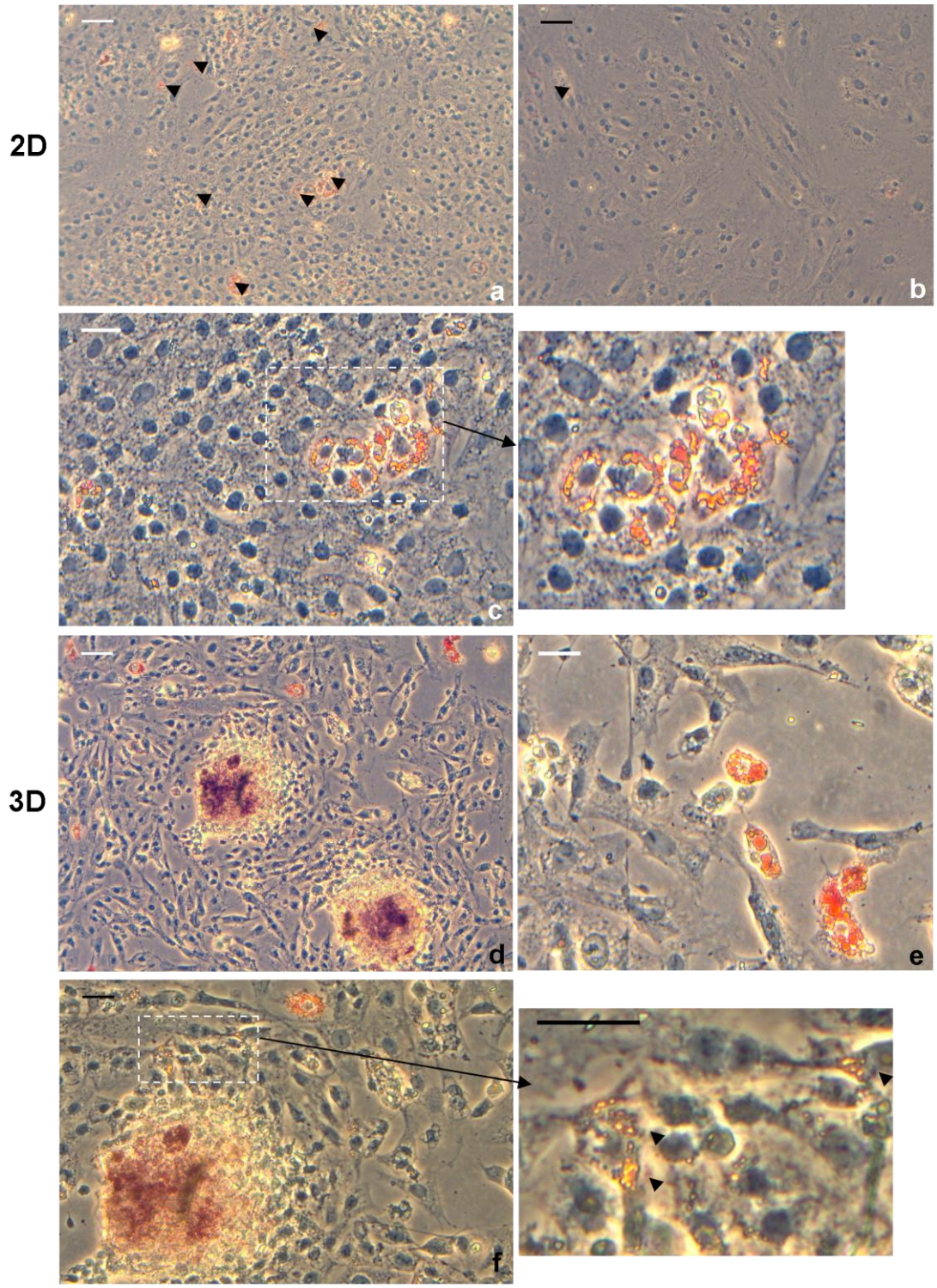

Figure 3.9: Lipid accumulation in E16.5 2D and 3D cell culture. E16.5 dermal cells were seeded at a density of 24,000 cells/well and cultured for 6 days before ORO staining (a-c). Stained cells are marked by black arrowheads. Small lipid droplets started to join together into larger globules (c). 6000 cell spheres were transferred to 2D after 4 days after cultured for a further 2 days before ORO staining (d-f). Cells are differentiated to different degrees with some containing large fat droplets (e) and others having many small droplets (f). Scale bars: a,b,d = 60μm; c,e,f = 30μm

Some intact E16.5 spheres were frozen for analysis after two days. This gave a developmental age equivalent to E18.5, which is the earliest point at which lipid droplets have been observed in the lower dermis *in vivo.* Expression of C/EBPα, one of the main transcription factors involved in adipogenesis showed nuclear staining in a number of cells, identifying preadipocytes undergoing the differentiation process (Figure 3.10 A). Only a very small amount of ORO staining, however, was visible in some sphere sections at this time (Figure 3.10 B).

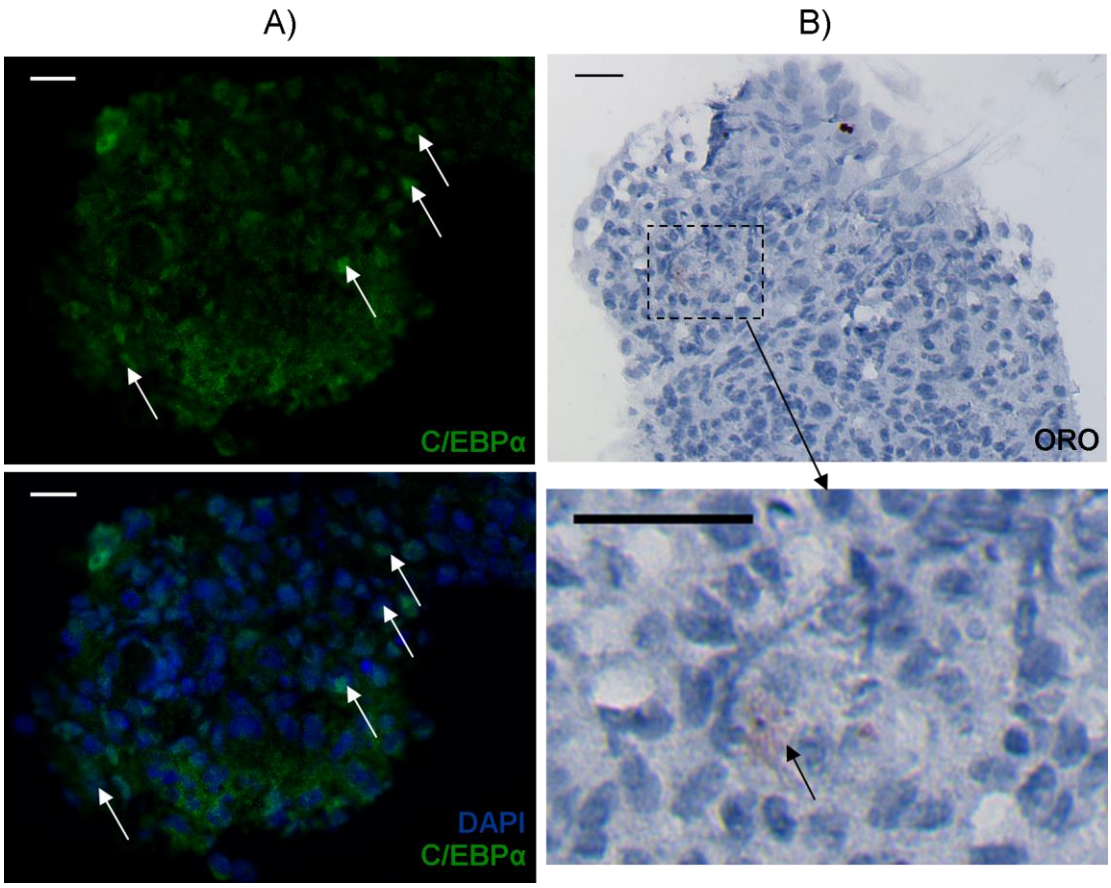

Figure 3.10: Analysis of E16.5 dermal cell 3D spheres after 2 days of culture. A) C/EBPα (green) expression is predominantly within nuclei. There is only minimal lipid accumulation at this stage (B). Scale bars = 15μm

C/EBPα staining of spheres frozen after 6 days of culture showed non-nuclear expression of the transcription factor, suggesting that the protein had left the nucleus once differentiation was complete (Figure 3.11 c). When intact E16.5 spheres were stained after 6 days in culture, many of the cells contained fat as shown by Oil Red O staining. However the distribution of

cells with visible staining was not uniform. In some sections nearly all the cells were stained, in other sections virtually none were (Figure 3.11 a and b). The widest sections contained the most fat-filled cells suggesting they were segregating from undifferentiated cells and gathering in the centre of the sphere (Figure 3.11 a). This was also supported by sections from the edge of spheres which did not contain any ORO staining (Figure 3.11 b).

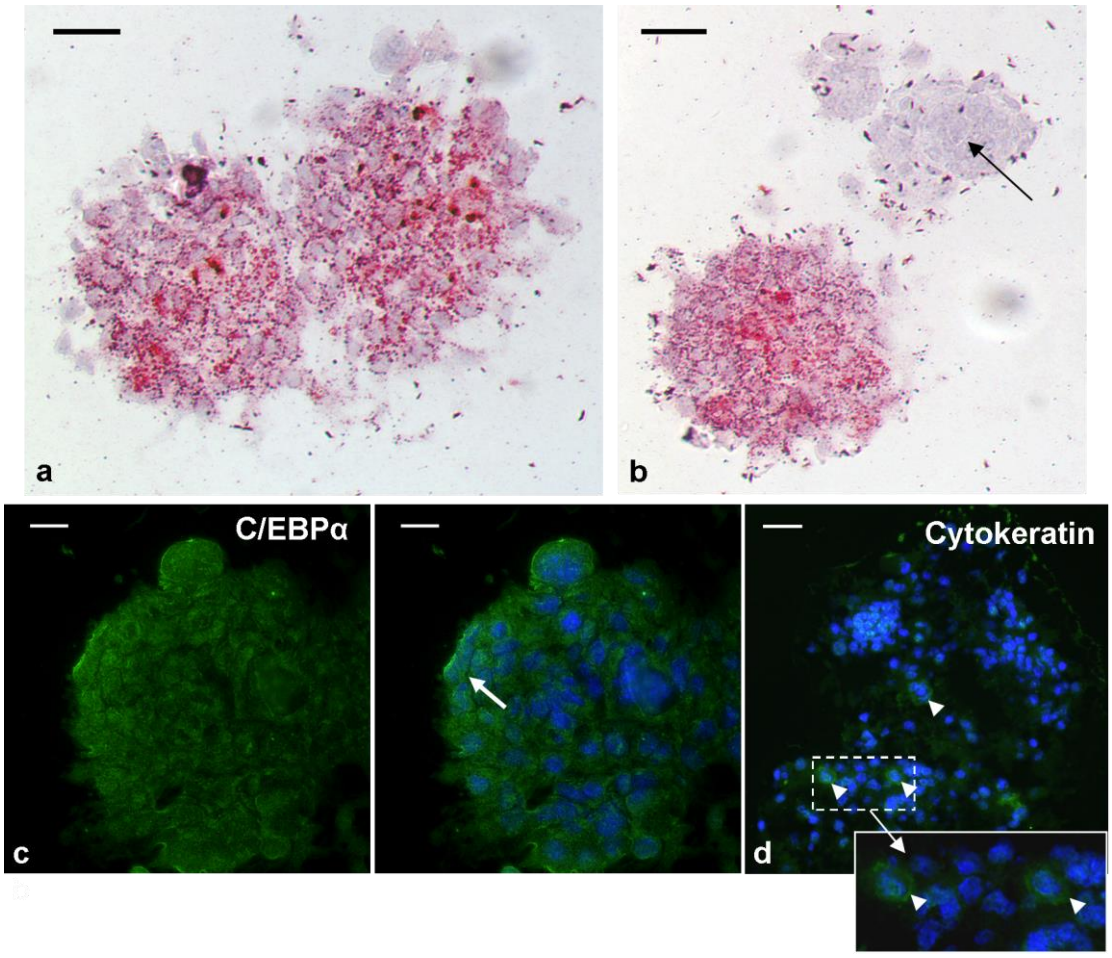

Figure 3.11: Analysis of E16.5 3D sphere sections after 6 days of culture. ORO staining showed extensive fat accumulation (a) in mainly in small droplets although not in all sections, especially at the edge of the sphere (b, arrow). There was some expression of the transcription factor C/EBPα (green) after 6 days of culture but the labelling was diffuse and not contained in nuclei (c, arrow). E16.5 dermal cell spheres contained a small amount epidermal contamination shown by cytokeratin expression (d). Scale bars: a,b = 30μm; c,d = 15 μm

E15.5 dermal cells cultured in 2D and 3D for 3 and 7 days (repeated twice) showed similar results to cells from E16.5 dermis. In spheres, positive C/EBPα expression was predominantly nuclear after 3 days of culture but by

7 days there was less positive staining and it was no longer nuclear (Figure 3.12 a, c). The amount of ORO staining increased from only a small amount in the centre of the sphere after 3 days to widespread numbers of fat cells after 7 days (Figure 3.12 b, d). Similar to cultures of other ages, a greater number of lipid containing fat cells formed after cells were cultured in 3D and then put into 2D compared with cells cultured for the same length of time continuously in 2D (Figure 3.12 e-g).

Age	2D cell density	Repeats	3D cell density	Repeats	Outcome
E18.5	6000 cells	1	3000 cells	1	2D cells sporadically placed; large number of spheres washed off
E18.5	24 000 cells	1	6000 cells	2	Majority of cells and spheres remained during staining
E17.5	24 000 cells	1	6000 cells	1	Majority of cells and spheres remained during staining
E16.5	24 000 cells	3	6000 cells	3	Very variable staining between experiments with number of cells remaining on dish and level of uptake of ORO stain
E15.5	24 000 cells	2	6000 cells	2	Variable outgrowth from spheres and variable number of spheres remaining during staining

Table 3.2: Summary of cell cultures carried out during the establishment of the model system. The density of cells in a 6-well plate was increased from 6000 to 24,000 cells per well. Spheres were made from 6000 cells. Four spheres were transferred to each well of a 6-well plate for staining, or frozen down in blocks.

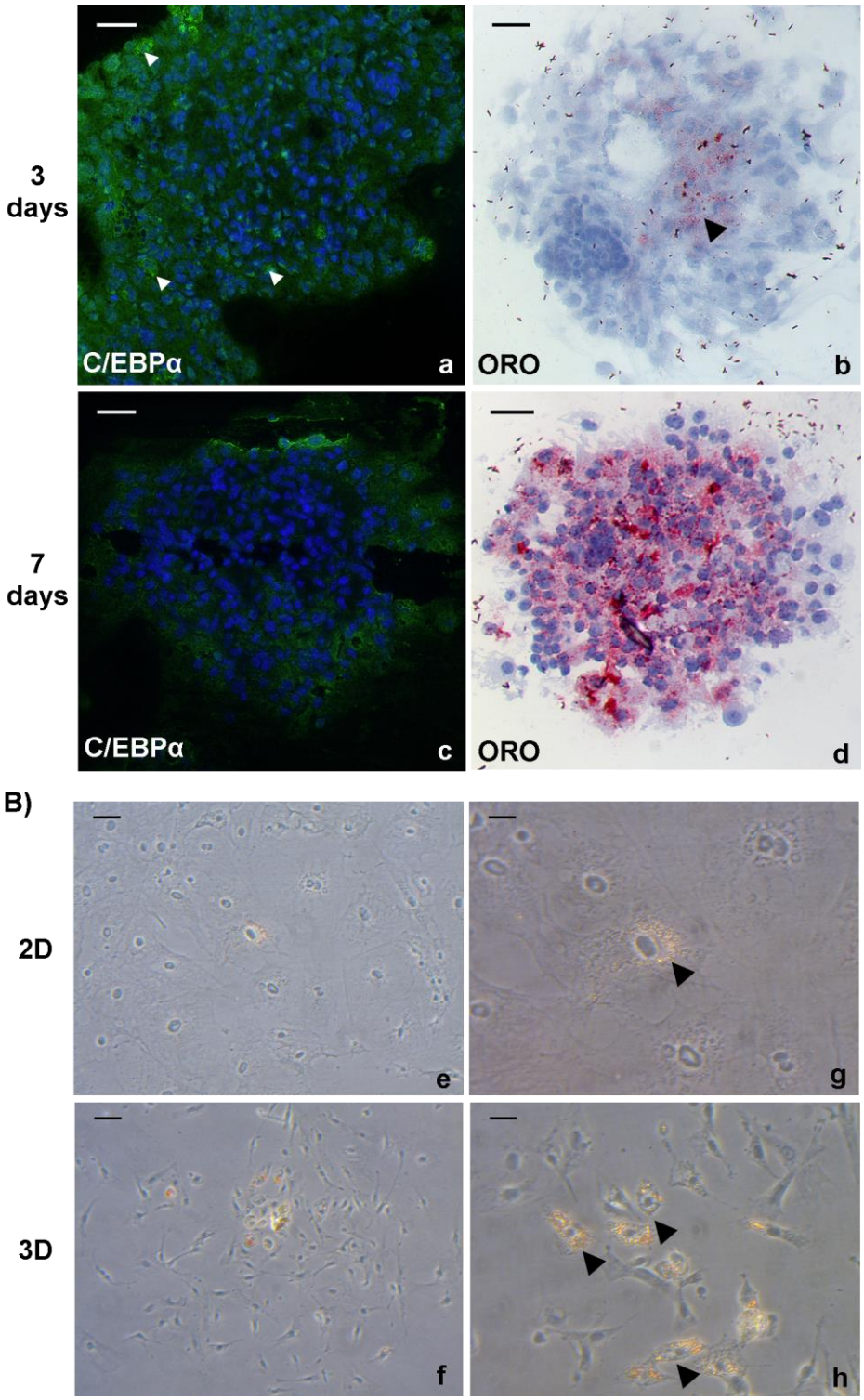

Figure 3.12: Analysis of C/EBPα expression and lipid accumulation in E15.5 2D and 3D cell cultures. A) After 3 days of spherical culture, E15.5 dermal cells had some nuclear specific expression of C/EBPα (a, arrowheads). This contrasted to expression after 7 days of culture where minority of cells had diffuse cytoplasmic C/EBPα staining (c). ORO staining showed a large increase in fat droplets with small lipid droplets in the centre of the sphere after 3 days (b, arrowhead) but widespread staining, and larger droplets, after 7 days (d). B) Comparison of 2D and 3D culture showed many more lipid filled cells after 3D culture (e-f). In 2D culture only a minority of cells started differentiating and contained small lipid droplets (g, arrowhead). 3D spherical culture grown out on 2D allowed more extensive differentiation (h, arrowheads.) Scale bars: a-d= 15μm; e,f= 60μm; g,h= 30μm

3.2.2.3 Epidermal contamination

Dense areas of cells in close association were again observed in E16.5 sphere sections, and shown to be epidermal contamination through immunofluorescent staining with cyto-keratin (3.11 d (arrowheads)). To determine the effect of these epidermal cells on preadipocyte differentiation, mixed spheres were created deliberately using cells from the dermal and epidermal layers of the skin. Fat droplets were observed in cells in the E15.5 and E16.5 mixed spheres grown out in 2D (Figure 3.13 b, e; arrows). The numbers of lipid containing cells were comparable for E15.5 dermal and mixed cell cultures. There were less in the E16.5 mixed cell culture due to some cells being washed off during the staining process (Figure 3.13e).

Density gradient centrifugation, using Ficoll, was explored as a means of removing epidermal contamination from the culture. The two Ficoll densities used were 1.05g/ml, for fibroblasts, and 1.06 g/ml, for epidermal cells (Ficoll PM400 Data File; Brysk et al., 1981; Reiners, Jn. and Slaga, 1983). The technique did not work effectively with these densities as epidermal contamination was not completely removed. Indeed it appeared that preadipocytes may have been removed. Slight adjustments to the Ficoll densities may have helped, however, as younger skin is easier to separate cleanly, it was decided not to pursue this method.

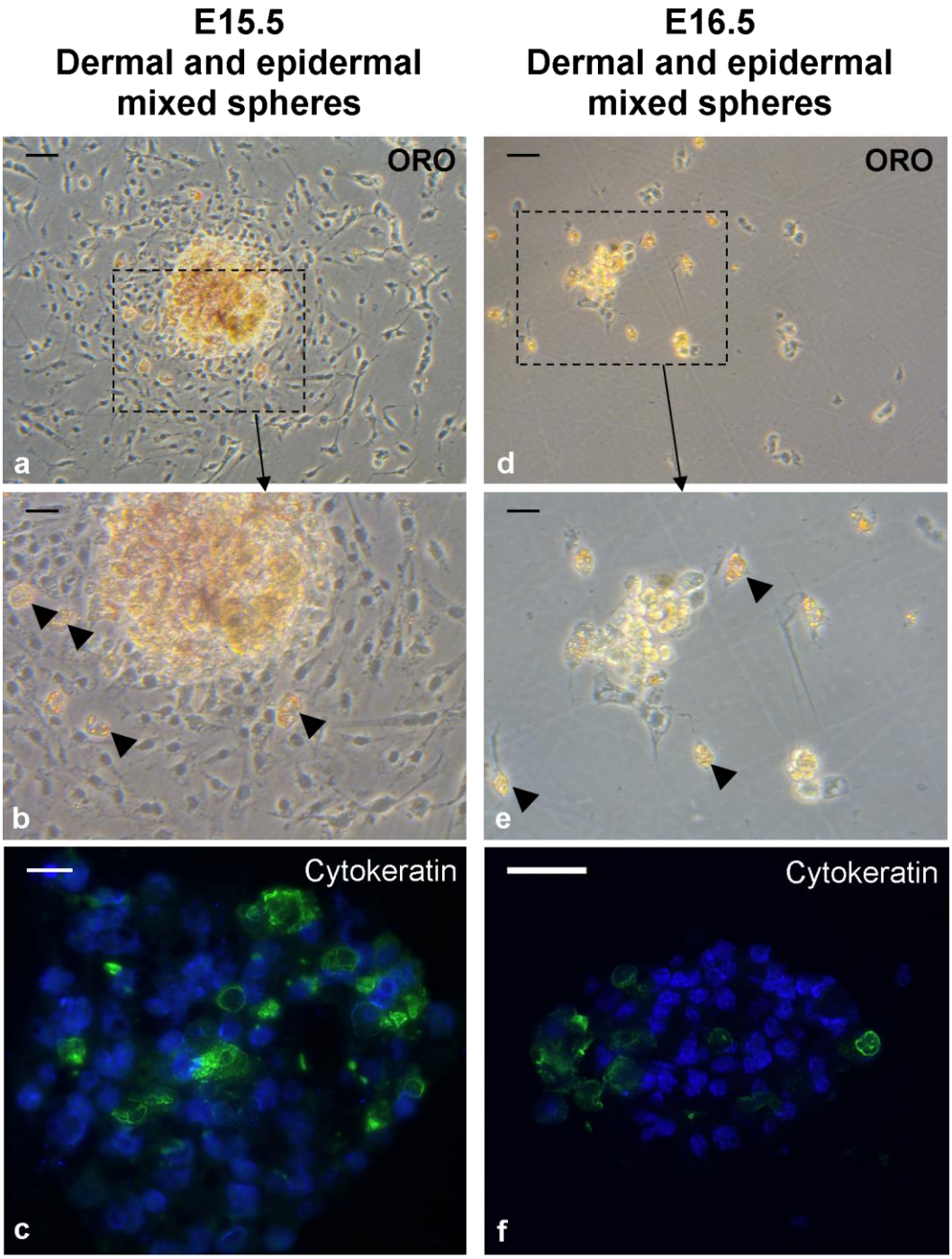

Figure 3.13: Analysis of dermal and epidermal cell mixed spheres from E15.5 and E16.5 embryonic mice. Spheres were made at a density of 6000 cells/sphere from a mixture of dermal and epidermal cells. Cytokeratin staining confirms the presence of epidermal cells (c,f). E15.5 spheres include differentiated lipid-containing cells which can be seen grown out on a 2D plate (b). Most E16.5 spheres were washed off during staining but some fat-containing cells can still be observed (e). Scale bars: i,ii= 60μm; iii,iv= 30μm; v,vi= 15μm

3.2.3 Quantification of Oil Red O staining

A method of quantifying the amount of oil red O staining has been described in a number of papers (Laughton, 1985; Gu et al., 2007; Tekkatte, 2012) and was attempted for the cell cultures described in this chapter. Oil red O was eluted out of stained fat cells using 100% isopropanol. The colour of the resulting solution was measured at 510 nm using a spectrophotometer. This was compared against a standard curve to gain a value for the concentration of Oil Red O.

Although this method has been described and published, a number of problems were encountered for specific use in this study. Accurate quantification relies on complete uptake of oil red O stain to all of the fat cells in the culture. This could not be guaranteed particularly for the spheres grown out onto 2D culture. Additionally, the spheres were only delicately attached to the culture dish meaning extensive washing was not possible during the staining process. This resulted in non-specific staining and clumped oil red O stain which could not then be removed prior to quantification.

A less precise method of quantification was employed to gain confirmation of the trends observed. Pictures of ORO staining of 2D cells and 3D spheres grown out onto 2D plates at 20x magnification were used. The number of nuclei per picture and number of cells containing fat droplets were counted. Where a cell was dividing, the nuclei were both counted if they had completely separated from one another. Although this method was subject to bias of the picture location, it did give a basic form of quantification resulting in the graph below (Figure 3.14).

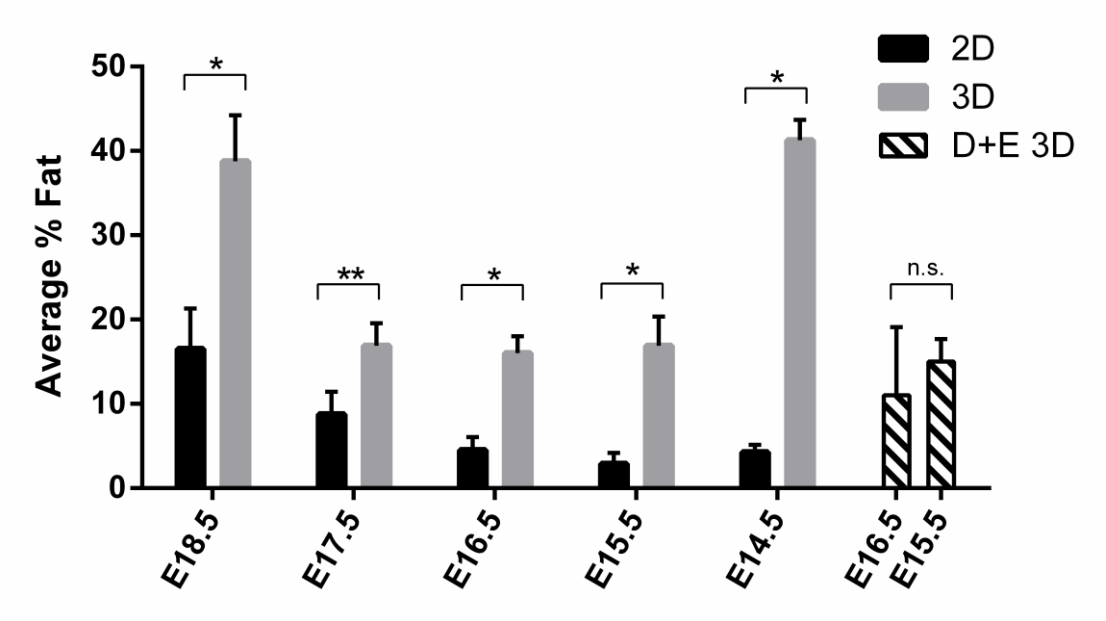

Figure 3.14: Average percentage of fat cells in dermal cell and mixed cell 3D spheres. The total number of cells and the number of cells containing Oil Red O staining were counted in cell culture pictures for each age and culture type. Data are mean ± s.e.m.; 3D & 2D n=8; D+E 3D n=4 (* P < 0.01, ** P < 0.05, n.s. not significant; Student's t-test).

3.2.4 The timing of adipogenesis in the dermal fat layer

As previously mentioned, the culture systems were originally established with a view to using them to investigate the role of miRNAs in adipogenesis through modulation of the adipogenesis process. However when E14.5 cell cultures were found to produce fat, the question shifted to focus on the secondary question of the timing of adipogenesis in the lower dermal fat layer and when the cells were becoming committed.

As discussed in the introduction, *in vivo* the first fat droplets are observed in the lower dermis at approximately embryonic day 18. It was previously hypothesised that the differentiation process may start around E16 and the organ culture system had been established with skin from E16.5 allowing fat droplets to be observed after 3 days of culture.

3.2.4.1 Cell culture of E14.5 dermal cells

3D cell culture of dermal cells from E14.5 mouse back skin (as described in section 2.2) was repeated three times and on each occasion a high proportion, almost 50% (Figure 3.14), of the cells contained fat droplets

after 8 days (Figure 3.15). A minority of the differentiated cells had much larger fat globules, or a single large lipid droplet, where the initial small droplets had joined together (Figure 3.15d arrows). These cells had also changed from a fibroblastic shape to the smaller, rounded shape characteristic of mature white adipocytes. There were also less well-developed cells containing only a few small lipid droplets which were still fibroblastic in shape (Figure 3.15d arrowheads). There were fewer cells without any fat droplets than equivalent cultures of older dermal cells, except E18.5 which contained a similar proportion of adipocytes. Oil Red O staining showed that the fat containing cells still had the tendency to group together in the middle of the sphere as was seen with other ages (Figures 3.15 and 3.16). Cells were also grown in 2D culture and it was found that, in contrast to the spheres, there were very few adipocytes after 8 days of culture (Figure 3.16).

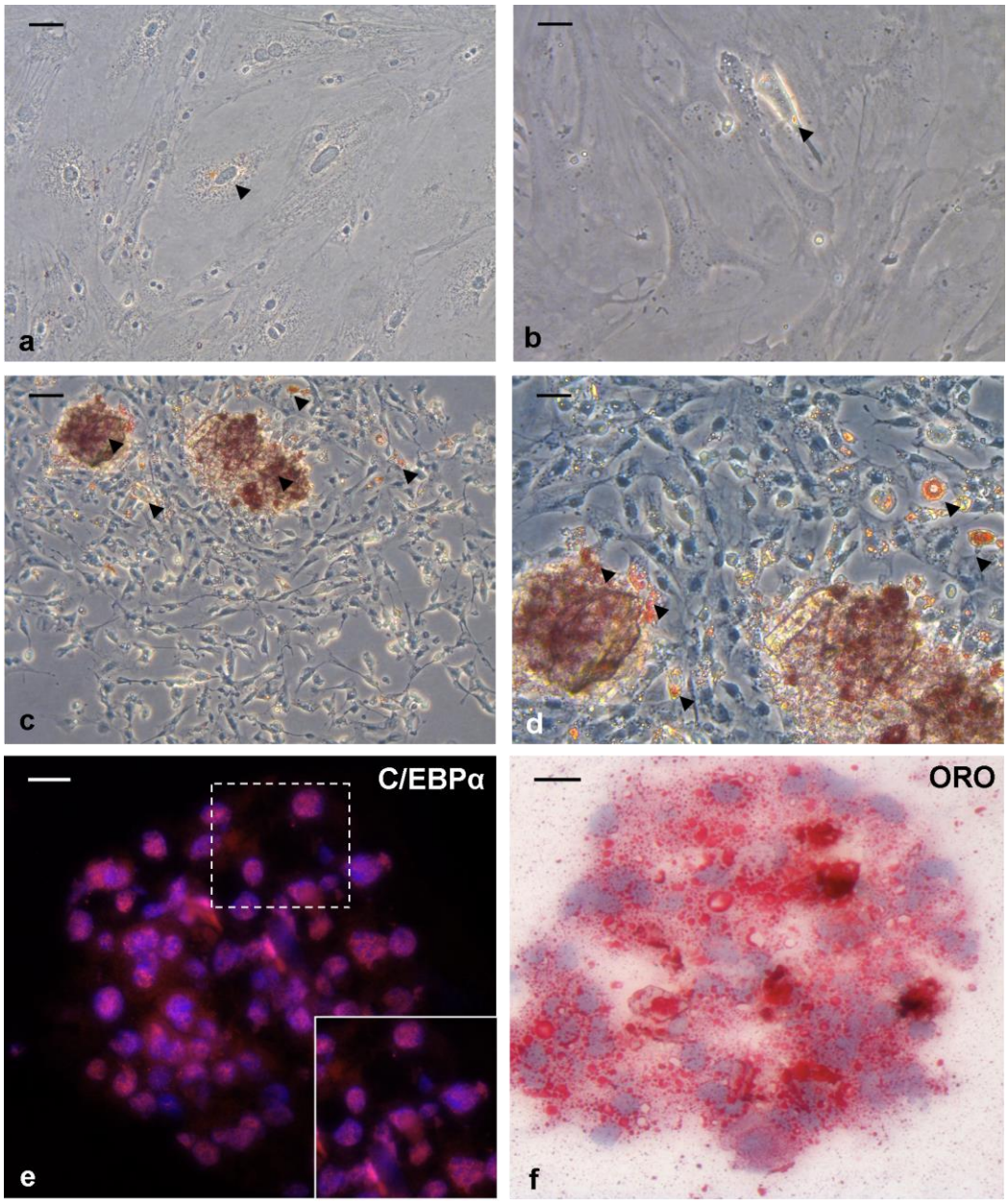

Figure 3.15: Analysis of E14.5 dermal cell 2D and 3D cultures after 8 days. 2D culture of E14.5 dermal cells resulted in very limited adipogenesis (a,b) in comparison to 3D (c,d). ORO staining showed only a minority of fibroblastic-shaped cells contained small lipid droplets in 2D culture (a,b arrows). 3D spheres grown out on 2D plates contained a high proportion of cells with lipid droplets (c,d) with many cells having the characteristic rounded shape of adipocytes (d). Sections through spheres showed almost entirely nuclear expression of C/EBPα (e) and widespread large lipid droplets (f). Scale bars: a,c= 60μm; b,d= 30μm; e,f= 15μm

Intact E14 dermal cell spheres were also analysed after 2, 3, 4 and 6 days of culture by ORO staining for lipid, and immunofluorescent staining for C/EBPα expression (Figures 3.16-3.18). After two days of culture, there was clear C/EBPα expression however it was not yet completely nuclear (Figure

3.16 a, b). By three and four days the staining showed that the protein was almost exclusively contained within the nucleus of cells undergoing the differentiation process (Figure 3.17 a, d). Interestingly, in contrast to spherical culture of E16.5 cells where C/EBPα left the nucleus as differentiation advanced, staining of E14.5 spheres cultured for 6 and 8 days still showed C/EBPα localised in nuclei (Figures 3.18 a and 3.15 e). These staining patterns were the same for each of the three repeats of the E14.5 cell culture.

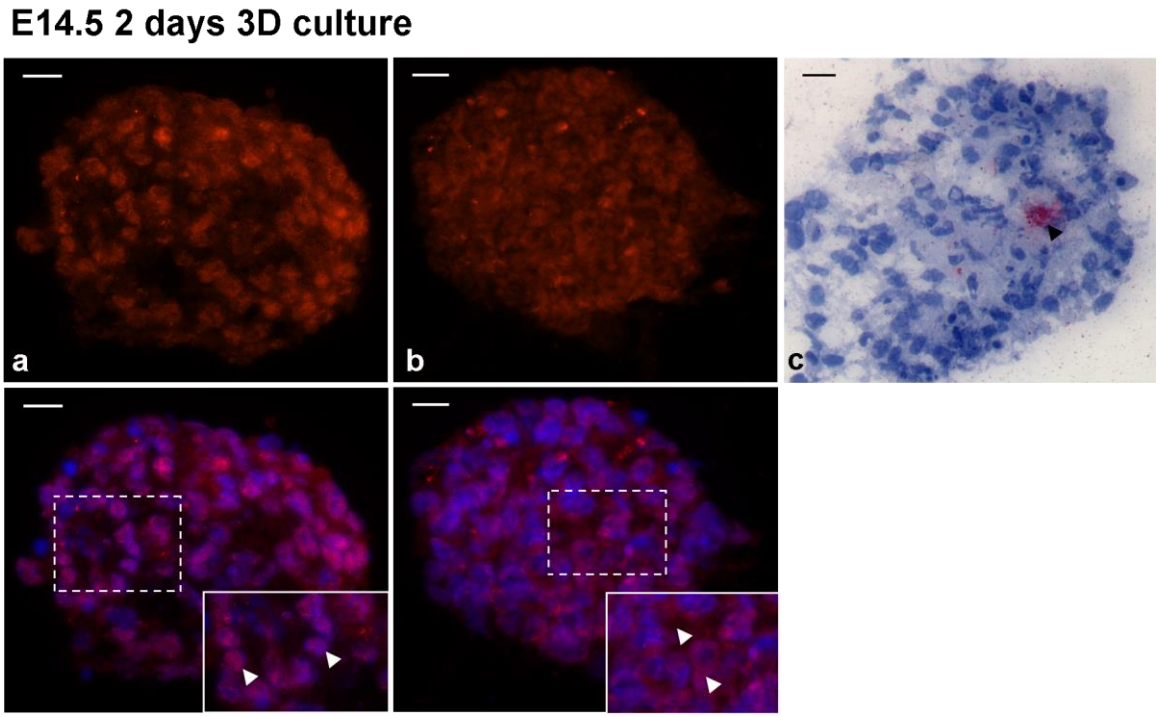

Figure 3.16: Analysis of E14.5 dermal cell spheres cultured for 2 days. C/EBPα expression (a,b) at this early culture stage was already beginning to become nuclear (a). Some sections still showed diffuse expression in the cytoplasm (b). After 2 days there were only a minority of cells contained small lipid droplets. The cells were located towards the centre of the sphere (c). Scale bars = 15μm

Spheres which were only cultured for two days before being frozen had very minimal ORO staining indicating that fat had not accumulated in the cells in this short time (Figure 3.16 c). By contrast, spheres which had developed for 3 days showed a large amount of heterogeneity in the amount of fat containing cells. Some of the sphere sections only had a small number of fat droplets in the centre of the sphere (Figure 3.17 b). In other sections the staining was widespread with nearly all of the cells containing fat droplets (Figure 3.17 c).

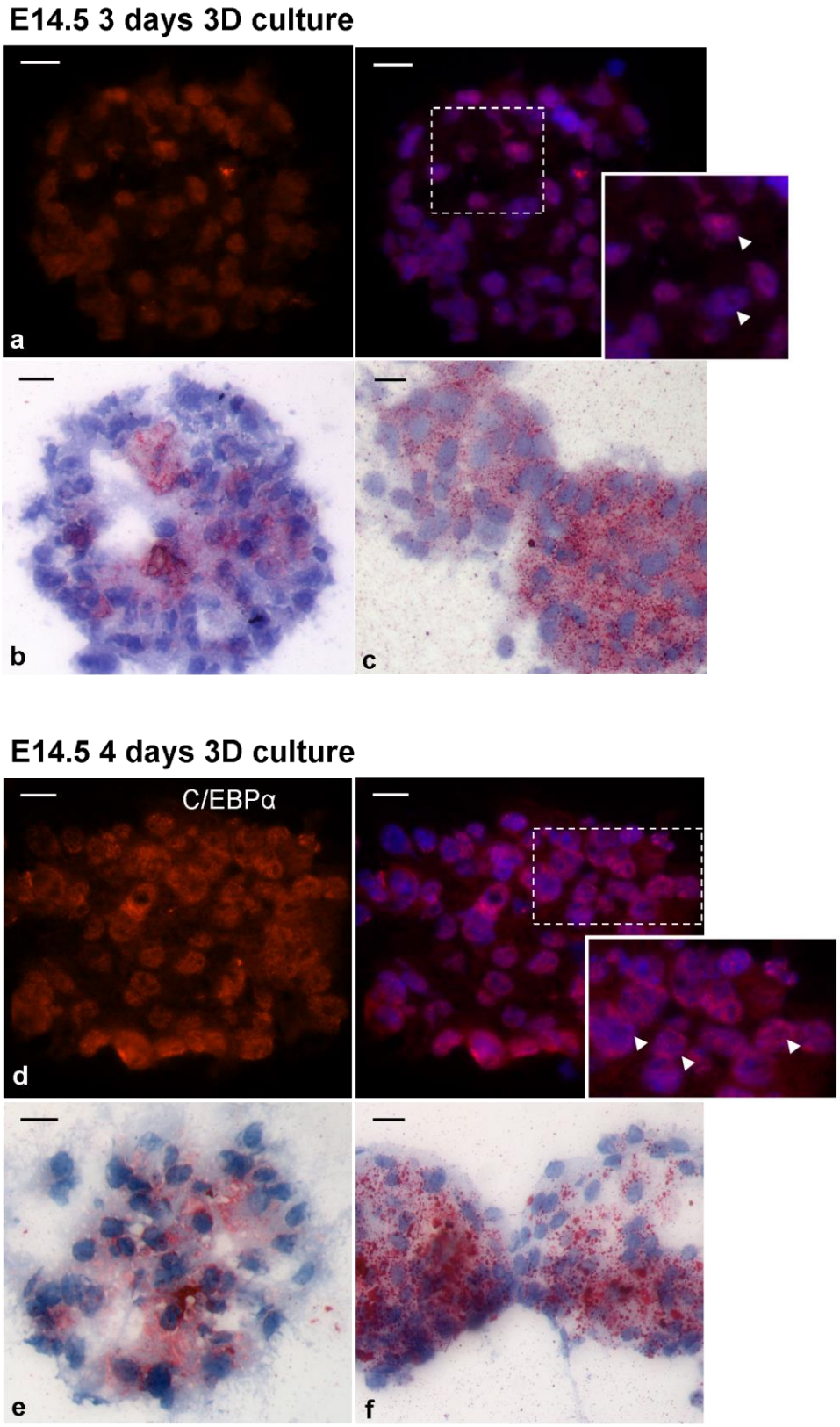

Figure 3.17: Analysis of E14.5 dermal cell spheres cultured for 3 and 4 days Spheres cultured for 3 and 4 days had almost completely nuclear C/EBPα expression (d,g). There was widespread ORO staining but it was not distributed evenly throughout the spheres (e,f,h,i). Scale bars = 15μm

After 4 days of culture, sections through the sphere were more uniform in the level of staining. The number of fat droplets was similar to spheres after 3 days but they had begun to increase in size (Figure 3.17 e, f). These cells were mainly in the centre of the sphere. The number and size of fat droplets continued to increase, until, by 8 days of culture, almost half of the cells had accumulated fat into droplets and a number were beginning to take on the characteristics of fully developed white adipocytes: a round shape filled by one large lipid globule (Figure 3.15d).

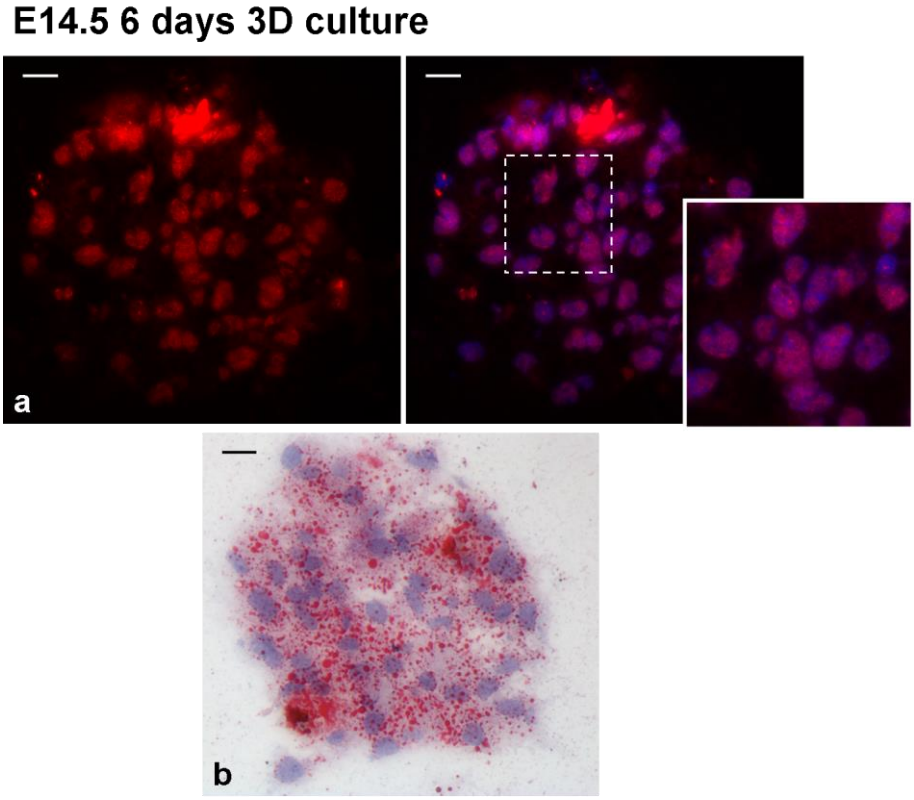

Figure 3.18: Analysis of E14.5 dermal cell spheres cultured for 6 days. After 6 days of culture, expression of C/EBPα remained strong and still within the nucleus (a). ORO staining of sphere sections showed that fat droplets were beginning to join together into larger droplets (b). Scale bars = 15μm

3.2.4.2 Organ culture of E14.5 mouse dorsal lateral back skin

Cell culture experiments and collagen IV staining showed that E14-E14.5, or even earlier, is likely to be an important developmental age for adipose tissue development in the lower dermis. As a result, a preliminary experiment was carried out for the organ culture of E14.5 back skin. Collagen IV staining (Figure 3.19) showed that there is already a distinct difference between the upper and lower dermis at E14.5, with much greater expression of the protein in the lower dermis.

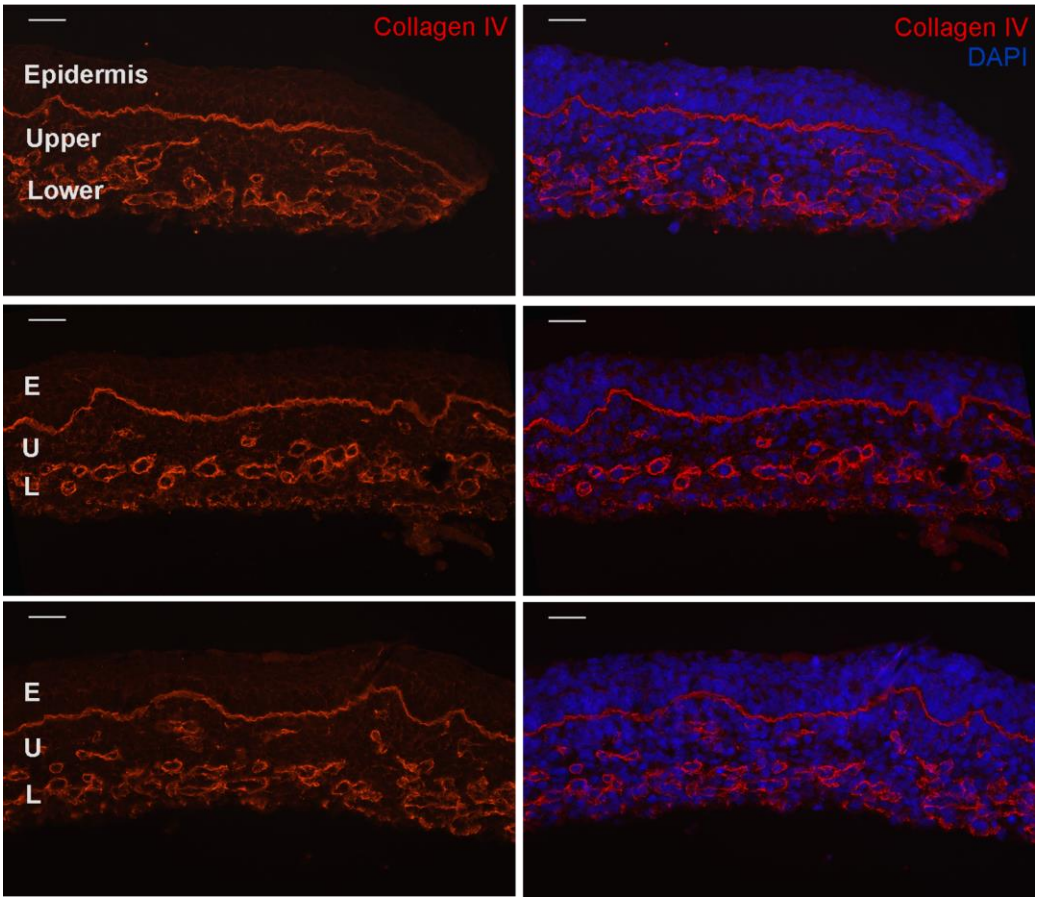

Figure 3.19: Collagen IV expression differs between the upper and lower dermis of mouse back skin at E14.5. Images show three representative examples of E14.5 mouse back skin sections stained with collagen IV and counterstained with DAPI. Labels identify the epidermis (E), upper (U) and lower (L) dermis. Scale bars = 30μm

Skin taken from E14.5 mouse dorsal lateral back was cultured in the organ culture system for three or four days. Skin from this younger age was easier to culture and did not lead to as much variability as was seen starting with E16.5 back skin. Hair follicle development begins around E14.5 and so more fully developed follicles were a good indication of healthiness in the cultured skin (Figure 3.20 A).

After 3 or 4 days in culture, adipocyte development had not progressed far enough to see any ORO staining (Figure 3.20 e, h). Earlier stages of fat development could be analysed, however, through immunofluorescent staining with earlier markers such as FABP4 (Figure 3.20 B). FABP4 was specifically found along the lower dermis, particularly near hair follicles, but also in the interfollicular dermis.

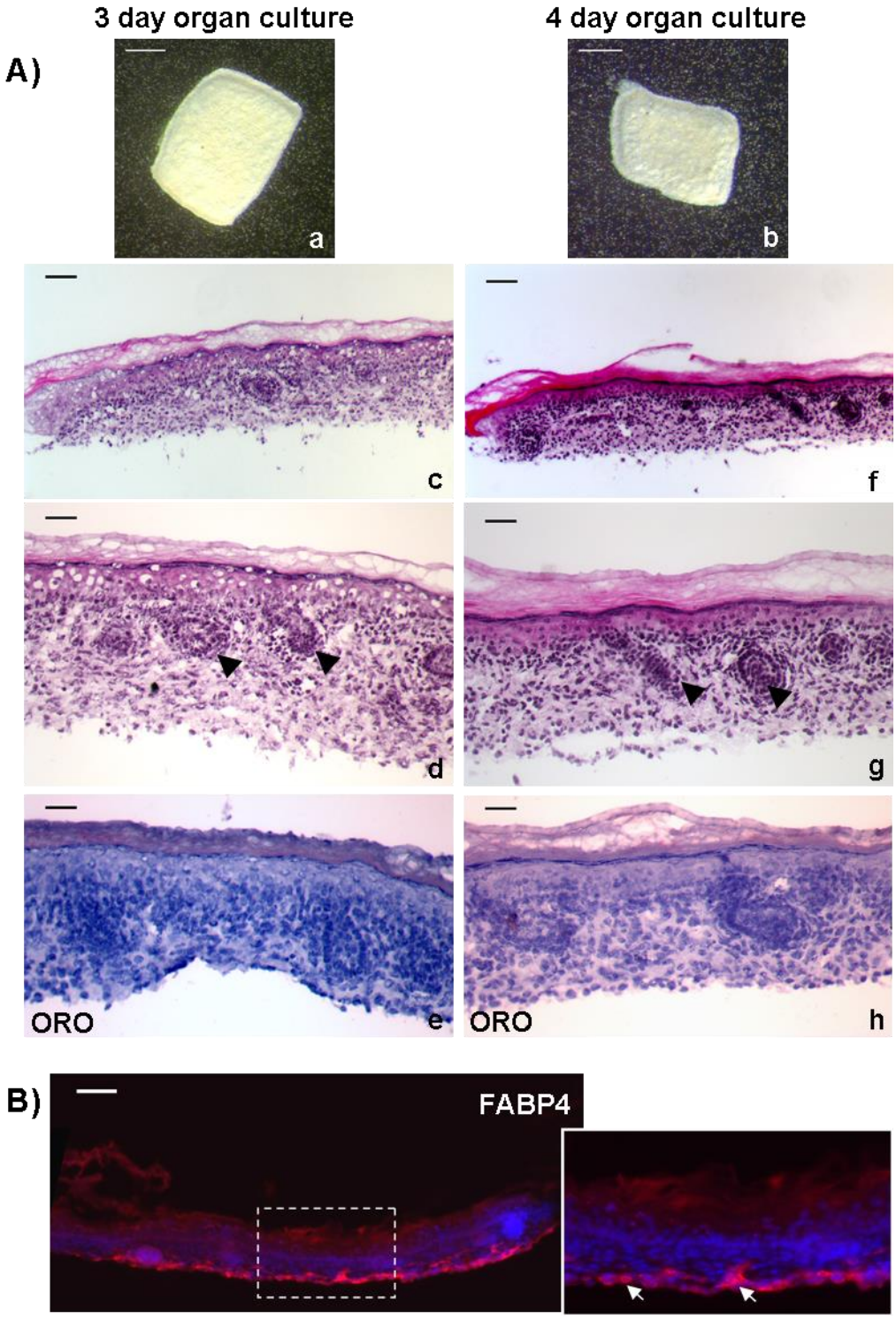

Figure 3.20: Organ culture of E14.5 mouse back skin allows adipogenesis over three and four days of culture. A) Culture pictures and H&E staining showed that E14.5 skin in the organ culture system remained healthy after 3 (a,c,d) or 4 (b,f,g) days of culture with a compact dermal structure and developing hair follicles (arrowheads). ORO staining did not show any lipid droplets meaning fat accumulation did not proceed to a sufficient level to be visible in this time (e,h). B) FABP4 staining of skin fixed after 3 days showed strong expression along the lower dermis, especially around hair follicles. Scale bars: A) a,b= 250µm; c,f,= 65µm; d,e,g,h= 30µm; B) 65µm

3.3 Discussion

The primary aim of the first part of this chapter was to establish a model system to develop a better understanding of adipose tissue development *in vivo*. There is a need for models such as these as there is increasing evidence that growing cells, even primary cells, in 2D culture changes the nature of the cells and is not representative of processes *in vivo*. Of the two models presented, 3D cell culture was most successfully established and used for further study into the timing of adipogenesis *in vivo*.

3.3.1 The substrate organ culture system

The substrate organ culture system allows the further development of the skin *ex vivo*. It has been previously shown that skin from E16.5 mouse back skin does not yet contain fat droplets (Figure 3.1). After three days in organ culture pieces of skin were observed to have fat droplets along the length of the lower dermis, however the quality and healthiness of the skin was very variable. The quality of the cutting of the skin did have an effect on the health of the skin after 3 days however this was not the only factor as skin which was comparable at the start of the culture differed by the end. The different media and serum concentrations tried also did not result in any combination which gave greater reliability. Although William's media, as a more nutrient rich medium, gave better results there were also some pathological pieces of skin produced in these cultures.

ORO staining of organ cultured skin showed that many had accumulated lipids during the period of the culture however the healthiest pieces of skin, judged through H&E staining, often had the least lipid droplets. This led to the conclusion that much of the ORO staining being seen was actually due to a stress response rather than normal adipose tissue development (Widnell et al., 1990; Özcan et al., 2004). The organ culture system would be most useful for adding or blocking factors thought to be involved in adipogenesis. The variability seen in lipid accumulation seen between different control pieces of skin however would make any results

invalid as normal development cannot be differentiated from a stress response.

Due to time constraints, organ culture of E14.5 dorsal lateral back skin was only repeated once however younger skin has previously been cultured in the Jahoda lab with a much higher success rate than was found with E16.5 starting material (Richardson et al., 2009). Three or four days in culture was not long enough for fat accumulation to be visible by ORO staining however the development could be analysed through staining with FABP4. The results presented in this chapter show that adipogenesis is likely to start at around E14.5 therefore organ culture of skin from this age, with the addition or inhibition of factors such as from signalling pathways, or miRNAs, will be interesting to pursue further.

3.3.2 Collagen IV expression in E14.5 mouse back skin

The differential expression of collagen IV between the upper and lower dermis as early E14.5 was an indication of the differences already being exhibited by the cells in each area. The expression of collagen IV was much greater in the lower dermis which matches an observation made in porcine subcutaneous fat development of collagen IV expression preceding adipose tissue formation (Hausman and Dodson, 2012). It would be interesting to investigate the expression of collagen IV at E13.5 firstly to see whether it is expressed at this age at all; and secondly, to see whether it is already different between the upper and lower dermis and this age.

3.3.3 The 2D and 3D cell culture of dermal cells

This model system was successfully established for dermal cells from mouse back skin between E14.5 and E18.5. The starting hypothesis was that 3D culture would allow better adipose tissue development and this proved to correct, as discussed later. Importantly for a model system, spherical culture was also highly reproducible (see appendix IV). Repeats showed that the primary cells were able to grow in 2D and also formed into spheres of the same size for all ages. E18.5 2D culture contained the most differentiated fat cells of 2D cultures at all of the ages; just over 15% of the cells contained fat

droplets. This is likely to be because the cells were already well progressed through the differentiation process when they were put into culture. 2D culture of cells from all of the other ages only produced 4-5% cells with lipid droplets.

The 3D spheres were analysed in two different ways: direct freezing and sectioning, and transfer to 2D. Transferring the spheres back onto 2D plates and allowing them to grow out not only showed that the cells remained viable and were undergoing genuine adipogenic differentiation, it also allowed direct comparison to 2D adipogenesis. This was extremely useful and allowed comparison through cell counting. Disparate cell numbers between the two culture types, however, decreased the accuracy of the method. Despite EdU analysis of cell division showing division in spheres (Chapter 4), when re-plated the 3D spheres produced less cells than 2D which had divided to cover the plate. The spheres also did not completely grow out onto the plate before analysis and some cells were lost during staining. The level of oil red O, and therefore adipogenesis, in 3D is likely to have been underestimated. Accurate quantification of oil red O stain using an extraction method was undertaken but was came up against a number of problems not least the bias against 3D cultures due to the smaller cell numbers.

As hypothesised, however, 3D culture produced a larger number of differentiated cells at all ages, possibly due to the greater amount of cell-cell contact. The end point timing at which all the cultures was analysed was equivalent to 22 days of development. At this age in mice the lower dermis adipose tissue is almost completely filled with fat cells. Assuming that the lower dermal cells made up half of the cells put into culture, E18.5 and E14.5 cell cultures, with approximately 40% differentiated cells, therefore relate well to *in vivo*.

There is strong evidence that many features of 3D culture provide a more realistic model system than 2D culture. An important attribute of 3D culture is the much greater cell-cell contact allowed providing the opportunity

for local signalling, and exchange of materials through gap junctions (Kuzma-Kuzniarska et al., 2014). Culture on a two-dimensional plate causes a flattened morphology of the cells with most of the cell surface in contact with the plastic surface below, or the culture medium above the 2D layer (Beningo et al., 2004). The production of gap junctions is therefore severely limited as the areas of cell surface touching are much reduced compared to 3D or the *in vivo* situation. As well as exchange of small molecules, gap junctions are also important for modulation of collagen production, mechanical properties of cells, and strain-induced cell death (Kuzma-Kuzniarska et al., 2014).

Another problem with 2D culture, particularly of cell lines, is changes in gene expression compared to the tissue of origin (Birgersdotter et al., 2005). The range of gene expression is often restricted which is not helpful for studying complex developmental processes involving entire networks of genes. The above discussion is concerned with features of cell culture which are improved by a 3D environment, however static 3D culture can produce the problem of hypoxia for cells not in direct contact with the culture medium (Volkmer et al., 2008). The small size of the spheres made in the method in this chapter should minimise this problem, and indeed, although it was not directly investigated, cells in the centre of the sphere did not appear to be hypoxic.

3.3.4 Adipogenesis in the lower dermis starts at an earlier age than previously hypothesised

Analysis of the 3D cell cultures by counting nuclei and lipid droplet containing cells, revealed similar number of adipocytes in E18.5 and E14.5 cell cultures, with far fewer in the ages between. This was a surprising observation as we expected to continue finding fewer differentiated cells for cell cultures from younger ages.

Cells from E14.5 dermis clearly already contained the potential to develop into adipocytes, and were able to do so in the 3D cell culture system however the timing of lipid accumulation and C/EBPα expression differed from what has previously been observed in mouse back skin. As described in

the introduction, both fat droplets and nuclear C/EBPα expression are first observed in mouse lower dermis at E18.5. By contrast, E14.5 dermal cell spheres which had been cultured for two days, therefore equivalent to E16.5, already had a very small number of fat droplets and some nuclear C/EBPα expression. By the time spheres had been in culture for 3 days, making them equivalent to 17-17.5 embryonic days, most of the cells had nuclear C/EBPα and fat droplets were becoming widespread. In general, fat accumulation in spheres appeared to happen at an earlier stage than in back skin. Organ cultured skin also had not started to accumulate lipid droplets in 3 or 4 days of culture.

An important factor in the differences observed between the 3D cell culture model and back skin is the absence of epidermal cells. In the spheres cell counts showed that approximately 50% of the cells differentiated into adipocytes and accumulated fat droplets, although sections through frozen spheres appeared to show a higher number than this. The very high level of staining in sphere sections raised a puzzling question as to the commitment of dermal cells to the adipogenic lineage. A number higher than 50% of the cells becoming adipocytes suggests that upper dermal cells were also able to follow the adipogenic pathway. It is possible that under normal developmental conditions in the organism the epidermis has an inhibitory role in preventing adipogenesis in the upper dermis. The high rate of adipogenesis, however, does strongly suggest that at E14.5 the lower dermal cells are committed to become adipocytes. In respect to the low rate of adipogenesis seen in the E14.5 2D cell culture it is possible that once the cells entered the differentiation process they were outcompeted on the 2D surface as the fibroblasts proliferated very rapidly.

The earlier timing of fat accumulation in spheres may be due to the close contact, and relatively small number, of cells in each sphere allowing more paracrine signalling. A study of epididymal fat development using a similar hanging drop technique found that most cells became lipid filled adipocytes even without adipogenic medium (Han et al., 2011). In this study they postulated that cell-ECM interactions were important for differentiation of

predetermined cells into epididymal adipose tissue therefore it would be interesting to investigate ECM proteins in the spherical culture system.

Intriguingly, although spheres quickly accumulated fat into small droplets, and the droplets did increase in size, most of the lipid was still within relatively small droplets by the end of the culture (8 days). Differences in the age of mice at birth does not make it possible to exactly correlate sphere days in culture with post natal days, however 8 days in culture make the spheres approximately equal to 1/2 days postnatal. By this time in mouse back skin the fat droplets are much larger than those seen in culture (K. Wojciechowicz et al., 2013) suggesting that although 3D culture allows adipogenesis to proceed, it is not sufficient for complete differentiation.

Another interesting observation was the difference in adipocyte numbers between E14.5 spherical culture and that of dermal cells from older embryonic ages. E14.5 and E18.5 dermal cell spherical culture produced very similar numbers of adipocytes whereas the in between ages of E15.5 - E17.5 had lower numbers. Interruption of the adipogenesis pathway could be the explanation for this diversity. Taking cells at E14.5, at the start of the differentiation process, allows all of the molecular signals to continue as they would during normal development. Equally cells from E18.5 are already far through differentiation. It is possible that taking cells from E15.5 – E17.5 dermis causes a disruption to the molecular sequence of events resulting in smaller number of adipocytes.

Similar to fat droplet accumulation, C/EBPα expression was also more advanced in the spherical cell culture than in back skin of an equivalent age. Nuclear expression of the protein, in E14.5 dermal spheres, started after only two days in culture and throughout the culture period up to the final culture time point of 8 days. Two days of culture starting with E14.5 dermal cells puts the spheres an equivalent developmental age to E16.5 back skin. As discussed in the introduction, C/EBPα expression is first seen in back skin at around E18.5-19 days (Wojciechowicz et al., 2008). In *in vitro* studies, C/EBPα is also expressed in the nucleus from two days after hormonal

induction and the expression peaks on the third day of culture (Hausman, 2000; Jiang and Lane, 2000). Before this time transcription is inhibited through repressor complexes bound to the DNA (Jiang and Lane, 2000; Zuo et al., 2005). Similarly to results found in the spherical cell culture system presented in this chapter, C/EBPα expression precedes fat accumulation with protein already present at the plating of porcine S-V cells (Hausman, 2000).

The timing of adipogenesis in E14.5 spheres appeared to closely relate to differentiation in 3T3-L1 cells without the need for hormonal induction. In 3T3-L1 cells, expression of C/EBPα is seen from the second day after induction onwards (Tang and Lane, 1999). Similarly in E14.5 dermal spheres C/EBPα staining was found in spheres frozen after 48 hr and continued to be expressed for the whole culture duration of 8 days. It is unknown whether expression started before 48 hr as, from a technical standpoint, this was the earliest time at which spheres could be frozen. In the E14.5 spheres, the earliest fat droplets could be seen after 2 days although the majority of fat droplets were not seen until at least 3 days of culture. 3T3-L1 cells are able to spontaneously differentiate once they reach confluence and very small fat droplets can be seen before induction (Wang et al., 2003; Gu et al., 2007). After induction, fat droplets continue to increase in size from 1-2 days after induction (Wang et al., 2003).

3.3.4.1 Microarray data of E13.5 and E14.5 dermis confirmed early expression of adipogenic genes

To look for molecular evidence of adipogenic commitment in embryonic mouse skin around e14.5, I examined a microarray of E13.5 and E14.5 mouse back skin whole dermis, previously produced by the Jahoda lab. This revealed early expression of a number of genes which have been linked to adipogenesis (Table 3.3). Three of the genes listed (IGF-2, RBP4, and Rgs5, in red) have been identified as suppressors of adipogenesis whereas the others are all important for fat development.

Gene Name	Up in 13.5	Up in 14.5	Gene symbol	Gene name
1415931_at	7.2		IGF-2	Insulin-like growth factor 2
1422243_at	5.4		FGF7 (KGF)	Fibroblast growth factor 7
1419519_at	3.3		IGF-1	Insulin-like growth factor 1
1427559_a_at	2.4		ATF2	Activating transcription factor 2
1454906_at	2.1		RARβ	Retinoic acid receptor, beta
1451679_at	2.1		Arxes2	Adipocyte-related X-chromosome expressed sequence
1418901_at	0.5	2.0	C/EBPβ	CCAAT/enhancer binding protein, beta
1423023_at	0.5	2.2	sFRP-5	Secreted frizzled-related sequence protein 5
1454791_a_at	0.4	2.2	RBP4	Retinoblastoma binding protein 4
1417023_a_at	0.4	2.6	FABP4	Fatty acid binding protein 4
1450333_a_at	0.3	3.1	GATA2	GATA binding protein 2
1417466_at	0.1	8.3	Rgs5	Regulator of G-protein signalling 5

Table 3.3: Selected genes from microarray of E13.5 and E14.5 mouse dermis

C/EBPβ is a member of the family of CCAAT/enhancer binding proteins which are thought to be essential for adipogenesis. The microarray showed that mRNA of C/EBPβ is present at E13.5 but particularly upregulated in the dermis at E14.5. In cell culture models of adipogenesis, C/EBPβ is one of the first proteins to be expressed after hormonal induction, the protein appearing within 4 hours (Cao et al., 1991). Fatty acid binding protein 4, FABP4, is another important protein involved in the early stages of adipogenesis (Birsoy et al., 2011; Wojciechowicz et al., 2013). Similarly to C/EBPβ, the microarray shows FABP4 present at E13.5 but further upregulated at E14.5.

IGF-1 and RXRβ were both upregulated at E13.5. These genes are interesting as IGF-1 is one of the components used for hormonal induction and is thought to be essential for adipogenic differentiation. *In vivo* however there is a report suggesting IGF-1 and IGF-1R signalling is not needed for the differentiation process (Kloting et al., 2008). The ligand of RXRβ, retinoic

acid, is similarly required for commitment of mouse embryonic fibroblasts to the adipogenic lineage (Dani et al., 1997).

The expression of these genes as early as E13.5 and E14.5 corroborates the results found of the potential of E14.5 dermal cells to develop into adipocytes. The microarray was taken of the complete dermal thickness including the upper dermis which does not contain adipocytes. The presence of inhibitory genes in the array therefore raises the possibility that the upper dermis is being inhibited from the adipogenic lineage at the same time as lower dermal cells become committed to adipogenesis. Immunofluorescent staining would help to confirm the expression localisation of these proteins and may provide a very early marker for fat differentiation.

Chapter 4

An investigation into cell division in the lower dermis of murine skin during adipogenesis

4.1 Introduction

Adipogenesis has largely been investigated in cell culture models in particular using 3T3 cell lines, such as 3T3-L1. Evidence from these model systems has resulted in the process of adipogenesis being divided into three general stages: 1) Commitment, 2) Clonal expansion, 3) Differentiation, ending with terminal differentiation of cells as mature adipocytes. The second stage, mitotic clonal expansion (MCE), is the focus of this chapter.

The most common cell line, 3T3-L1, was refined over a number of generations. It was originally derived from cultures of cells from Swiss mouse embryos between 17-19 days. The cells were passaged every three days until they could be stably cultured as a fibroblastic cell line (3T3 cells) (Todaro and Green, 1963). Confluent cultures of 3T3 cells were observed to have clusters of lipid-containing cells. Through the specific isolation of these lipid-rich areas over successive generations, two subclone cell lines 3T3-L1 and 3T3-L2 were established (Green and Kehinde, 1974). They are described as preadipocytes as they are already committed to the adipogenic lineage and are able to make fat with or without the use of hormonal induction (Gu et al., 2007). Nevertheless a higher proportion of the cells follow the adipogenic pathway after hormonal treatment.

In the most frequently used protocol for adipogenic differentiation of these cells, they are allowed to grow until they are confluent and become growth arrested. Two days after this, differentiation is induced using three hormones, insulin or IGF-1 (I), Dexamethasone (DEX), and Methylisobutylxanthine (MIX), in medium also containing Fetal Bovine Serum (FBS). Within the first 16h after induction with this hormonal mixture, 3T3-L1 cells are observed to synchronously re-enter the cell cycle for 1-2 rounds of cell division, known as mitotic clonal expansion. It has been shown that cells generally traverse the G1-S phase transition in the cell cycle at approximately 16h after induction (Tang and Lane, 2012).

There are differing theories for the role of MCE in the process of adipogenesis. One side of the argument maintains that it is an essential step

require before differentiation can take place (Tang et al., 2002; 2012), whereas others argue that it is an artefact of the cell line model of adipogenesis (Qiu et al., 2001). *In vitro* experiments have been carried out that provide evidence to support both of these theories.

The researchers that maintain that MCE is essential have found that adipogenesis in 3T3-L1 cells is arrested by blocking cell division (Tang et al., 2002 a). Others argue that the synchronous re-entry into the cell cycle followed by 1-2 rounds of cell division is in fact an artefact of the hormonal mixture used to stimulate adipogenesis (Qiu et al., 2001; Martini et al., 2009) although there is disagreement over which component is the cause of cell division. Qiu et al., suggest that insulin is responsible through interaction with the MAPK/ERK signalling pathway. They found that a MEK-1 inhibitor could block MCE whilst still allowing differentiation to continue. Cho and Jefcoate, 2004, also found that removing insulin and fresh serum from the hormonal induction media removed the mitotic stage from adipogenesis in 10T1/2 cells, a mouse embryonic cell line. More recently it was found that methylisobutylxanthine (MIX) was causing MCE in 3T3-L1 cells through PKA-dependent cAMP signalling. cAMP has two separate mechanisms by which it can act in the cell and it was found that whereas PKA was causing MCE, cAMP signalling was required for normal adipose differentiation through PKA-independent EPAC (exchange proteins directly activated by cAMP) signalling (Martini et al., 2009)

The above results demonstrate that, although there are now several reports suggesting that MCE is not a necessary process, this is still a confused and controversial area. Culture of primary cells has provided further evidence that MCE is not required. Human bone marrow stem cells could be differentiated into adipocytes without going through mitotic clonal expansion, even though they were induced with the standard differentiation protocol used for 3T3 cell line culture (Qian et al., 2010). Similarly, cultured primary porcine stromal-vascular (S-V) cells do not undergo MCE (Wright and Hausman, 1994); however *in vivo* preadipocyte clusters are observed which

may be the result of a burst of proliferative activity before differentiation (Hausman and Kauffman, 1986; Hausman and Dodson, 2012).

A microarray of gene expression in the lower at E17, E18, and E19 time points was previously undertaken in the Jahoda lab. The results from this work did not identify a large number of the cell cycle genes which have been identified as being upregulated in 3T3-L1 adipogenesis. Further work presented in the previous chapter, however, contends that the adipogenesis process in the lower dermis starts at a younger age, around E14. Cells from the dermis of E14.5 mouse back skin were able to develop into adipocytes. For the process of mitotic clonal expansion to occur, it would therefore be likely to happen around this time or earlier.

The aim of this chapter is to investigate the presence of the mitotic clonal expansion step *in vivo* during the adipogenic differentiation of cells in the lower dermis of the skin. More generally the observations presented in this chapter offer a view of the quantity and location of cell division during murine skin development. The principal method used for exploration of cell division was incorporation of a nucleotide substitute 5-ethynyl-2´-deoxyuridine (EdU) into organ cultured pieces of skin. A short two hour "pulse" of incorporation was undertaken using skin from three embryonic different ages: E14, E15, and E16. Further experiments used the 3D cell culture system to investigate EdU incorporation in parallel with C/EBPα expression.

EdU is a thymidine analogue which gets incorporated into DNA during the DNA replication phase of cell proliferation. It can easily be detected by 'click' chemistry: a Cu(I) catalysed [3+2] azide-alkyne cycloaddition reaction by which a fluorescently tagged azide specifically reacts with part of the EdU molecule. This is a fast detection method, using water as a solvent, offering advantages over the common cell proliferation assay using BrdU (Hill et al., 2007).

4.2 Results

4.2.1 An overview of cell division in developing mouse back skin

Incorporation of EdU into back skin sections performed at 14-14.5, 15-15.5, and 16-16.5 days gestation (Figure 4.1, H&E) allowed a general investigation of cell division at these ages. Overall a large amount of cell division was observed at all ages, particularly E14, seen by the number of nuclei positive for EdU although the distribution varied slightly between the ages.

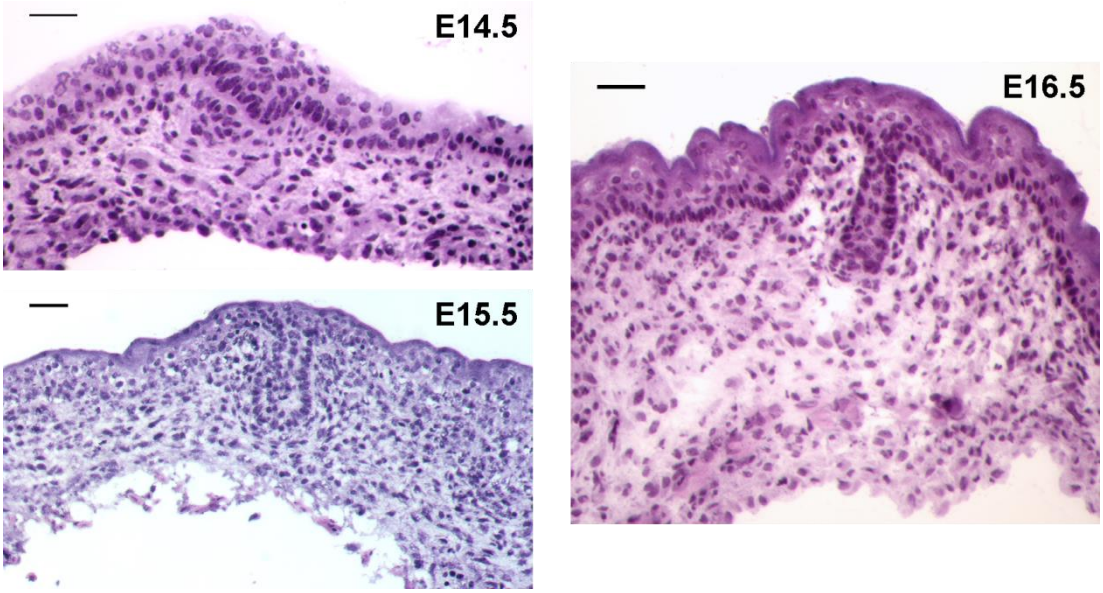

Figure 4.1: Structure of E14.5, E15.5, and E16.5 mouse back skin. Hematoxylin and Eosin stain; Scale bars = 30μm

All pieces of E14.5 skin (six pieces in total from three embryos) showed incorporation of EdU into the epidermis and both upper and lower dermis (Figure 4.2 A). Labelled cells could be observed along the entire length of each specimen. As expected, most of the dividing cells in the epidermis were in the innermost layer next to the basement membrane; over half the cells in this layer had divided and incorporated EdU during the two hour pulse (Figure 4.2 A and B). The epidermis at this age is only two to three cell layers thick at the deepest points and there were nuclei that had incorporated EdU in all layers. However, there were decreasing numbers of stained nuclei moving up through the layers, with only approximately 1% of the outermost (topmost) cells stained (Figure 4.2).

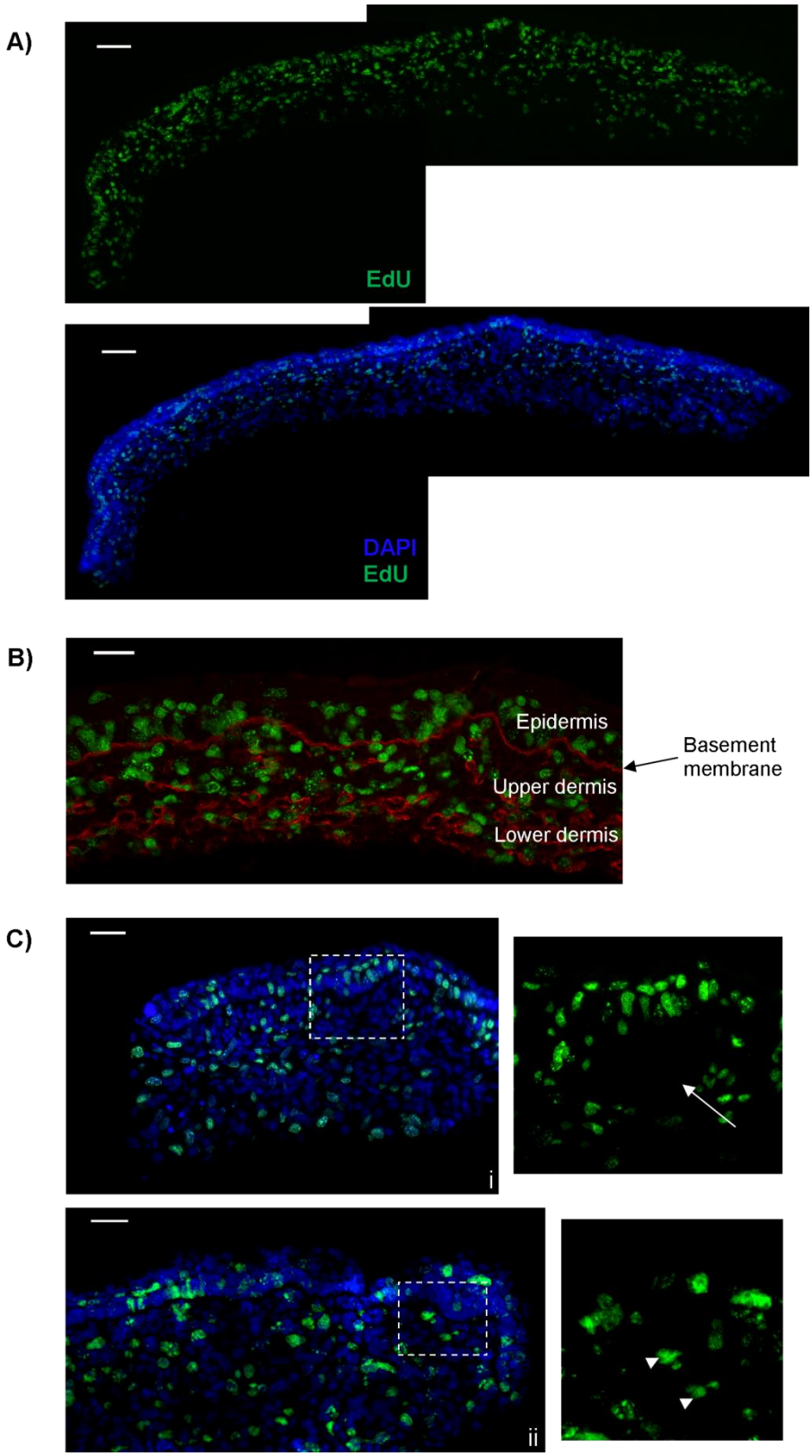

Figure 4.2: Extensive cell division is visible throughout the epidermis and dermis at E14.5. Representative sections of skin after 2h EdU pulse. Cell division is evenly distributed throughout the width of the skin (A). The underlying structure is visualised by staining with Collagen IV (red) showing substantial division in the epidermis and dermis (B). C) Dermal condensations below developing hair follicles are generally devoid of EdU staining (i, arrow) although occasionally a couple of stained nuclei can be seen (ii, white arrowheads). Scale bars: 65μm A), 30μm B), C)

At E14.5 most of the cells in the epithelial part of the developing hair follicle, the hair placode, also divided during the two hour EdU pulse however the area of the dermis underneath these the hair placodes, known as the dermal condensation, had a clear lack of label uptake. This absence of labelling was found in the upper dermis in a crescent shape under the epidermal hair placode and was common to almost all dermal condensations found (Figure 4.2 C i). Very occasionally a developing hair follicle could be found at this age which had one or two stained nuclei in the dermal condensation (Figure 4.2 C ii).

The EdU labelling seen in E15.5 mouse back skin, examined in four pieces of skin from two embryos, was still widespread in the epidermis and dermis (Figure 4.3A). In the interfollicular epidermis, over half of the cells next to the basement membrane stained positively for EdU incorporation. By this age, however, the positive nuclei were almost exclusively contained in the basal epidermis with far fewer observed in the developing layers above (Figure 4.3B). Cell division was also visible throughout the upper and lower dermis, apparently evenly spread through the interfollicular dermis (Figure 4.3B and C).

By E15.5 the hair follicles had began to lengthen down through the dermis and as they did so they became more visibly organised into layers. The outer layer(s) in particular contained a large number of nuclei which had taken up label during the two hour pulse period (Figure 4.3 A and B).

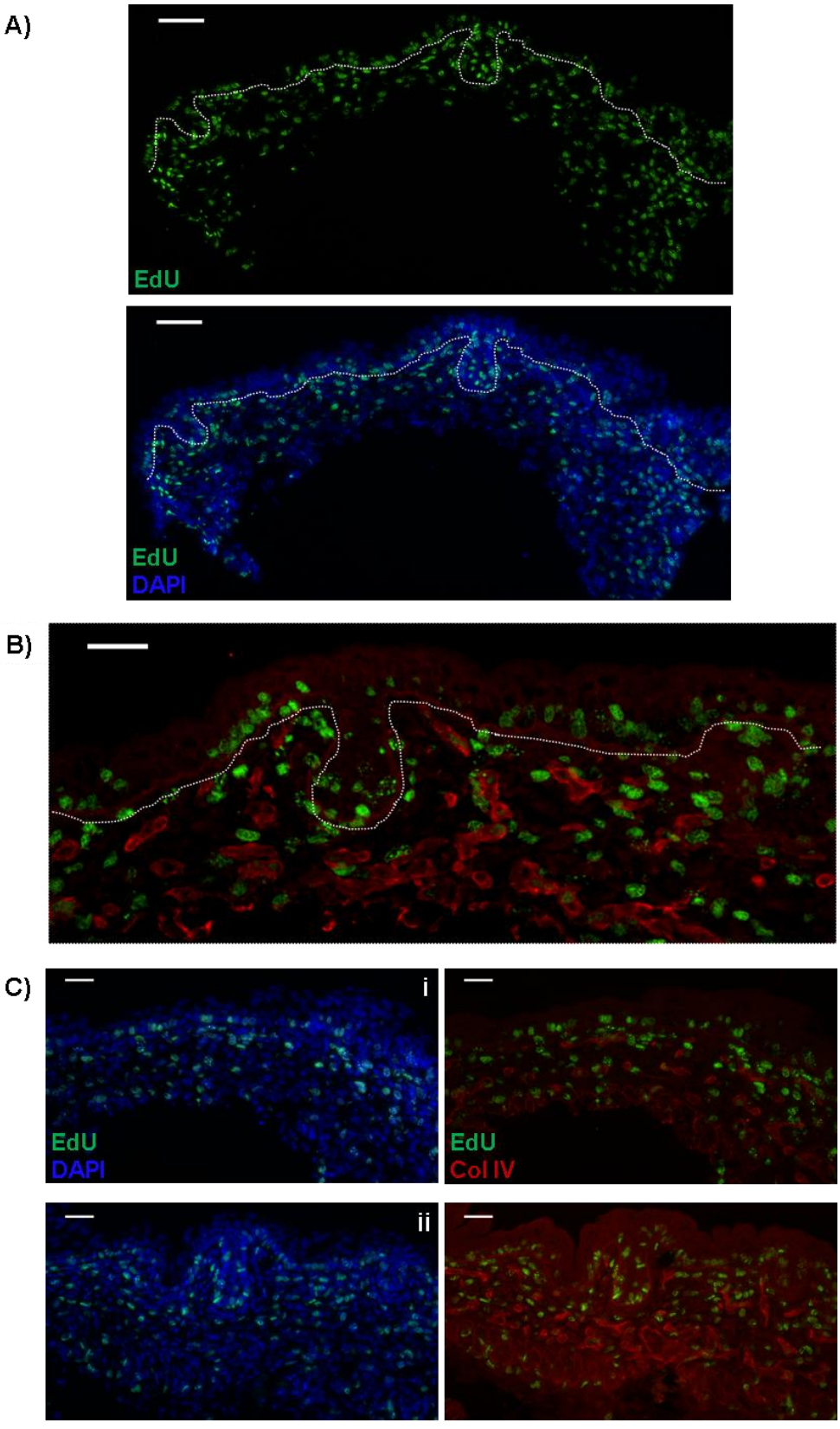

Figure 4.3: Cell division continues to be widespread at E15.5 particularly in the basal epidermis and hair follicles. White dotted lines indicate epidermal basement membranes. A) Representative example of EdU incorporation into E15.5 mouse back skin. B) Cell division in the epidermis is confined to basal layer and the epidermal portion of the hair follicle. C) Two examples of E15.5 mouse back skin showing division in the dermis is evenly distributed along the width of the skin. Scale bars: A) 65μm, B-C) 30μm

H&E of E16.5 back skin showed it to be thicker than the skin of preceding ages and the cornified layers of the epidermis had started to form (Figure 4.1). DAPI staining of the nuclei showed that they were less compacted in the epidermis than at E14.5 as the different layers had started become more defined (Figure 4.4A). EdU was incorporated exclusively into cells of the basal epidermis (Figures 4.4A and 4.4B, 1) indicating further differentiated cells were not dividing, and that labelled cells had not migrated upwards within the two hour pulse period.

Many hair follicles were well developed by E16.5 and a large amount of labelling could be seen throughout the follicle (Figure 4.4B, 2), particularly in the bulb region (Figure 4.4C) and around the outer epithelial layers (Figure 4.4D). In the interfollicular dermis, cell labelling was evenly spread along the length of the specimens with approximately a quarter of the cells having incorporated EdU during the two hour pulse (Figure 4.4A).

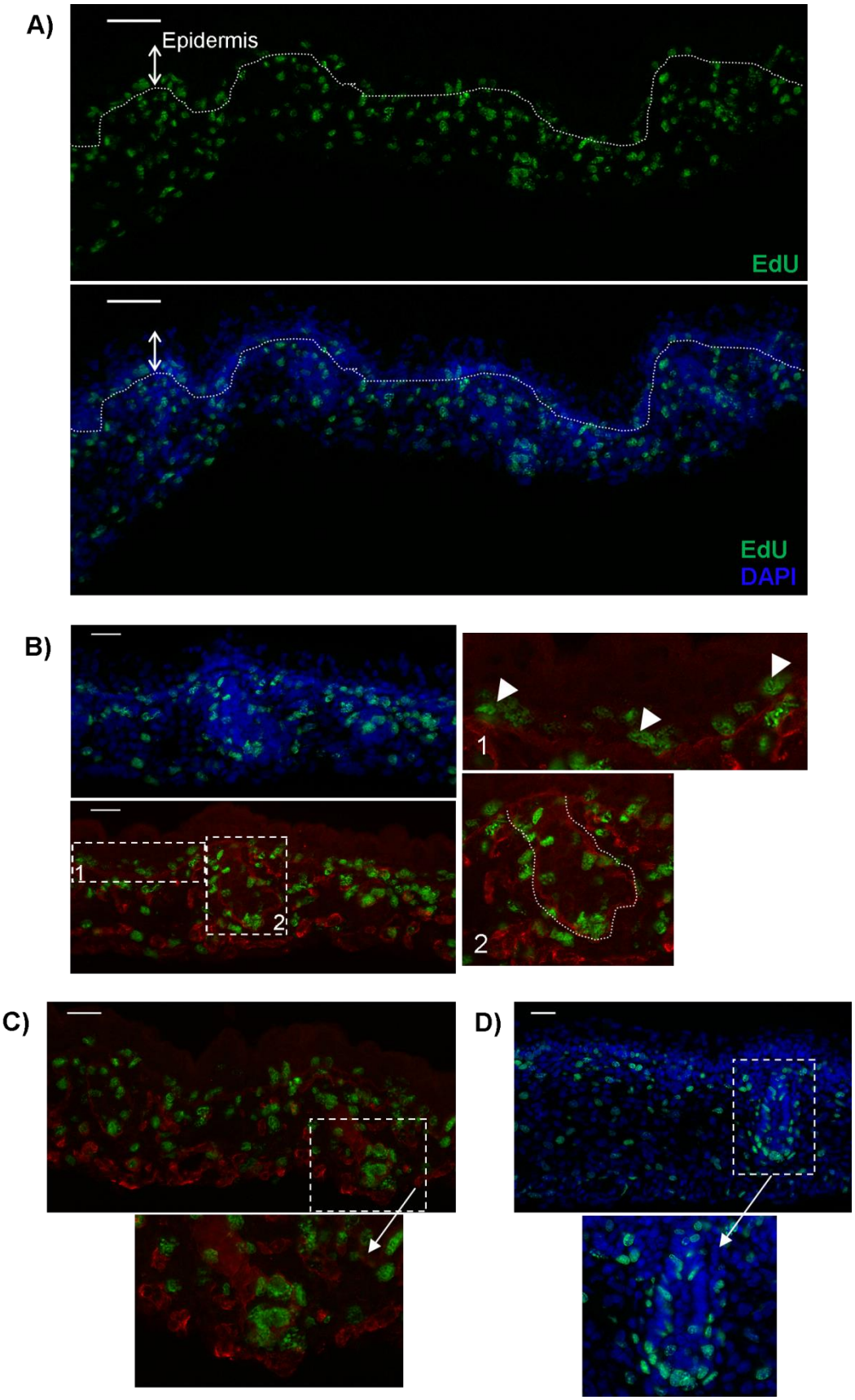

Figure 4.4: Cell division at E16.5 is widely distributed and particularly prevalent in hair follicles. A) Representative section of E16.5 mouse back skin with EdU incorporation showing cell division across the whole width (dotted line indicates epidermal basement membrane). B) Cell division in the epidermis (1) is restricted to basal cell layer next to the

basement membrane. Developing follicles have division (2) in the epithelial and mesenchymal derived portions (dotted line outlines hair follicle). Some hair follicles have extensive EdU incorporation in the bulb region (C) with others dividing particularly in the outer epithelial layers (D). Scale bars: 65μm A, 30μm B, C, D

4.2.2 Cell counts and analysis of EdU incorporation into mouse back skin

The amount of staining in the upper and lower dermis at each age was examined for specific evidence of a mitotic clonal expansion stage taking place in the lower dermal adipose tissue depot. Visual inspection of the EdU marking, alone, did not reveal any obvious difference in the amount of labelling between the upper and lower dermis, although across a large number of skin pieces there appeared to be slightly more division in the upper dermis at each age. Nuclei counts (for raw data see Appendix 3) were performed to gain a greater understanding of the amount of cell division taking place. Images of skin pieces at E14.5, E15.5, and E16.5 were subdivided into upper and lower dermis using collagen IV staining, and the total and EdU-positive nuclei were counted (for further detail and example images, see section 2.8.1). The counts revealed that for each age and skin piece the proportion of labelled cells was almost always greater in the upper dermis (Figure 4.5).

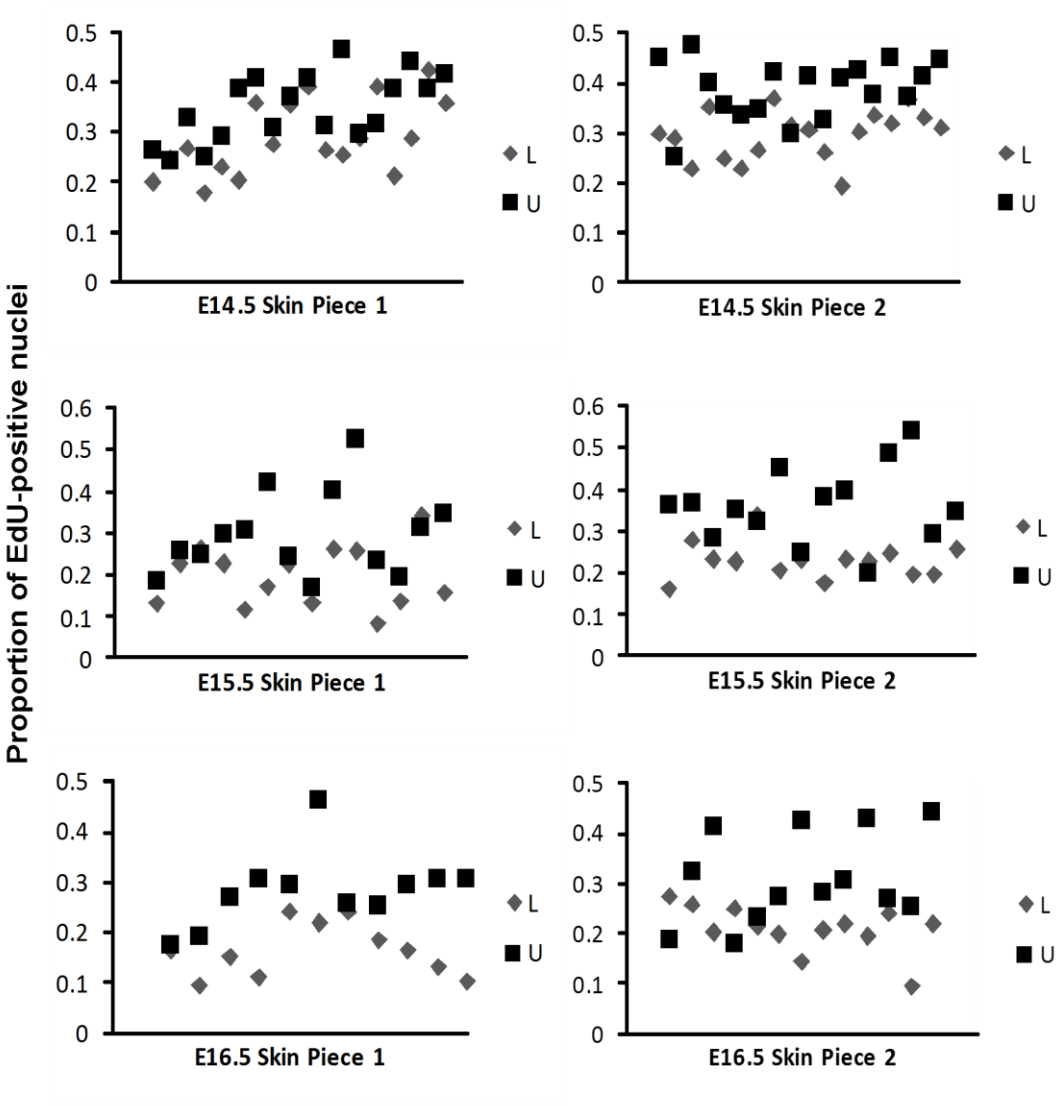

Figure 4.5: The proportion of EdU-stained nuclei is greater in the upper than the lower dermis. The proportion of stained EdU-positive nuclei vs. total number of nuclei has been plotted for the upper (red square) and lower (blue diamond) dermis. Each point represents the proportion for one area counted. Areas counted were paired so that an area of upper dermis was directly above its corresponding area of lower dermis (see Methods section 2.8.1). For statistical analysis see table 4.1 below.

Statistical analysis of the cell counts showed strong evidence that the fraction of stained cells differed between lower and upper dermis for all ages (see table 4.1 for likelihood ratio test values, G_1). Mean percentage values for the number of EdU-positive nuclei are greater in the upper dermis than the lower dermis for each age (Table 4.1 and Figure 4.6).

Age	Skin piece	G_1	P	Mean no. of stained cells (lower dermis) %	Mean no. of stained cells (upper dermis) %
E14.5	1	6.65	0.010	28.5	35.0
	2	20.2	7.07×10^{-6}	29.0	38.1
	Avg	**-**	**-**	**28.75**	**36.55**
E15.5	1	8.66	0.003	19.2	28.7
	2	19.7	8.81×10^{-6}	22.5	34.8
	Avg	**-**	**-**	**20.85**	**31.75**
E16.5	1	13.7	2.14×10^{-4}	16.5	28.2
	2	11.3	7.69×10^{-4}	20.6	31.1
	Avg	**-**	**-**	**18.55**	**29.65**

Table 4.1: Summary of results of likelihood ratio test between the upper and lower dermis for E14.5, E15.5, and E16.5 dorsal lateral back skin. Counts of total nuclei and EdU-positive nuclei were carried out in images of two pieces of skin from each age. Likelihood ratio test values (G_1) showed strong evidence that the fraction of stained cells differed between the upper and lower dermis. P values, which differ for each age and skin piece, are shown in the table.

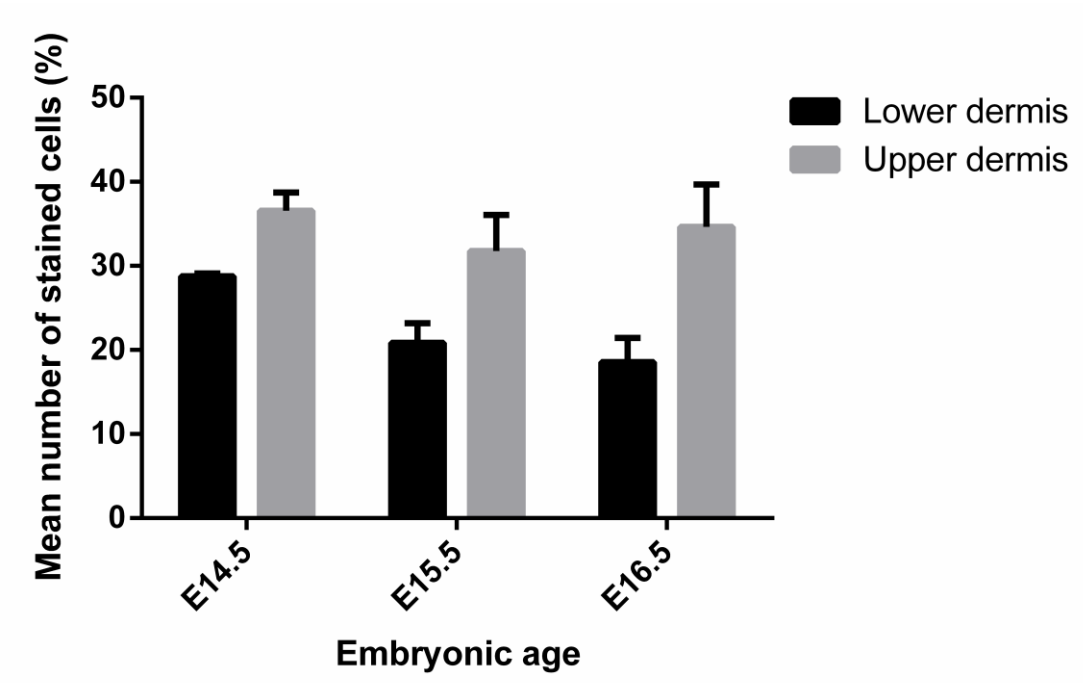

Figure 4.6: Mean number of EdU stained cells at E14.5, E15.5, and E16.5. See table 4.1 above for analysis. Data are mean ± s.e.m.; n=2.

4.2.3 Investigation of cell division in the 3D cell culture system

Back skin grown in the organ culture system was delicate meaning it was not possible to continue culturing back skin after an EdU pulse as originally planned. The skin became pathological after changing the media to remove EdU. Instead the 3D dermal sphere method was used to investigate whether mitotic expansion was a pre-requisite for adipogenic differentiation.

Two separate pulse chase experiments were used to examine the cell division in spheres. EdU was added to medium for the first two days of the culture. This was the period during which the single cell suspension in drops formed into spheres. Some of these spheres were frozen straight away at the end of this 48 hour period. Interesting, and somewhat unexpectedly, nearly all of the cells making up each sphere had taken up label in these first 48 hours leaving only a small number without EdU staining (Figure 4.7A). Other spheres were transferred to new medium, not containing any EdU, and cultured for a further one or two days, respectively. Most of the nuclei in these later spheres stained much more faintly for EdU indicating that the cells had continued to divide since the removal of EdU from the medium (Figure 4.7B). Some of the cells still stained brightly suggesting they had not divided, or if they had, only once or possibly twice.

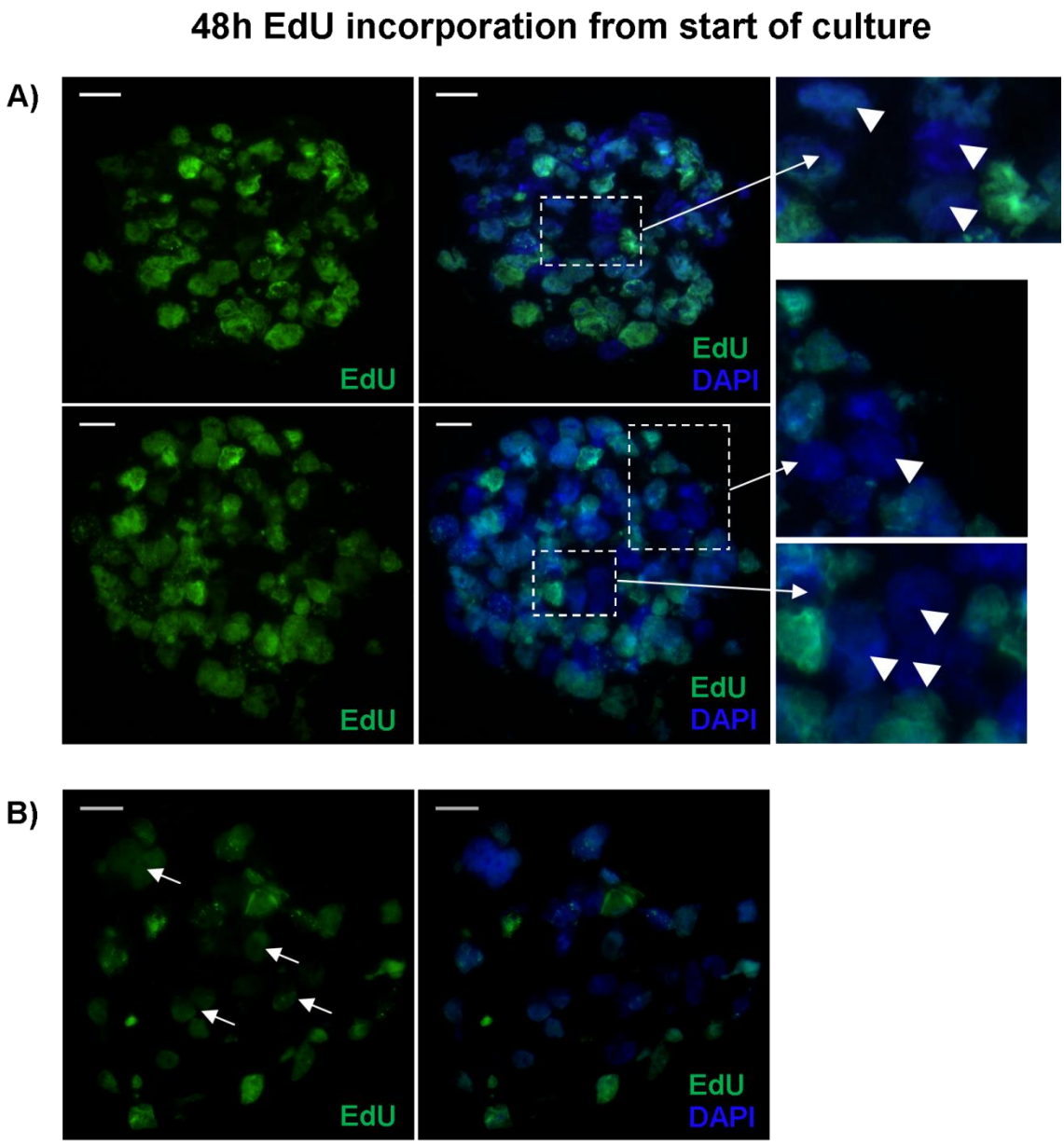

Figure 4.7: The majority of cells in dermal spheres divide in the first 2-3 days of culture. A) Representative sections of spheres were frozen down at 48h of culture directly after the EdU pulse. The majority of nuclei are positive for EdU staining after 48h indicating widespread DNA replication. Only a minority are not labelled with EdU (white arrowheads). B) Some spheres were cultured for a further 2 days after changing the media to remove EdU. Staining is generally much fainter (white arrows) although a couple of brightly stained nuclei remain visible indicating most cells continued to divide. Scale bars: 15μm

A more accurate way of determining the level of cell division after the first 48 hours, and the rate of cell division, was also used. Spheres were subjected to a four hour pulse with EdU on the third day of culture. The analysis of spheres frozen immediately after this pulse confirmed that approximately 10% of the cells were incorporated label during the pulse (Figure 4.8 A). After the pulse, some of the spheres were again transferred to new medium not containing EdU. They were left for a further 1 or 5 days so that they had been cultured for 4 or 8 days in total. Fluorescent staining of these spheres showed that division continued throughout the 8 days of culture. The relatively small proportion of cells with nuclei containing EdU after the 4 hour pulse on day 3 had divided, so that approximately half of the nuclei were labelled after a further 1 day of culture (Figure 4.8B). After 5 days more in culture nearly all of the nuclei contained some EdU, although most only stained very faintly (Figure 4.8C).

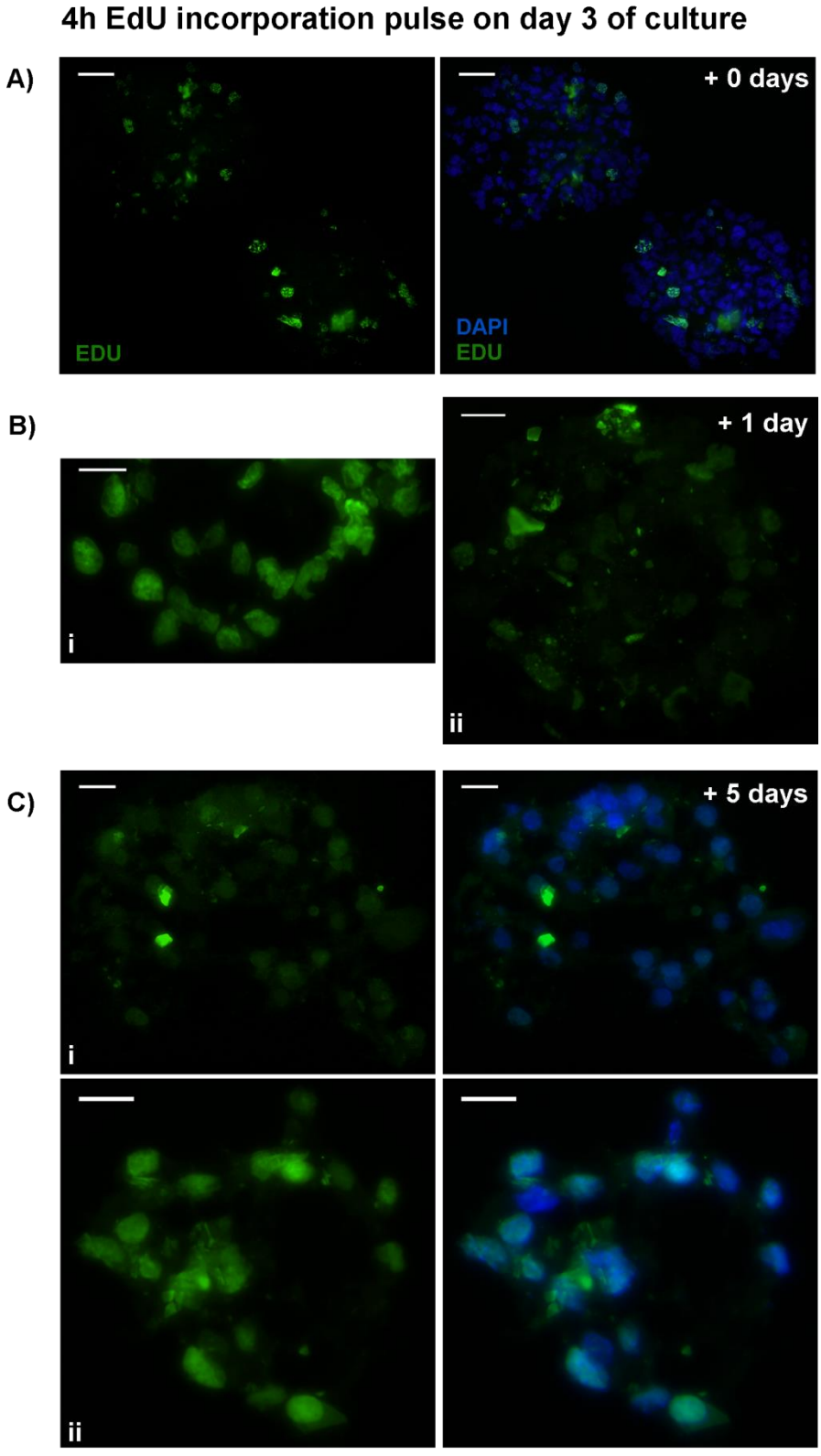

Figure 4.8: E14.5 dermal cells in 3D culture continue to divide for the length of the culture. A) Approximately 10% of nuclei are brightly stained with EdU following a 4h pulse. B) After 1 day of further culture without EdU a greater proportion of nuclei are positive for EdU. There is heterogeneity between nuclei with some brightly stained (i) and others only faintly positive for EdU (ii). C) Five days after the EdU pulse (8 days culture in total) the majority of nuclei of positive for EdU. Again there is a mixture of faintly (i) and brightly (ii) stained nuclei. Scale bars = 15μm

4.2.4 Co-staining of EdU with C/EBPα in E14.5 dermal cell spheres

Cell division and adipogenesis were investigated together by the co-staining of EdU with C/EBPα. As seen with staining presented in the previous chapter, C/EBPα was expressed in the all of the spheres from 2 days of culture onwards however it became more nuclear as the length of culture increased. All of the spheres stained showed co-localisation of C/EBPα with EdU positive nuclei. Spheres incubated with EdU for 48 hours before being frozen did not yet have nuclear C/EBPα in all sections however amongst the expression that was nuclear there were some cells that had not divided (Figure 4.9A). After a further day of culture, the expression of C/EBPα was more decisively nuclear and there were a number of cells which did not even have faint EdU staining (Figure 4.9B).

The majority of cells in spheres which had been subjected to a limited pulse of EdU and then cultured for a further 5 days had positive nuclear staining for both EdU and C/EBPα. Approximately 10% of nuclei did not stain for EdU after the "chase" period of 5 days. The strength of EdU staining varied between different nuclei, ranging from very faint to bright (Figure 4.10 A and B). There were also differences in the levels of C/EBPα expression, however the two did not appear to correlate as the strongest EdU expression was not necessarily matched with the strongest C/EBPα staining, and vice-versa (Figure 4.10 a, b and c). Interestingly within the heterogeneity, there were cells that were both strongly labelled with EdU and with C/EBPα.

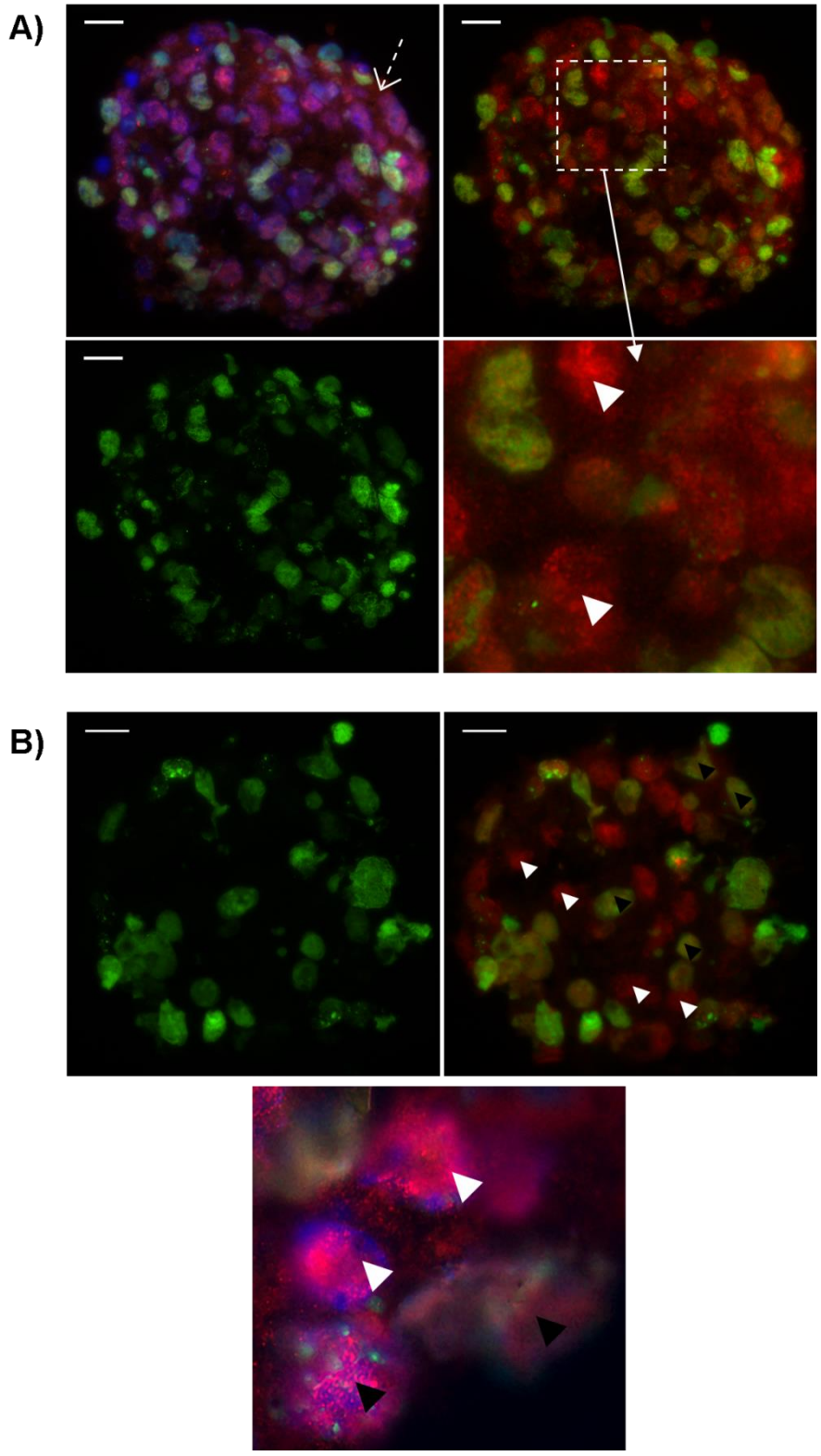

Figure 4.9: Co-localisation of EdU and C/EBPα is heterogeneous after a 48h EdU pulse A) After 48h culture C/EBPα had begun to be expressed although not entirely nuclear specific (white dotted arrow; cytoplasmic C/EBPα). Nuclear expression was apparent both in EdU positive cells; and in nuclei which had not incorporated EdU during the 48h pulse (white arrowheads). B) Spheres which were cultured for a further one day without EdU (48h pulse + 1 day) have very clear nuclear expression of C/EBPα both in EdU stained (black arrowheads) and non-stained (white arrowheads) cells. C/EBPα (red), DAPI (blue), EdU (green); Scale bars = 15μm

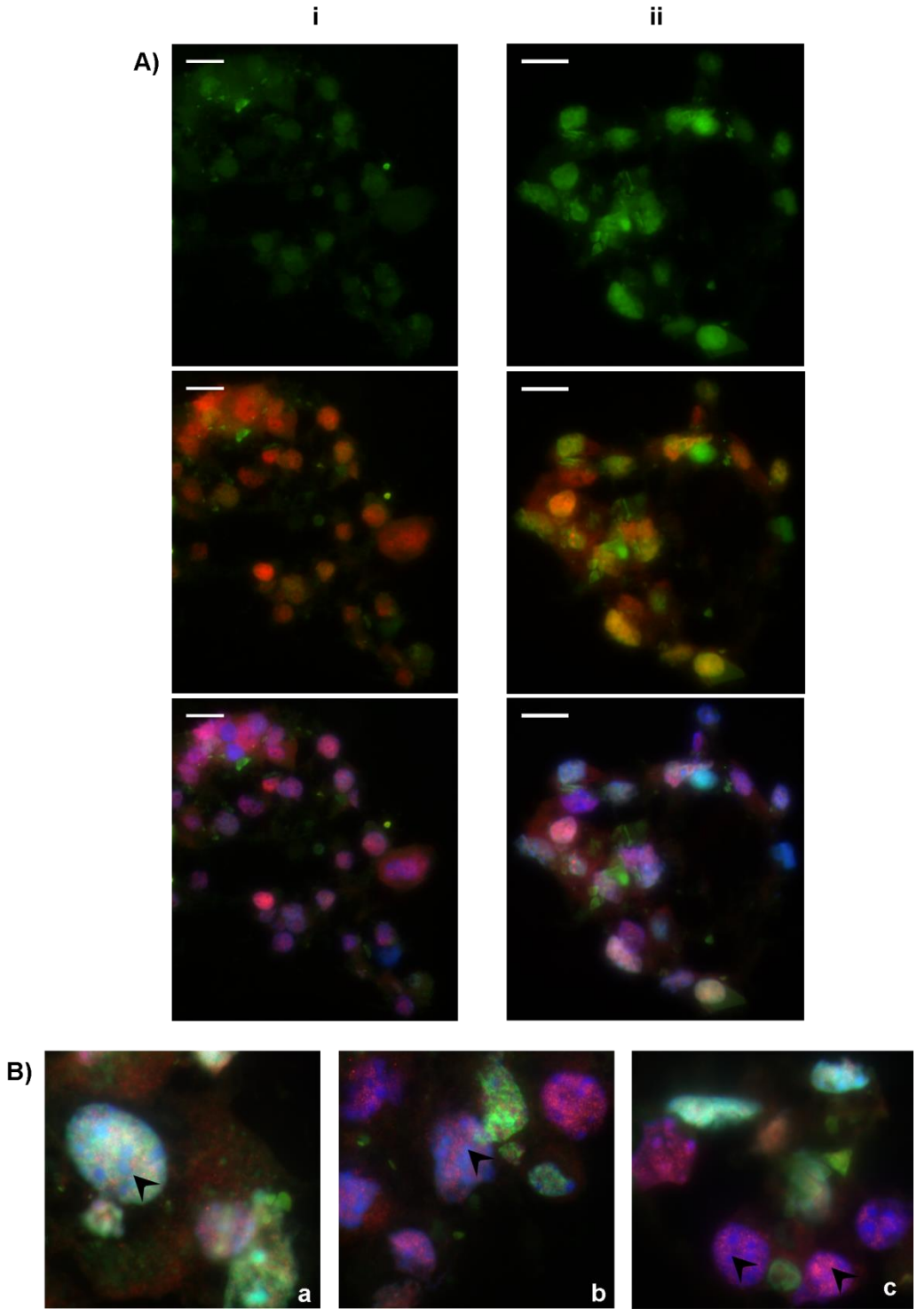

Figure 4.10: Heterogeneous C/EBPα and EdU staining and co-localisation is visible after a short 4h pulse and 5 day chase period. A) and B) E14.5 spheres cultured for a total of 8 days with a 4h EdU pulse on day 3. Representative sphere sections (i and ii) show heterogeneity of EdU incorporation and retention after 8 days. B) C/EBPα expression and EdU incorporation are not correlated as strong C/EBPα expression is visible in cells with strong EdU staining (a), weak EdU staining (b), or with no EdU staining (c). C/EBPα (red), DAPI (blue), EdU (green); Scale bars = 15μm

4.3 Discussion

In this chapter cell division was investigated in the skin during development, and in dermal cell spheres from embryonic skin, through the use of EdU incorporation into nuclei. The primary question being explored through these two model systems was the dependency of adipogenesis on cell division. The processes of cell division and differentiation have been reported to be intricately linked in adipogenesis through mitotic clonal expansion (MCE), the supposed obligatory first stage of differentiation. MCE has been assumed by many to be required in adipogenesis as it is the first phase which 3T3 cells go through after the standard hormonal induction mixture of insulin/IGF-1, dexamethasone, methylisobutylxanthine is applied to the culture system. The results presented in this chapter show the simple model in adipogenesis of 3T3-L1 cells of induction-mitotic clonal expansion-differentiation is not evident in 3D spheres or in the skin. In the dermal spheres especially, there was a great deal of heterogeneity in the timing of cell division in relation to the expression of C/EBPα, one of the key transcription factors involved in adipogenesis.

4.3.1 Cell division occurs in the back skin during development

Although employed as a method for investigating MCE, EdU pulses also allowed a more general analysis of cell division in mouse back skin during development to be undertaken. As expected, division was observed throughout the skin in the epidermis, dermis and developing hair follicles. The distribution of the division did change between the different ages. Counting of stained cells in the dermis showed that the total amount of division decreased from E14.5 to E16.5 by about 10% in the upper dermis and 7-8% in the lower dermis. Cell counting combined with a likelihood ratio test showed that the proportion of stained cells was almost universally greater in the upper dermis than the lower dermis. The likelihood ratio test showed that were approximately 10% more positive cells in the upper dermis in all three ages (E14.5, E15.5 and E16.5). Although the hypothesis being tested was against the presence of mitotic clonal expansion *in vivo*, this difference was still not foreseen as more equal proportions of cell division were expected. The results strongly suggest that there is not a clonal expansion phase

although it does not completely dispute the suggestion that cell division is essential for adipogenesis to proceed (Tang et al., 2003).

It has previously been observed that there is an absence of division in the dermal condensation of developing hair follicles (Wessels and Roessner, 1965). EdU incorporation into E14.5 back skin confirmed this result as there was a crescent shaped break in staining underneath the epidermal placode in almost all instances. Occasionally one or two EdU positive nuclei could be seen in the dermal condensation, possibly indicating a slightly further developed hair follicle.

EdU incorporation at E15.5 showed that the hair peg had started to grow down through the dermis facilitated by cell division in the epidermal and dermal parts of the developing follicle. Wessels and Roessner, 1965, noted that ^{3}H-Thymidine incorporation continued at a low frequency even once the hair peg had grown down in to the dermis and surrounded the dermal condensation to form the distinctive bulb region. Although staining here did show that EdU incorporation was greater in the epithelial cells of the follicles, there was also some staining in the dermal/mesenchymal portions of the developing hair follicle. By E16.5, when a distinct follicle bulb was visible, in some specimens the majority of follicle mesenchyme cells had been labelled during the two hour pulse, suggesting that cell division in the dermal part of the hair follicle is greater than previously described.

From a biological perspective, it is not surprising that there is cell division in the dermal portion of the developing hair follicle. The initial small number of cells in the dermal condensation has to go on to form the dermal papilla, and the dermal sheath along the side of mature hair follicle. Also from a technical point of view, the greater number of labelled cells than previously described could be due to superior sensitivity of EdU compared to BrdU or tritiated thymidine. Indeed, studies have given indications that EdU allows for more sensitive labelling. Research in 2008 found that the lower signal to noise ratio of EdU click chemistry labelling compared to BrdU immunofluorescent detection gave much better sensitivity in U2-OS and

HL60 cell lines (Cappella et al., 2008). The simpler detection method for EdU compared to BrdU has also been shown to preserve better the structural integrity of the sample (Chen et al., 2011)

The distribution of cell division in the epidermis matched what has been observed. Stem cells responsible for maintaining the different layers of the epidermis are contained within the basal stratum; hence the most division was seen in this layer next to the basement membrane (Braun et al., 2003). At E14.5 the epidermis was only two-to-three layers and there was some division in all layers although the most was in the innermost layer. As the epidermis thickened into more layers the division became confined to these basal cells adjacent to the basement membrane.

The original experimental plan was to use the organ culture model for investigation of mitotic clonal expansion through pulse chase experiments; however this had more problems than expected. As discussed in chapter 3, the substrate organ culture model was unreliable over 3/4 days as the skin often became pathological and produced fat through a stress response rather than adipogenesis. This was exacerbated by the requirement of changing the culture medium to remove EdU for the "chase" period. Aside from the unreliability of the culture system, it would also have been difficult to clearly link EdU-positive nuclei with cells undergoing adipogenesis in the skin. Therefore, focus shifted to the 3D spherical cell culture model which yielded some interesting results.

4.3.2 Cell division in 3D spherical cell culture

Uptake of EdU into DNA in cells within spheres was seen after the long 48h pulse. It was also seen after spheres were incubated with EdU for just 4 hours. Most of the cells were strongly immunoreactive for EdU after they had been incubated with the analogue for 48h. This suggests that most of them were preparing to divide and may have done so during that time. Culture of some spheres continued after removal of EdU from the medium. The EdU staining became progressively weaker dependent on the number of days of culture after removal of EdU. Equally the small number of cells

strongly labelled during the 4h pulse, increased to many weakly labelled cells after a further five days of culture. These two observations together strongly imply that cells continued to divide throughout the length of the culture.

One of the key features of mitotic clonal expansion in the standard cell line model of adipogenesis is the synchronous nature of re-entry into the cell cycle after induction and the subsequent quiescence after one/two rounds of cell division. This single progression of events was not evident in dermal cells in the spherical cell culture model. Double staining of cells with EdU and C/EBPα showed a lot of heterogeneity in the strength of immunoreactivity. As shown in the results, some cells were stained brightly for EdU and C/EBPα. These cells fit with the model of quiescence before terminal differentiation as the strong presence of EdU analogue within the DNA makes it unlikely that they had divided many times. Several other cells, however, only had very weak staining of EdU suggesting it had been diluted out through many rounds of DNA replication cell division.

A particularly interesting observation about cells with weak EdU staining was that they simultaneously immunoreactive for C/EBPα. In the spheres, it appeared that cells continued dividing throughout the culture even after they became reactive for C/EBPα. It is generally accepted that both C/EBPα and PPARγ are anti-mitotic hence their appearance in cultured cells only after MCE has taken place (Jiang and Lane, 2000). The 30 kDa isoform of C/EBPα, however, has been reported to lack anti-mitotic activity (Lin et al., 1993). Finally, there were also cells visible which had no EdU staining but had strong C/EBPα expression. This lack of EdU expression could either be due to the cell not taking up label during the pulse, or alternatively the EdU could have become entirely diluted out of the DNA by a large number of subsequent divisions. The heterogeneity of EdU staining described strongly suggests that cells in this 3D model do not need to undergo MCE before differentiation.

Chapter 5

Bioinformatic analysis of microarrays for the identification of miRNAs involved in adipogenesis, and verification through qPCR

5.1 Introduction

MicroRNAs are small, endogenous, non-coding pieces of RNA about 20-25 nucleotides in length. They were originally discovered in C. elegans but are now known to exist in plants, vertebrates and invertebrates (Lee et al., 1993; Rana, 2007; Romao et al., 2011). Since their discovery, a very large number of different miRNAs have been identified and linked to a range of developmental and metabolic processes (Esau et al., 2004; Lin et al., 2009). miRNAs have been profiled by microarray to try and gain an understanding of their role in adipogenesis however, due to differences in model systems, induction media, and array platforms there has been very little agreement between different studies. This has led to a large number of miRNAs being identified as being up- or down-regulated during the adipogenic pathway with very few being investigated further. In order to carry out a preliminary investigation of microRNA activity during adipogenesis *in vivo* I adopted a dual approach. This involved retrospectively interrogating microarray data existing in the Jahoda laboratory to identify miRNAs potentially associated with regulation of adipogenesis, and that were also referred to in the literature. Additionally, other microRNAs highlighted solely by the literature were also investigated.

miRNA-143 has been identified in several different arrays as being upregulated during adipogenesis possibly having an effect through the ERK signalling pathway. Its expression has mainly been investigated in primary human adipocytes however it has also been shown to be upregulated on microarrays of 3T3-L1 cells during adipogenesis. Inhibition of miR-143 stops adipogenic differentiation however overexpression is not enough to stimulate adipogenesis without another adipogenic stimulant. Investigation of protein levels identified ERK5 (extracellular signal-related kinase) as a potential target of miR-143 (Esau et al., 2004). A heparin-binding growth factor, pleiotrophin (PTN) has also been suggested to be a miR-143 target (Yi et al., 2011). One report contradicted other theories suggesting that miR-143 is not important for adipose tissue development; however the knockdown technique was only employed in newborn mice from one day onwards which could have been too late to show an effect (He et al., 2012). This study also found that

ERK5 was not a target for miR-143 in mice, instead identifying FGF-7. miR-143 has also been implicated in porcine adipogenesis (Wang et al., 2011).

Multiple members of the let-7 gene family (particularly a, b, and g) have also been identified on microarrays carried out in 3T3-L1 and epididymal fat cells. The results surrounding this miRNA are confused as it has been shown to be upregulated from day 1 of the differentiation process leading to the conclusion that it is pro-adipogenic, however ectopic expression in 3T3-L1 cells before hormonal induction inhibited differentiation (Sun et al., 2009). It has been proposed that it is involved in exit from the cell cycle through interaction with HMGA2 (High motility group AT-hook 2). A recent paper first linked miR-374 to porcine adipogenesis (Pan et al., 2013). Both miR-374a and miR-374b are thought to target C/EBPβ, an early acting adipogenesis gene. Dexamethasone treatment of primary porcine adipocytes upregulated miR-374a and b, ultimately promoting terminal differentiation and accumulation of fat droplets (Pan et al., 2013).

MiR-130a and miR-27b are thought to inhibit adipogenesis. The miR-27 gene family is one of the most widely studied. Both members of the family, miR-27a and miR-27b, are anti-adipogenic. Microarray data shows them to be downregulated during adipogenesis and overexpression in 3T3-L1 preadipocyte cultures inhibits their differentiation into mature adipocytes (Lin et al., 2009). Overexpression of miR-27 also inhibited the adipogenic differentiation of OP9 cells, a multipotent mesenchymal cell line, when they were treated with adipogenic stimulants (Lin et al., 2009). In 3T3-L1 preadipocytes, adipogenesis was strongly suppressed through overexpression of miR-130a, and enhanced by a knockdown method (Lee et al., 2011). It is thought to target PPARγ, one of the transcription factors involved in adipogenesis.

In this chapter I describe preliminary qPCR work on five miRNAs which have been linked to adipogenic development, focusing on expression in mouse back skin. The miRNAs investigated were miR-374, miR-143, miRNA let-7a, miR-130a, and miR-27b.

5.2 Results

5.2.1 Selection of potential microRNAs

A large number of miRNAs have been identified in the literature as being potentially involved in adipogenesis, mainly through microarray of preadipocyte cell lines before and after differentiation. Relatively few of these have been verified through PCR or blotting techniques however. In order to narrow down the selective and gain some idea of miRNAs relevant in the dermal fat layer, bioinformatic analysis was undertaken of microarray data from E17, E18, and E19 upper and lower dermis (K. Wojciechowicz, PhD thesis). Microarray raw data was analysed using the iGET FIRE software which identifies DNA and RNA regulatory binding motifs within genes in the array data (Elemento et al., 2007).

The majority of regulatory motifs identified by the programme were at the 5' end mapping to transcription factors however 3'-untranslated region (UTR), the location of miRNA binding, motifs were also identified. Of these, only a small number were associated with identified miRNAs. Due to time restraints and the small scale of this study it was decided to only investigate miRNAs which had already been linked to adipogenesis. MicroRNA-374 and let-7a were therefore selected from the FIRE results to be investigated further as they had previously been shown to be involved in adipose tissue development. Three more miRNAs were selected purely from literature searches: miRNA-143, miRNA-27b, and miRNA 130a. Of the five microRNAs selected for investigation, three are thought to be pro-adipogenic and the other two anti-adipogenic (Table 5.1).

MicroRNA	Identification method	Adipogenic effect	Sequence and chromosome (chr)
miR-374	FIRE and literature	Pro-adipogenic	AUAUAAUACAACCUGCUAAGUG Chr X
let-7a	FIRE and literature	Pro-adipogenic	UGAGGUAGUAGGUUGUAUAGUU Chr 13
miR-143	Literature	Pro-adipogenic	UGAGAUGAAGCACUGUAGCUC Chr 18

miR-27b	Literature	Anti-adipogenic	UUCACAGUGGCUAAGUUCUGC Chr 13
miR-130a	Literature	Anti-adipogenic	CAGUGCAAUGUUAAAAGGGCAU Chr 2

Table 5.1: miRNAs selected for quantification in mouse back skin using qPCR. miRNAs chosen for investigation were selected through bioinformatic analysis of microarray data using a motif identification software (FIRE), or through literature searches.

5.2.2 Quantitative polymerase chain reaction of microRNAs

To explore the role of selected miRNAs in adipogenesis in the lower dermal adipose tissue depot, samples were prepared from back skin of embryos at embryonic days 14.5, 16.5, and 17.5. Aside from laser capture microdissection there is no way to separate the cells of the upper and lower dermis therefore RNA was from the whole dermis, which had been enzymatically separated from the epidermis above, and the subcutaneous fat depot below the skin. RNA was also taken from the separated epidermis at each age. Expression was explored using qPCR and fold changes were calculated using E14.5 samples as the baseline. Due to time restraints the data presented in the following graphs are only representative of one biological sample and would therefore need to be repeated for verification of the results.

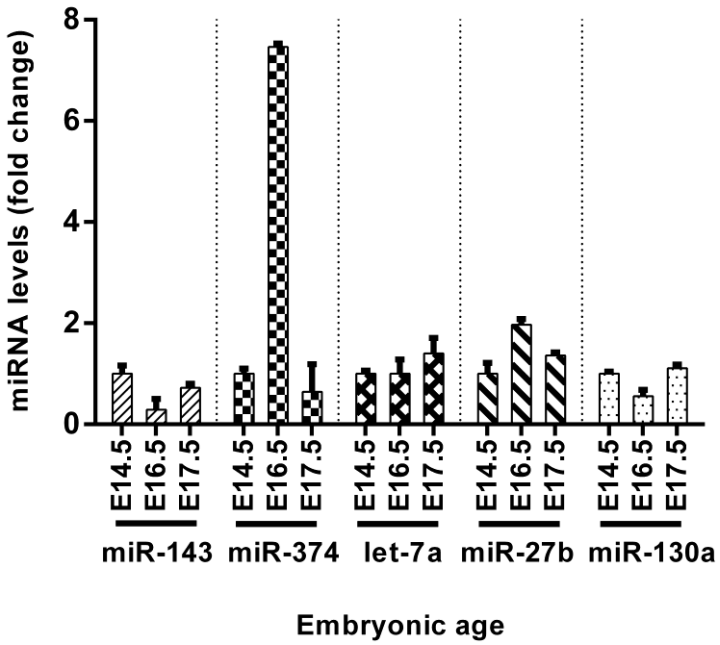

Figure 5.1: qPCR of E14.5, E16.5 and E17.5 dermal samples. MicroRNA expression levels remained similar between E14.5 and E17.5 except miR-374 which was greatly upregulated between E14.5 and E16.5. RNA samples were prepared from mouse back skin dermis at each age. Expression of each miRNA is shown as a fold change from E14.5. Data shows mean ± s.e.m. n=3 (technical replicates)

The results showing expression of the miRNAs in the dermis and epidermis are shown in Figure 5.1 and 5.2 and the first observation was that all of the miRNAs investigated were present in both tissues at all time points (E14.5, E16.5 and E17.5). In the dermis the miRNAs generally stayed at a similar expression level between the ages. miR-374 was the only one which showed considerable increase between E14.5 and E16.5 before decreasing at E17.5. Both miR-143 and -130a decreased between E14.5 and E16.5 before increasing at E17.5. Conversely, miR-27b increased from E14.5 to E16.5 and then dropped again at E17.5. The expression level of microRNA let-7a remained constant between E14.5 and E16.5, and then increased slightly at E17.5 (Figure 5.1).

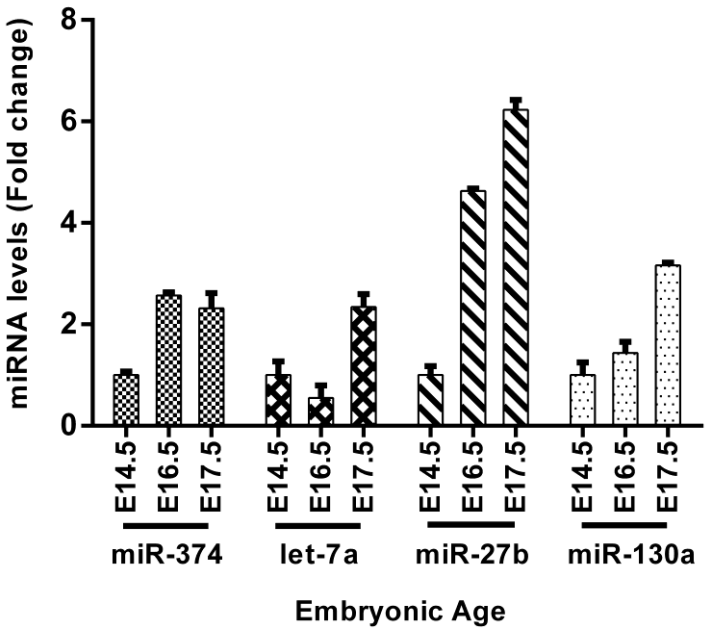

Figure 5.2: qPCR of E14.5, E16.5, and E17.5 epidermal samples. There was a general upward trend of the investigated miRNAs from E14.5 to E17.5. RNA samples were prepared from mouse back skin epidermis at each age. Expression of each miRNA is shown as a fold change from E14.5. Data shows mean ± s.e.m. n=3 (technical replicates)

MicroRNA levels in the epidermis changed more noticeably between the ages than in the dermis. The two anti-adipogenic miRNAs (miR-27b and -130a) in particular showed the same upward trend with increasing embryonic age. miR-27b expression increased slightly between E14.5-E16.5 and then more at E17.5 (Figure 5.2). mi-130a expression largely increased between E14.5 and E16.5 with a smaller increase to E17.5. Expression of let-7a was the only one which decreased between E14.5 and E16.5 but it then increased at E17.5. miR-374 also increased from E14.5 to E16.5 and then dropped slightly by E17.5 (Figure 5.2).

5.3 Discussion

Research into microRNAs is a growing area of interest as it is clear that they have important roles in regulating gene expression. A number of functions have already been identified particularly in development and cancer biology (Sayed and Abdellatif, 2011). The work presented in this chapter explored the expression of five miRNAs in the epidermis and dermis of embryonic mouse back skin.

5.3.1 miRNA expression in the dermis

The five miRNAs investigated were all found to be present in the dermis at each timepoint (E14.5, E16.5, and E17.5). Work presented in chapter 3 outlines a hypothesis that fat development in the lower dermis starts at around E14.5 therefore it is unsurprising that the miRNAs investigated are already present in the dermis at this time. It is hard to decipher the variations in miRNA dermal expression, however, as the RNA was extracted from the whole dermis and not just the lower dermis where fat development is occurring. It is possible that their expression simultaneously increases and decreases in the upper and lower dermis respectively. In addition, although all of these miRNAs were being investigated from the point of view of their role in adipogenesis, it must be pointed out that miRNAs are thought to act on several targets therefore they could also have separate roles in the skin in parallel with fat development.

The point made above about the difficulty in interpretation is particularly relevant for the dermal expression of miR-130a and miR-27b. These two miRNAs are proposed to be anti-adipogenic as their expression levels decrease during adipogenesis (Lin et al., 2009; Lee et al., 2011). As such it may have been expected that they would reduce in expression in older dermal samples. This was not entirely the case as miR-27b increased from E14.5 to E16.5 before decreasing slightly, and miR-130a decreased before returning to almost the same expression level at E17.5 as at E14.5. Although these expression levels will need to be verified in biological replicates, it does suggest that these miRNAs may be increase in the upper

dermis to suppress adipogenic differentiation whilst concurrently decreasing in the lower dermis to allow adipogenesis to proceed.

Both miR-27b and miR-130a have previously been examined in cell culture and are thought to directly target PPARγ mRNA with binding sites in the coding region and the 3'-UTR (Karbiener et al., 2009; Kim et al., 2010; Lee et al., 2011). miR-27b over-expression inhibited differentiation in 3T3-L1 preadipocytes, OP9 MSCs, and human multipotent adipose-derived stem cells (Karbiener et al., 2009; Lin et al., 2009). It was found that transfection of miR-27b at the before, or at the same time as, induction inhibited differentiation, but if it was transfected after 24 or 48h there was no significant effect (Lin et al., 2009). Over-expression of miR-130a in 3T3-L1 cells similarly inhibited adipogenesis (Lee et al, 2011).

miR-374, identified through FIRE analysis of microarray data, had the greatest increase in dermal expression between E14.5 and E16.5 suggesting it is important for the differentiation process. This fits well with a recent paper identifying C/EBPβ as a target of miR-374 in dexamethasone-induced differentiation of porcine adipocytes. miR-374 binds C/EBPβ at a highly conserved site in the 3'-UTR targeting the mRNA for degradation. If miR-374 is ectopically added to the culture before induction of differentiation, it has an inhibitory effect, adding support for its role being later in differentiation (Pan et al., 2013).

Let-7a was the other miRNA identified from FIRE analysis. The qPCR results showed that expression of let-7a remained level between in E14.5 and E16.5 dermis. Previous research has shown that, in 3T3-L1 cells, let-7a decreased on the first day after induction before increasing again and continuing to gain in expression throughout differentiation (Sun et al., 2009). Additional ages would need to be analysed to establish if this also occurs in back skin however the constant expression seen suggests that it is already being expressed at E14.5.

Let-7a has been suggested to have a role in cell proliferation as over-expression in culture impairs mitotic clonal expansion and reduces the number of cells in the S-phase of the cell cycle (Sun et al., 2009). Over-expression in mice reduces their body mass which may initially seem a strange observation as let-7a is proposed to be pro-adipogenic. It is suggested however that this effect is a result of progenitor cells having reduced proliferation and instead being pushed to differentiate (Frost and Olsen, 2011). The role of let-7a would be interesting to investigate in the spherical cell culture model as it was found that cells in the spheres are able to proliferate and differentiate simultaneously.

The final microRNA explored was miR-143 which has also been one of the most extensively investigated in culture, in 3T3-L1 cells and porcine preadipocytes, and *in vivo*. Although it is generally thought to be pro-adipogenic acting to accelerate adipogenesis (Esau et al., 2004; Xie et al., 2009), an *in vivo* study concluded that it was not important fat development as adipose tissue was not affected by knock-down of endogenous miR-143 (He et al., 2011). This study, however, was conducted using post-natal animals up to 1 month after birth which may have been too late for knockdown to have an effect. The expression of miR-143 was present in the dermis at all three ages investigated and there was only a small fold change between the ages. Expression decreased slightly at E16.5 and then increased again at E17.5. This pattern suggests that it may be important early in differentiation.

Several targets for miR-143 have been suggested including ERK5, which can act as part of the MAPK signalling pathway, and KGF (FGF7). In human preadipocytes it was found that knockdown of miR-143 expression upregulated ERK5 after 7-10 days of differentiation (Esau et al., 2004). In 3T3-L1 cells and primary mouse preadipocytes, however, miR-143 was not able to inhibit ERK5 expression but FGF7 was significantly reduced in both types of cells (He et al., 2012).

As stated at the opening of this discussion, the results of miRNA expression in the dermis are extremely difficult to interpret due to extraction from the whole dermis. The results presented are only drawn from one biological replicate however it may have more significance to use laser capture microdissection to separately collect samples from the upper and lower dermis for comparison. These results do, however, confirm the presence of the examined miRNAs in the dermis. The availability of mimics and inhibitors of miRNAs would allow investigation of their role through modulation of the model systems described in chapter 3.

5.3.2 miRNA expression in the epidermis

Although not the primary focus of this study, the expression of four of the miRNAs was also explored in the epidermis. Contrary to the variable results in the dermis, expression in the epidermis generally showed an upward trend from E14.5 to E17.5. In particular miR-130a and miR-27b were both upregulated from E14.5 to E17.5 in the epidermis. This is consistent with their proposed role in inhibition of fat development and lipid accumulation (Lin et al., 2009; Lee et al., 2011). miR-130a, in particular was highly upregulated between E14.5 and E16.5 suggesting that it may also have another distinct function in development of the epidermis. Although, recently it was found to be involved in inhibition of cutaneous wound healing (Pastar et al., 2012).

The expression of miRNA let-7a in the epidermis shows a pattern of decreasing expression before increasing. It is possible that this is due to some fat accumulation, such as in sebaceous glands (Picardo et al., 2009). Let-7a is expressed in a wide range of tissues, however, and is thought to have a role in cell proliferation and so it could have another distinct role in the epidermis (Wulczyn et al., 2007; Legesse-Miller et al., 2009). Of all the miRNAs investigated, the least is currently known about miR-374. The increase in expression in the epidermis between E14.5 and E16.5 suggests that it may be involved in the development process.

Chapter 6

Final Discussion and Future work

6.1 Investigation into the timing of adipogenesis in the lower dermis through *in vivo*-like model systems

As described in chapter 1, the majority of research into the process of adipogenesis, particularly the molecular events, has been done with 2D culture of fibroblastic or preadipocyte cell lines such as 3T3-L1 cells. The work in chapter 3, therefore, aimed to establish a 3D model system with characteristics more similar to the *in vivo* situation. Although the substrate organ culture model had previously been used in the Jahoda lab for a small study of EGFR in adipogenesis, the work in this thesis shows that the results are highly unreliable due to large variations in the healthiness of cultured skin. Of the two models developed, the spherical cell culture model has so far given the most intriguing results.

The work presented in chapter 3 of this thesis shows that dermal cells isolated from young embryonic mice, E14.5 onwards, are able to develop into adipocytes and accumulate lipids. This discovery has opened up several further avenues for investigation related to the timing of adipogenesis in the lower dermis. Experiments in both model systems established should reveal more interesting information. Collagen IV staining of mouse back skin at E14.5 revealed differences between the upper and lower dermis already present. This raises the question of when distinctions between the two layers begin to manifest and at what age cells first become committed to a developmental lineage.

Another interesting question is the signalling being exerted on lower dermal cells influencing them to undergo adipogenesis. A possibility is that the adipocyte lineage is actually the default pathway and it is signalling from the epidermis above which prevents cells in the upper dermis from differentiating. However, without epidermal influence (examined carefully with cytokeratin staining) in the 3D spherical culture model, still only approximately 50% of cells underwent adipogenesis. This suggests that at the young age of E14.5, cells in the upper and lower dermis are already committed to distinct developmental lineages. Culture of dermal cells from E13.5 mouse back skin would therefore be interesting to explore, firstly, to

discover whether they are able to differentiate, and secondly, the proportion which do so.

It has also been suggested that adipogenesis is closely linked with hair follicle development (Schmidt and Horsley, 2012). In pigs, outer subcutaneous fat contains clusters located around the base of hair follicles which differ in their developmental properties to other outer adipocytes (Hausman and Kauffman, 1982). The discovery that adipogenesis in the lower dermis starts at around E14.5 at the same as hair follicle development further strengthens this theory. It would therefore be interesting to examine the effects of blocking hair follicle development.

The spherical cell culture model was also used in chapter 2 to investigate the expression of C/EBPα. The results show that during culture of E14.5 dermal cells, C/EBPα is specifically expressed in the nucleus of differentiating cells from approximately 3/4 days until the end of the culture at 8 days. Intriguingly, expression of this protein was less clearly nuclear in spheres of older dermal cells. The expression also appeared to leave the nucleus by the end of the culture. C/EBPα, along with PPARγ, has previously found to be continually expressed in mature adipocytes, thought to be in order to maintain adipocyte-specific gene expression (Siersbaek et al., 2012). Thus, it is interesting that expression in spheres of dermal cells from E15.5-E17.5 mice showed loss of expression of C/EBPα by the end of the culture time. It may be that taking cells from older embryonic mice, which were already part way through the differentiation process when they were isolated, resulted in differing expression of the transcription factor. E14.5 cells, by contrast, cultured from early in the adipogenic pathway, may have allowed specific nuclear expression of the transcription factor. Culturing E14.5 spheres for 2/3 more days would reveal whether C/EBPα does also eventually leave the nucleus in these cells or if expression is maintained.

The C/EBPα transcription factor is one of the key proteins involved in the molecular control of adipogenesis however it is only one component of a hugely complex and tightly controlled network. It would be interesting,

therefore, to explore the timing of expression of other proteins thought to be involved particularly C/EBPβ and δ which are among the earliest transcription factors expressed in 3T3-L1 cells (Tang and Lane, 2000; Hishida et al., 2009). These two transcription factors reportedly act together to activate later transcription factors, including C/EBPα and PPARγ (Siersbaek et al., 2012).

To summarise, contrary to prior research which suggests adipogenesis in the lower dermis begins around E16.5 (Wojciechowicz, 2011), work in this thesis suggests that the developmental processes start earlier, at approximately embryonic day 14. Cells from this age are capable of developing into adipocytes, and E14.5 skin cultured for three or four days clearly shows specific adipogenic differentiation in the lower dermis by the expression FABP4.

6.2 The mitotic clonal expansion stage

As discussed in the introduction to chapter 4, the mitotic clonal expansion stage of 1-2 rounds of cell division prior to adipogenesis is a controversial process in cell culture. The first experiments in 3T3-L1 cells using hormonal induction always observed this stage and so it became accepted as part of adipogenic differentiation. In further investigation however, Qui et al., 2001, countered this with experiments to block cell division showing that adipogenesis could still proceed. Tang et al., 2002, however, still argue that it is a required synchronous process. A number of other theories have been put forward in including a hypothesis that cells need to progress through the S-phase of mitosis in order to commit to differentiate, but do not require the 1-2 rounds of complete cell division seen in MCE (Cho and Jefcoate, 2004).

Work in chapter 4 attempted to answer the question of whether cell division is required before adipogenesis can proceed and the results follow the conclusion that it is not. Firstly, in back skin sections: exploration of cell division in the back skin of three ages (E14.5, E15.5, and E16.5) did not show evidence for a clonal expansion phase taking place in the lower dermis. Indeed contrary to this, nuclei counts, and subsequent statistical analysis,

actually revealed more cell division in the upper dermis. Secondly spherical culture of dermal cells gave interesting heterogeneous results. Cells were able to differentiate with or without several rounds of cell division. These results strongly suggest that cell division is not a requirement in adipogenesis, however, a logical next stage of experimentation would be to block cell division in the spherical culture. It would not be feasible inhibit cell division in cultured back skin as it would also interfere with other processes such as hair follicle development, and therefore would not be a genuine test of mitotic clonal expansion. Cho and Jefcoate, 2004, also proposed that DNA replication in the S-phase of the cell cycle, but not complete movement through mitosis therefore it may be interesting to explore this further through inhibition of G2-M phase transition.

In summary, the controversial process of mitotic clonal expansion does not appear to be required for adipogenesis in the lower dermis. In agreement with other research, adipogenesis in the spherical culture appeared to be able to proceed without the cells first dividing. Equally contrary to dogma on MCE, cells continued through the cell cycle after expression of C/EBPα and accumulation of lipids.

6.3 MicroRNAs in adipogenesis

The discovery of miRNAs has revealed a new level of control for protein expression. MicroRNAs act by binding to the 3' UTR of their target mRNA, either suppressing translation, or targeting the mRNA for degradation (Rana, 2007). Exploration of miRNAs in the adipogenic process, many through microarrays of *in vitro* preadipocytes before and after hormonal induction, has resulted in extensive lists of potential miRNAs. In the most part, verification of these, however, is yet to be carried out, particularly *in vivo*.

The work in chapter 5 provides a small insight into miRNAs present in mouse back skin at E14.5, E16.5, and E17.5. The five miRNAs explored were all found to be present in the dermis and epidermis in all of these ages although in differing levels. The qPCR work presented however is only

representative of one biological sample therefore the first stage of future work would be to achieve replicates of this data. For each miRNA, the expression levels were compared to those at E14.5. Chapter 3, however, concludes that adipogenesis appears to already be underway at this timepoint therefore it may be more beneficial to acquire data from an earlier age for use as the baseline of expression. Interestingly, miR-374 was found to greatly upregulated at E16.5 compared to E14.5 suggesting that it acts later in the differentiation program. This timescale links in well with the suggested target for miR-374: C/EBPβ (Pan et al., 2013), which is thought to be one of the earliest acting transcription factors which is then downregulated after 1-2 days (Payne et al., 2010).

All of the miRNAs investigated have been linked to adipogenesis in the literature however their specific roles are generally unknown, although potential targets have been identified (Esau et al., 2004; Pan et al., 2013). Inhibitors and mimics of miRNAs are available providing the opportunity to interfere with adipogenesis in both of the model systems established in chapter 3. The spherical cell culture model, in particular, has the potential to show the isolated effect of miRNAs in dermal cells, whereas the substrate organ culture model could provide a more holistic view. Using material at different ages should also allow analysis of when each miRNA is acting.

To summarise, the investigation of miRNAs in adipogenesis is still in the early stages and their role is not yet fully understood and appreciated. In the small study in chapter 5, it was found that the five miRNAs investigated are all present in the back skin of embryonic mice. Now that their presence has been confirmed, research can be undertaken to elucidate each of their roles.

Chapter 7

Bibliography

Alonso, L. and Fuchs E. (2006). The Hair Cycle. *J. Cell Sci.* **119**, 391-393

Arner, E., Westermark, P.O. Spalding, K.L., Britton, T., Rydén, M., Frisén, J., Bernard, S., Arner, P. (2010). Adipocyte turnover: relevance to human adipose tissue morphology. *Diabetes*. **59**, 105-109

Asaki, T., Konishi, M., Miyake, A.,Kato, S., Tomizawa, M., Itoh, N. (2004). Roles of fibroblast growth factor 10 (Fgf10) in adipogenesis in vivo. *Mol. Cell. Endocrinol.* **218**, 119-128

Ban, A., Yamanouchi, K., Matsuwaki, T., Nishihara, M (2008). In vivo gene transfer of PPAR gamma is insufficient to induce adipogenesis in skeletal muscle. *J. Vet. Med. Sci.* **70**, 761-767

Banerjee, S. S., Feinberg, M. W., Watanabe, M., Gray, S., Haspel, R. L., Denkinger, D. J., Kawahara, R., Hauner, H., Jain, M. K. (2003). The Kruppel-like factor KLF2 inhibits peroxisome proliferator-activated receptor-gamma expression and adipogenesis. *J. Biol. Chem.* **278**, 2581-2584

Beningo, K. A., Dembo, M., Wang, Y. (2004). Responses of fibroblasts to anchorage of dorsal extracellular matrix receptors. *PNAS*. **101**, 18024–18029

Billon, N., Monteiro, M.C., Dani, C. (2008). Developmental origins of adipocytes: new insights into a pending question. *Biol. Cell.* **100**, 563-575

Billon, N., Monteiro, M.C., Glavieux-Pardanaud, C., Richardson, W.D., Kassaris, N., Dani, C., Dupin, E. (2007). The generation of adipocytes by the neural crest. *Development*. **134**, 2283-2292

Birgersdotter A, Sandberg R, Ernberg I. (2005) Gene expression perturbation in vitro - a growing case for three-dimensional (3D) culture systems. *Semin. Cancer Biol*. **15**, 405-412

Birsoy, K., Berry, R., Wang, T., Ceyhan, O., Tavazoie, S., Friedman, J.M., Rodeheffer, M.S. (2011). Analysis of gene networks in white adipose tissue development reveals a role for ETS2 in adipogenesis. *Development.* **138**, 4709-4719

Bost,F., Caron,L., Marchetti, I., Dani, C., Le Marchand-Brustel, Y. Binetruy, B. (2002). Retinoic acid activation of the ERK pathway is required for embryonic stem cell commitment into the adipocyte lineage. *Biochem. J.* **361**, 621-627

Bowers R.R., Lane, M.D. (2008). Wnt signalling and adipocyte lineage commitment. *Cell cycle*. **7**, 1191-1196

Braun, K.M., Niemann, C., Jensen, U.B., Sundberg, J.P., Silva-Vargas, V., Watt, F.M. (2003). Manipulation of stem cell proliferation and lineage commitment: visualisation of label-retaining cells in wholemounts of mouse epidermis. *Development.* **130**, 5241-5255

Breen, E.P., Gouin, S.G., Murphy, A.F., Haines, L.R., Jackson, A.M., Pearson, T.W., Murphy, P.V., Porter, R.K. (2006). On the mechanism of uncoupling protein 1 function. *J. Biol. Chem.* **281**, 2114-2119

Brysk, M., Snider, J.M., Smith, E.B. (1981). Separation of newborn rat epidermal cells on discontinuous isokinetic gradients of Percoll. *J. Invest. Dematology*. **77**, 205-209

Calonje, J.E., Brenn, T., Lazar, A.J., McKee, P.H. (2011). McKee's Pathology of the Skin.

Cao, Z., Umek, R.M., McKnight, S.L. (1991). Regulated expression of three C/EBP isoforms during adipose conversion of 3T3-L1 cells. *Genes & Dev.* **5**, 1538-1552

Cappella, P., Gasparri, F., Pulici, M., Moll, J. (2008). A novel method based on click chemistry, which overcomes limitations of cell cycle analysis by classical determination of BrdU incorporation, allowing multiplex antibody staining. *Cytometry Part A*. **73**, 626-636

Chen, M., Qu, D., Chi, W., Ren, X., Cong, S., Liang, P., Feng, S., Zhang, B. (2011). 5-Ethynyl-2′-deoxyuridine as a molecular probe of cell proliferation for high-content siRNA screening assay by “click” chemistry. *Science China Chemistry*. **54**, 1702-1710

Chuong, C. M., Nickoloff, B. J., Elias, P. M., Goldsmith, L. A., Macher, E., Maderson, P. A., Sundberg, J. P., Tagami, H., Plonka, P. M., Thestrup-Pedersen, K., Bernard, B. A., Schroder, J. M., Dotto, P., Chang, C. H., Williams, M. L., Feingold, K. R., King, L. E., Kligman, A. M., Rees, J. L., Christophers, E. (2002). What is the ‘true’ function of skin? Viewpoint 1. *Exp. Dermatol.* **11**, 159-163

Cinti, S. (2001). The adipose organ: morphological perspectives of adipose tissues. *P. Nutr. Soc.* **60**, 319-328

Cinti S (2007) In: Fantuzzi G and Mazzone T (Eds.) *Nutrition and Health: Adipose Tissue and Adipokines in Health and Disease*, pp. 3-19. © Humana Press Inc., Totowa, NJ. ISBN: 978-1-58829-21-1

Clarke, S. L., Robinson, C. E., Gimble, J. M. (1997). CAAT/enhancer binding proteins directly modulate transcription from the peroxisome proliferator-activated receptor gamma 2 promoter. *Biochem. Biophys. Res. Comm.* **240**, 99-103

Dani, C., Smith, A.G., Dessolin, S., Leroy, P., Staccini, L., Villageois, P., Darimont, C., Ailhaud, G. (1997). Differentiation of embryonic stem cells into adipocytes in vitro. *J. Cell Sci.* **110**, 1279-1285

Date, T., Doiguchi, R., Nobuta, M., Shindo, H. (2004). Bone morphogenetic protein-2 induces differentiation of multipotent C2H10T1/2 cells into osteoblasts, chondrocytes, and adipocytes in vivo and in vitro. *J. Orthop. Sci.* **9**, 503-508

Esau, C., Kang, X., Peralta, E., Hanson, E., Marcusson, E.G., Ravichandran, L.V., Sun, Y., Koo, S., Perera, R.J., Jain, R., Dean, N.M., Freier, S.M., Bennett, C.F., Lollo, B., Griffey, R. (2004). MicroRNA-143 Regulates Adipocyte Differentiation. *J. Biol. Chem.* **279**, 52361-52365

Farmer, S.R. (2005). Regulation of PPAR gamma activity during adipogenesis. *Int. J. Obesity.* **29**, S13-S16

Foty, R. (2011). A simple hanging drop cell culture protocol for generation of 3D spheroids. *J. Vis. Exp.* **51**, 2720

Fuchs, E. (1990). Epidermal differentiaion: the bare essentials. *J. Cell. Biol.* **111**, 2807-2814

GE Healthcare. Ficoll PM400 Data File 18-1158-27 AB

Genever, P.G. (2010). The generation of three-dimensional tissue strucutres with mesenchymal stem cells. *ATLA*. **38**, 31-34

Gerin, I., Bommer, G.T., McCoin, C.S., Sousa, K.M., Krishnan, V., MacDougald, O.A. (2010). Roles for miRNA-378/378* in adipocyte gene expression and lipogenesis. *Am. J. Physiol. Endocrinol. Metab.* **299**, 198-206

Gesta, S., Blüher, M., Yamamoto, Y., Norris, A.W., Berndt, J., Kralisch, S., Boucher, J., Lewis, C., Kahn, C.R. (2006). Evidence for a role of developmental genes in the origin of obesity and body fat distribution. *Proc. Natl. Acad. Sci. USA.* **103**, 6676-6681

Green, H. and Kehinde, O. (1974). Sublines of mouse 3T3 cells that accumulate lipid. *Cell*. **1**, 113-116

Green, H., Mueth, M. (1974). Established pre-adipose cell line and its differentiation in culture. *Cell*. **3**, 127-133

Gu, D., Yu, B., Ye, W., Lv, Q., Hua, Z., Ma, J., Zhang, Y. (2007) The effect of pleiotrophin signaling on adipogenesis. *FEBS Letts.* **581**. 382-388

Gudjonsson, J.E., Johnston, A., Dyson, M., Valdimarsson, H., Elder, J.T. (2007). Mouse models of psoriasis. *J. Invest. Dematol.* **127**, 1282-1308

Hamm, J.K., Park, B.H., Farmer, S.R. (2001). A role for C/EBP beta in regulation peroxisome proliferator-activated receptor gamma activity during adipogenesis in 3T3-L1 preadipocytes. *J. Biol Chem.* **276**, 18464-18471

Han, J., Lee., J.E. Jongho, J., Lim, J.S., Kim, K., Chang, S.I., Shibuya, M., Kim, H., Koh, G.Y. (2011) The spatiotemporal development of adipose tissue. *Development*. **138**, 5027-5037

Hausman, G.J. (2000). The influence of dexamethasone and insulin on expression of CCAAT/enhancer binding protein isoforms during preadipocyte differentiation in procine stromal-vascular cell cultures: Evidence for very early expression of C/EBPα. *J. Anim. Sci.* **78**, 1227-1235

Hausman, G.J. and Dodson, M.V. (2012). Stromal vascular cells and adipogenesis: Cells within adipose depots regulate adipogenesis. *J. Genomics*. **1**, 56-66

Hausman, G.J., Hausman, D.B. (2007). What are subcutaneous adipocytes really good for? *Exp. Dematol.* **16**, 45-70

Hausman, G.J. and Kauffman, R.G. (1986a). The histology of developing porcine adipose tissue. *J. Anim. Sci.* **63**, 642-658

Hausman, G.J. and Kauffman, R.G., (1986b). Mitotic activity in fetal and early postnatal porcine adipose tissue. *J. Anim. Sci.* **63**, 659-673

Hausman, G.J. and Martin, R.J. (1982). The development of adipocytes located around hair follicles in the fetal pig. *J. Anim. Sci.* **54**. 1286-1296

He, Z., Yu, J., Zhou, C., Ren, G., Cong, P., Mo, D., Chen, Y., Liu, X. (2012). MiR-143 is not essential for adipose development as revealed by in vivo antisense targeting. *Biotech. Lett.* **35**, 499-507

Hill, D.M., Clarke, S.T., Bradford, J.A., Buck, S.B., Johnson, I., Salic, A., Chen, Y.T. (2007). Click-chemistry based detection of S-phase adherent cells using automated microscopy and image analysis.

Hishida, T., Nishizuka, M., Osada, S., Imagawa, M. (2009). The role of C/EBPδ in the early stages of adipogenesis. *Biochimie*. **91**, 654-657

Jaager, K., Neuman, T. (2011). Human dermal fibroblasts exhibit delayed adipogenic differentiation compared with mesenchymal stem cells. *Stem cells Devel.* **20**, 1327-1336

Jiang, M.S., Lane, M.D. (2000). Sequential repression and activation of the CCAAT enhancer-binding protein-alpha (C/EBP alpha) gene during adipogenesis. *PNAS.* **97**, 12519-12523

Kajimoto, K., Naraba, H., Iwai, N. (2006). MicroRNA and 3T3-L1 pre-adipocyte differentiation. *RNA.* **12**, 1626-1632

Kajita, K., Mori, I., Kitada, Y., Taguchi, K., Kajita, T., Hanamoto, T., Ikeda, T., Fujioka, K., Yamauchi, M., Okada, H., Usui, T., Uno, Y., Morita, H.,

Ishizuka, T. (2013). Small proliferative adipocytes: identification of proliferative cells expressing adipocyte markers. *Endocrine J.* **8**, 931-939

Kanitakis, J. (2002). Anatomy, histology and immunohistochemistry of normal human skin. *Europ. J. Dermatol.* **12**, 390-401

Karbiener, M., Fischer, C., Nowitsch, S., Opriessnig, P., Papak, C., Ailhaud, G., Dani, C., Amri, E.Z., Scheideler, M. (2009). microRNA miR-27b impairs human adipocyte differentiation and targets PPARgamma. *Biochem Biophys Res Commun*. **390**, 247-251

Kennell, J.A., Gerin, I., MacDougald, O.A., Cadigan, K.M. (2008). The microRNA miR-8 is a conserved negative regulator of Wnt signalling. *PNAS*. **105**, 15417-15422

Kim, J.B., Wright, H.M., Wright, M., Spiegelman, B.M. (1998). ADD1/SREBP1 activates PPAR gamma through the production of endogenous ligand. *PNAS*. **95**, 4333-4337

Kim, S.Y., Kim, A.Y., Lee, H.W., Son, Y.H., Lee, G.Y., Lee J.W., Lee, Y.S., Kim, J.B. (2010). miR-27a is a negative regulator of adipocyte differentiation via suppressing PPARgamma expression. *Biochem Biophys Res Comun.* **392**, 323-328

Klein, J., Permana, P.A., Owecki, M., Chaldakov, G.N., Böhm, M., Hausman, G., Lapière, C.M., Atanassova, P., Sowiński, J., Fasshauer, M., Hausman, D.B., Maquoi, E., Tonchev, A.B., Peneva, V.N., Vlachanov, K.P., Fiore, M., Aloe, L., Slominski, A., Reardon, C.L., Ryan, T.J., Pond, C.M., Ryan, T.J. (2007). What are subcutaneous adipocytes really good for? *Exp. Dematol.* **16**, 45-70

Kuzma-Kuzniarska, M., Yapp, C., Pearson-Jones, T.W., Jones, A.K., Hulley, P.A. (2014). Functional assessment of gap junctions in monolayer and

three-dimensional cultures of human tendon cells using fluorescent recovery after photobleaching. *J. Biomed. Opt.* **19**, 15001

Kwon, H., Pessin, J.E. (2013). Adipokines mediate inflammation and insulin resistance. *Front Endocrinol. (Lausanne).* **4**, 71

Lafontan, M. and Berlan, M. (2003). Do regional differences in adipocyte biology provide new pathophysiological insights? *Trends in Pharma. Sci.* **24**, 276-283

Lafontan, M., Langin, D. (2009). Lipolysis and lipid mobilisation in human adipose tissue. *Progress in Lipid Research.* **48**, 275-297

Large, V., Peroni, O., Lextexier, D., Ray, H., Beylot, M. (2004) Metabolism of lipids in human white adipocyte. *Diabetes Metab.* **30**, 294-309

Lee, E.K., Lee, M.J., Abdelmohsen, K., Kim, W., Kim, M.M., Srikantan, S., Martindale, J.L., Hutchison, E.R., Kim, H.H., Marasa, B.S., Selimyan, R., Egan, J.M., Smith, S.R., Fried, S.K., Gorospe, M. (2011). miR-130 suppresses adipogenesis by inhibiting peroxisome proliferator-activated receptor γ expression. *Mol. Cell. Biol.* **31**, 626-638

Lee, K.Y., Russell, S.J., Ussar, S., Boucher, J., Vernochet, C., Mori, M.A., Smyth, G., Rourk, M., Cederguist, C., Rosen, E.D., Kahn, B.B., Kahn, C.R. (2013). Lessons on conditional gene targeting in mouse adipose tissue. *Diabetes*. **62**, 864-874

Lee, R.C., Feinbaum, R.L., Ambros, V. (1993). The C. elegans heterochronic gene *lin-4* encodes small RNAs with antisense complementarity to *lin-14*. *Cell*. **75**, 843-854

Legesse-Miller, A., Elemento, O., Pfau, S.J., Forman, J.J., Tavazoie, S., Coller, H.A. (2009). let-8 overexpression leads to an increased fraction of

cells in G2/M, direct down-regulation of Cdc34, and stabilisation of Wee1 kinase in primary fibroblasts. *J. Biol. Chem.* **284**, 6605-6609

Levy, V., Lindon, C., Harfe, B.D., Morgan, B.A. (2005). Distinct stem cell populations regenerate the follicle and interfollicular epidermis. *Developmental Cell*. **9**, 855-861

Lin, F., MacDougald, O.A., Diehl, A.M., Lane, M.D. (1993). A 30-kDa alternative translation product of the CCAAT/enhancer binding protein alpha: transcriptional activator lacking antimitotic activity. *Proc Natl Acad Sci U S A*. **90**; 9606–9610

Lin, Q., Gao, Z., Alarcon, R.M., Ye, J., Yun, Z (2009). A role of *miR-27* in the regulation of adipogenesis. *FEBS. J.* **276**, 2348-2358

Magerl, M., Tobin, D.J., Muller-Rover, S., Hagen, E., Lindner, G., McKay, I.A., Paus, R. (2001). Patterns of proliferation and apoptosis during murine hair follicle morphogenesis. *J. Invest. Dermatol.* **116**, 947-955

Matthias, A., Ohlson, K.B., Fredriksson, J.M., Jacobsson, A., Nedergaard, J., Cannon, B. (2000). Thermogenic responses in brown fat cells are fully UCP-1 dependent. UCP2 or UCP3 do not substitute for UCP1 in adrenergically or fatty acid-induced thermogenesis. *J.Biol. Chem.* **275**, 25073-25081

McGrath, J. A., Eady, R. A. J. and Pope, F. M. (2008) Anatomy and Organization of Human Skin, in Rook's Textbook of Dermatology, Seventh Edition (eds T. Burns, S. Breathnach, N. Cox and C. Griffiths), Blackwell Publishing, Inc., Malden, Massachusetts, USA.

Mikkelsen, T.S., Xu, Z., Zhang, X.L., Wang, L., Gimble, J.M., Lander, E.S., Rosen, E.D. (2010). Comparative epigenomic analysis of murine and human adipogenesis. *Cell*. **143**, 156-169

Miller, S.E. (2002). Molecular mechanisms regulating hair follicle development. *J. Invest Dermatol.* **118**, 216-225

Miyazaki Y., Mahankali A., Matsuda M., Mahankali S., Hardies J., Cusi K., Mandarino L.J., DeFronzo R.A. (2002). Effect of pioglitazone on abdominal fat distribution and insulin sensitivity in type 2 diabetic patients. *J Clin Endocrinol Metab*. **87**, 2784–2791

Nicholls, D.G. and Locke, R.M. (1984) Thermogenic mechanisms in brown fat. *Physiol. Rev.* **64**, 1-64

Pan, S., Zheng, Y., Zhao, R., Yang, X. (2013). miRNA-374 regulates dexamethasone-induced differentiation of primary cultures of porcine adipocytes. *Horm Metab Res.* **45**, 518-525

Pang, S.S., Le, Y.Y. (2006). Role of resistin in inflammation and inflammation-related diseases. *Cell Mol. Immunol.* **3**, 29-34

Pastar, I., Khan, A.A., Stojadinovic, O., Lebrun, E.A., Medina, M.C., Brem, H., Kirsner, R.S., Jimenez, J.J., Leslie, C., Tomic-Canic, M. (2012). Induction of specific microRNAs inhibits cutaneous wound healing. *J. Biol. Chem.* **287**, 29324-29335

Payne, V.A., Wo-Shing, A.U., Lowe, C.E., Rahman, S.M., Friedman, J.E., O'Rahilly, S., Rochford, J.J. (2010). C/EBP transcription factors regulate SREBP1c gene expression during adipogenesis. *Biochem. J.* **425**, 215-223

Picardo, M., Ottaviani, M., Camera, E., Mastrofrancesco, A. (2009) Sebaceous gland lipids. *Dermatoendocrinol.* **1**, 68-71

Pond, C.M. (2007). What are subcutaneous adipocytes really good for? *Exp. Dematol.* **16**, 45-70

Porse, B.T., Pedersen, T.A., Xu, X., Lindberg, B., Wewer, U.M., Friis-Hansen, L., Nerlov, C. (2001). E2F Repression by C/EBPα Is Required for Adipogenesis and Granulopoiesis In Vivo. *Cell*. **107**, 247-258

Porter, S.A., Massaro, J.M., Hoffman, U., Vasan, R.S., O'Donnel, C.J., Fox, C.S. (2009). Abdominal subcutaneous adipose tissue: A protective fat depot? *Diabetes Care.* **32**, 1068-1075

Proksch, E., Brandner, J.M., Jensen, J.M. (2008). The skin: an indispensable barrier. *Exp. Dermatol.* **17**, 1063-1072

Rana, T.M. (2007). Illuminating the silence: understanding the structure and function of small RNAs. *Nature Rev.* **8**, 23-36

Reiners, J.J. Jr. and Slaga. T.J. (1983) Effects of tumor promoters on the rate and commitment to terminal differentiation of subpopulations of murine keratinocytes. *Cell*. **32**, 247-255

Richardson GD, Bazzi H, Fantauzzo KA, Waters JM, Crawford H, Hynd P, Christiano AM, Jahoda CA. (2009). KGF and EGF signalling block hair follicle induction and promote interfollicular epidermal fate in developing mouse skin. *Development*. **136**, 2153-2164

Rogers, N.H., Landa, A., Park, S., Smith, R.G. (2012). Aging leads to a programmed loss of bown adipocytes in murine subcutaneous white adipose tissue. *Aging Cell*. **11**, 1074-1083

Romao, J.M., Jin, W., Dodson, M.V., Hausman, G.J., Moore, S.S., Guan, L.L. (2011). MicroRNA regulation in mammalian adipogenesis. *Exp. Biol. Med.* **236**, 997-1004

Rosen, E.D. and MacDougald, O.A. (2006). Adipocyte differentiation from the inside out. *Nat. Rev. Mol. Cell Bio.* **7**, 885-896

Rosen, E.D., Sarraf, P., Troy, A.E., Bradwin, G., Moore, K., Milstone, D.S., Spiegelman, B.M., Mortensen, R.M. (1999). PPARg is required for the differentiation of adipose tissue in vivo and in vitro. *Mol. Cell.* **4**, 611-617

Rosen, E.D., Walkey, C.J., Puigserver, P., Spiegelman, B.M. (2000). Transcriptional regulation of adipogenesis. *Gen. Dev.* **14**, 1293-1307

Sayed, D. and Abdellatif, M. (2011). MicroRNAs in development and disease. *Physiol. Rev.* **91**, 827-887

Schmidt, B. and Horsley, V. (2012). Unraveling hair follicle-adipocyte communication. *Experimental Dermatology*, **21**, 827-830

Seo, J.B., Moon, H.M., Noh, M.J., Lee, Y.S., Jeong, H.W., Yoo, E.J., Kim, W.S., Park, J., Youn, B.S., Kim, J.W., Park,S.D., Kim, J.D. (2004). Adipocyte determination- and differentiation-dependent factor1/sterol regulatory element-binding protein 1c regulates mouse adiponectin expression. *J. Biol. Chem.* **279**, 22108-22117

Snijder, M.B., Visser, M., Dekker, J.M., Goodpaster, B.H., Harris, T.B., Kritchevsky, S.B., De, R.N., Kanaya, A.M., Newman, A.B., Tylavsky, F.A., Seidall, J.C. (2005). Low subcutaneous thigh fat is a risk factor for unfavourable glucose and lipid levels, independently of high abdominal fat. *Deiabetologia.* **48**, 301-308

Sorrell, J.M. and Caplan, A.I. (2004). Fibroblast heterogeneity: more than skin deep. *J. Cell Sci.* **117**, 667-675

Spalding, K.L., Arner, E., Westermark, P.O., Bernard, S., Buchholz, B.A., Bergmann, O., Blonqvist, L., Hoffstedt, J., Naslund, E., Britton, T., Concha, H., Hassan, M., Rydén, M., Frisén, J., Arner, P. (2008). Dynamics of fat cell turnover in humans. *Nature*. **453**, 783-787

Sul, H.S., Smas, C., Mei, B., Zhou, L. (2000). Function of pref-1 as an inhibitor of adipocyte differentiation. *Int. J. Relat. Metab. Disord.* **24**, S15-S19

Sun, K., Kusminski, C.M., Scherer, P.E. (2011). Adipose tissue remodeling and obesity. *J. Clin. Invest.* **6**, 2094-2101

Sun, T., Fu, M., Bookout, A.L., Kliewer, S.A., Mangelsdorf, D.J. (2009). MicroRNA *let-7* regulates 3T3-L1 adipogenesis. *Mol. Endocrinol.* **23**, 925-931

Tanaka, T., Yoshida, N., Kishimoto, N., Akira, S. (1997). Defective adipocyte differentiation in mice lacking the C/EBPβ and/or C/EBPδ gene. *EMBO*. **16**, 7432-7443

Tang Q.Q., Lane, M.D. (1999). Activation and centromeric localization of CCAAT/enhancer binding proteins during the mitotic clonal expansion of adipocyte differentiation. *Gene Dev.* **13**, 2231-2241

Tang Q.Q., Lane, M.D. (2000). Role of C/EBP homologous protein (CHOP-10) in the programmed activation of CCAAT/enhancer-binding protein-β during adipogenesis. *PNAS.* **97**, 12446-12450

Tang, Q.Q., Lane, M.D. (2012). Adipogenesis: from stem cell to adipocyte. *Annu. Rev. Biochem.* **81**, 715-736

Tang, Q.Q., Otto, T.C., Lane, M.D. (2003) Mitotic clonal expansion: A synchronous process required for adipogenesis. *PNAS*. **100**, 44-49

Tchkonia, T., Giorgadze, N., Pirtskhalava, T., Tchoukalova, Y., Karagiannides, I., Forse, R.A., DePonte, M., Stevenson, M., Guo, W., Han, J.R., Waloga, G., Lash, T.L., Jensen, M.D., Kirkland, J.L. (2002). Fat depot origin affects adipogenesis in primary cultured and cloned human preadipocytes. *Am. J. Phys. Reg. Integ. Compara. Phys.* **282**, 1286-1296

Tibbitt, M.W. and Anseth, K.S. (2009). Hydrogels as extracellular matrix mimics for 3D cell culture. *Biotech. and Bioeng.* **103**, 655-663

Todaro, G.J. and Green, H. (1963). Quantitative studies of the growth of mouse embryo cells in culture and their development into established lines. *J. Cell. Biol.* **17**, 299-313

Tran, T.T., Tamamoto, Y., Gesta, S., Grella, E., Guigliano, F., Esposito, K., Scuderi, N., D'Andrea, F. (2004). Effect of liposuction on insulin resistance and vascular inflammatory markers in obese women. *Br. J. Plast. Surg.* **57**, 190-194

Trayhurn, P. and Beattie, J.H. (2001). Physiological role of adipose tissue: white adipose tissue as an endocrine and secretory organ. *P. Nutr. Soc.* **60**, 329-339

Umut Özcan, Qiong Cao, Erkan Yilmaz, Ann-Hwee Lee, Neal N. Iwakoshi, Esra Özdelen, Gürol Tuncman, Cem Görgün, Laurie H. Glimcher, Gökhan S. Hotamisligil (2004). Endoplasmic reticulum stress links obesity, insulin action, and type 2 diabetes. *Science.* **306**, 457-461

Valet, P., Tavernier, G., Castan-Laurell, I., Saulnier-Blache, J.S., Langin, D. (2002). Understanding adipose tissue development from transgenic animal models. *J. Lip. Res.* **43**, 835-860

Vorsmann, H., Groeber, F., Walles, H., Busch, S., Beissert, S., Walczak, H., Kulms, D. (2013). Development of a human three-dimensional organotypic skin-melanoma spheroid model for *in vitro* drug testing. *Cell Death Dis.* **4**, e719

Wang, Q., Li, Y.C., Wang, J., Kong, J., Qi, Y., Quigg, R.J., Li, X. (2008). miR-17-92 cluster accelerate adipocyte differentiation by negatively regulation tumor-supressor Rb2/p130. *PNAS.* **105**, 2889-2894

Wang, Q., Tao, C., Gupta, R.K., Scherer, P.E. (2013). Tracking adipogenesis during white adipose tissue development, expansion and regeneration. *Nature Medicine.* **19**, 1338-1344

Wang, S., Hwang, R., Greenberg, A.S., Yeo, H. (2003). Temporal and spatial assembly of lipid droplet-associated proteins in 3T3-L1 preadipocytes. *Histochem. Cell Biol.* **120**, 285-292

Wang, T., Li, M., Guan, J., Li, P., Wang, H., Guo, Y., Shuai, S., Li, X. (2011). MicroRNAs miR-27a and miR-143 regulate porcine adipocyte lipid metabolism. *Int. J. Mol. Sci.* **12**, 7950-7959

Wang, Y., Kim, K., Kim, J., Sul, H.S. (2006). Pref-1, a pre-adipocyte secreted factor that inhibits adipogenesis. *J. Nutr.* **136**, 2953-2956

Weller, R.P.J.B., Hunter, J.A.A., Savin, J., Dahl, M.V. (2008). Chapter 2: The function and structure of the skin in Clinical Dermatology, fourth edition. Blackwell Publishing, Inc., Malden, Massachusetts

Wessels, N.K., Roessner,, K.D. (1965). Nonproliferation in dermal condensations of mouse vibrissae and pelage hairs. *Developmental Biology.* **12**, 419-433

Weyer, C., Foley, J.E., Bogardus, C., Tataranni, P.A., Pratley, R.E. (2000). Enlarged subcutaneous abdominal adipocyte size, but not obesity itself, predicts type II diabetes independent of insulin resistance. *Diabetologia.* **43**, 1498-1506

Wibe, E, Berg, J.P., Tveit, K.M., Nesland, J.M., Lunde, S. (1984). Multicellular spheroids grown directly from human tumour material. *Int. J. Cancer.* **34**, 21-26

Wickett, R.R. and Visscher, M.O. (2006). Structure and function of the epidermal barrier. *Am. J. Infect. Control.* **34**, S98-S110

Widnell, C.C., Baldwin, S.A., Davies, A., Martin, S., Pasternak, C.A. (1990). Cellular stress induces redistribution of the glucose transporter. *FASEB J.* **4**, 1634-1637

Wojciechowicz, K., Markiewicz, E., Jahoda, C.A.B. (2008). C/EBPα identifies differentiating preadipocytes around hair follicles in foetal and neonatal rat and mouse skin. *Experimental Dermatology*. **17**, 675–680.

Wojciechowicz, K., Gledhill, K., Ambler, C.A., Manning, C.B., Jahoda, C.A.B. (2013) Development of the mouse dermal fat layer occurs independently of subcutaneous fat and is marked by restricted early expression of FABP4. *PLoS ONE.* **8**(3), e59811

Wright, J.T. and Hausman, G.J. (1994). Flow cytometric analysis of porcine preadipocyte replication. *J. Anim. Sci.* **72**, 1712-1718

Wulczyn, F.G., Smirova, L., Rybak, A., Brandt, C., Kwidzinski, E., Ninnemannm O., Strehle, M., Seiler, A., Schumacher, S., Nitsch, R. (2007). Post-transcriptional regulation of the let-7 microRNA during neural cell specification. *FASEB J.* **21**, 415-426

Xie, H., Lim, B., Lodish, H.F. (2009). MicroRNAs induced during adipogenesis that accelerate fat cell development are downregulated in obesity. *Diabetes*. **58**, 1050-1057

Young, D.A., Choi, Y.S., Engler, A.J., Christman, K.L. (2013). Stimulation of adipogenesis of adult adipose-derived stem cells using substrates that mimic the stiffness of adipose tissue. *Biomaterials.* **34**, 8531-8588

Zhang, Y., Proenca, R., Maffei, M., Barone, M., Leopold, L., Friedman, J.M. (1994). Positional cloning of the mouse *obese* gene and its human homologue. *Nature*. **372**, 425-432

Zuo, Y., Qiang, L., Farmer, S.R. (2006) Activation of CCAAT/Enhancer-binding protein (C/EBP) α expression by C/EBPβ during adipogenesis requires a peroxisome proliferator-activated receptor-γ-associated repression of HDAC1 at the *C/ebpα* gene promoter. *J. Biol. Chem*. **281**, 7960-7967

Zuk, P.A., Zhu, M., Mizuno, J., Huang, J., Futrell, J.W., Katz, A.J., Benhaim, P., Lorenz, H.P., Hedrick, M.H. (2001). Multi-lineage cells from human adipose tissue: implication for cell-based therapies. *Tissue Eng.* **7**, 211-228

Appendix I

List of reagents (Alphabetical order)

H&E, Immunofluorescent, and Oil Red O staining

Acid ethanol (100 ml)	Prepare 100 ml of 70% ethanol from 70 ml 100% ethanol and 30 ml dH_2O. Add conc. HCl to 70% ethanol to a final volume of 1%
Calcium formal (100 ml)	Prepare 100 ml of 4% formaldehyde (from 37% formaldehyde solution; Sigma) in dH_2O. Add calcium chloride (granular anhydrous; Sigma) to 4% formaldehyde to a final volume of 1%.
Mowiol	6 g glycerol 2.4 g mowiol 4-88 (Sigma) 6 ml dH_2O 12 ml 0.2 M Tris (pH 6.8) Leave stirring over-night at 37oC then leave for 10 min at 50^{o}C. Centrifuge and add to a supernatant DABCO (1.4-diazobicylo-(2.2.2)-octane) to final concentration of 2.5%. Aliquots kept at -20^{o}C.
Oil Red O (stock)	Dissolve 300 mg ORO solid (Sigma) in 100 ml 100% isopropanol
10x PBS (1 litre)	80g NaCl 2g KCl 14.4g Na_2HPO_4 2.4g KH_2PO_4 In 800 ml dH_2O Adjust pH to 7.4 with dil. HCl Add dH_2O up to 1 litre
4% paraformaldehyde (100 ml)	Slowly add 4g of paraformaldehyde (Sigma) to 100 ml PBS. Carefully heat to 50-60^{o}C with stirring until it dissolves and is transparent
0.1 / 0.5% Triton-X	0.1 / 0.5% TritonX-100 (Sigma) in 100 ml PBS

Epidermal-dermal separation and RNA extraction

5% Trypsin (100 ml)	Dissolve 5 g trypsin (BD) in 100 ml 1x Earle's (Gibco) Aliquots (1 ml) kept at -20^{o}C. Filter (0.2 mm syringe filter) before the use.
6% Pancreatin (100 ml)	Dissolve 6 g of pancreatin (Sigma) in 100 ml 1x Earle's (Gibco). Leave stirring over-night at 4^{o}C. Centrifuge and collect supernatant. Aliquots (1 ml) kept at -20^{o}C. Filter (0.2 mm syringe filter) before the use.
DEPC water (1 litre)	Add 0.1% DEPC (Sigma) to 1 litre dH_2O. Incubate O/N at RT and autoclave
DNase I (1 mg/ml stock)	Dissolve 0.01 g DNase I (Sigma) in 10 ml 1x Earle's (Gibco) Mix slowly.
DNAse I / Collagenase II (working solution)	Add approx. 3900 units of collagenase II (Worthington) and 100 μl of 1mg/ml DNase I into 15 ml of MEM (Sigma)

Appendix II

ORO cell counts

The Image J cell counter plugin was used to count ORO positive cells in culture pictures of 2D and 3D-2D cultures at each age. Nuclei were counted for the total number of cells (in the case of a dividing cell, nuclei were counted once if still joined together). All cells containing any ORO staining were counted as positive.

E18.5 2D

Nuclei	ORO cells	% Fat
53	4	8
63	4	6
13	3	23
16	1	6
5	1	20
8	3	38
11	0	0
13	4	31
		16

E18.5 3D-2D

Nuclei	ORO cells	% Fat
142	59	42
227	11	5
78	40	51
111	59	53
130	43	33
130	51	39
146	52	36
127	65	51
		39

E17.5 2D

Nuclei	ORO cells	% Fat
154	6	4
148	9	6
14	2	14
43	0	0
14	1	7
16	1	6
12	3	25
25	2	8
		9

E17.5 3D-2D

Nuclei	ORO cells	% Fat
122	33	27
142	28	20
37	5	14
46	7	15
68	18	26
164	12	7
131	9	7
158	30	19
		17

E16.5 2D

Nuclei	ORO cells	% Fat
37	0	0
61	1	2
168	11	7
32	1	3
119	2	2
45	1	2
185	12	6
28	4	14
		4

E16.5 3D-2D

Nuclei	ORO cells	% Fat
99	8	8
49	3	6
102	21	21
97	17	18
99	19	19
106	22	21
82	14	17
49	9	18
		16

E15.5 2D

Nuclei	ORO cells	% Fat
31	0	0
49	0	0
111	0	0
17	0	0
10	1	10
51	3	6
57	2	4
77	2	3
		3

E15.5 3D-2D

Nuclei	ORO cells	% Fat
23	4	17
20	1	5
32	2	6
26	4	15
25	5	20
30	11	37
52	10	19
25	4	16
		17

E14.5 2D

Nuclei	ORO cells	% Fat
50	2	4
22	1	5
46	1	2
14	0	0
36	1	3
18	1	6
15	1	7
14	1	7
		4

E14.5 3D-2D

Nuclei	ORO cells	% Fat
49	22	45
57	26	46
28	7	25
98	41	42
105	46	44
131	55	42
87	40	46
110	44	40
		41

E15.5 D+E 3D

Nuclei	ORO cells	% Fat
117	21	18
98	21	21
89	9	10
132	15	11
		15

E16.5 D+E 3D

Nuclei	ORO cells	% Fat
23	8	35
30	0	0
33	1	3
83	5	6
		11

Culture	% Fat
E18.5 2D	16
E17.5 2D	9
E16.5 2D	4
E15.5 2D	3
E14.5 2D	4
E15.5 D+E 3D	15

Culture	% Fat
E18.5 3D	39
E17.5 3D	17
E16.5 3D	16
E15.5 3D	17
E14.5 3D	41
E16.5 D+E 3D	11

Appendix III
Nuclei counts for analysis of EdU-incorporation

The total number and EdU-positive nuclei in E14.5, E15.5, and E16.5 back skin sections were counted on ImageJ using the "Image-based Tool for Counting Nuclei" plugin. See section 2.8.1 for full explanation and example pictures.

Age	Skin piece	Picture	Area (1, 2...)	Area (U/L)	N DAPI	n EDU
E14.5	1	1	1	U	85	22
E14.5	1	1	1	L	86	17
E14.5	1	1	2	U	83	20
E14.5	1	1	2	L	94	23
E14.5	1	2	1	U	126	41
E14.5	1	2	1	L	147	39
E14.5	1	2	2	U	126	31
E14.5	1	2	2	L	125	22
E14.5	1	3	1	U	52	15
E14.5	1	3	1	L	93	21
E14.5	1	3	2	U	307	118
E14.5	1	3	2	L	320	65
E14.5	1	4	1	U	91	37
E14.5	1	4	1	L	129	46
E14.5	1	4	2	U	36	11
E14.5	1	4	2	L	70	19
E14.5	1	5	1	U	90	33
E14.5	1	5	1	L	117	41
E14.5	1	5	2	U	64	26
E14.5	1	5	2	L	128	50
E14.5	1	6	1	U	68	21
E14.5	1	6	1	L	92	24
E14.5	1	6	2	U	82	38
E14.5	1	6	2	L	115	29
E14.5	1	7	1	U	58	17
E14.5	1	7	1	L	95	27
E14.5	1	7	2	U	51	16
E14.5	1	7	2	L	64	25
E14.5	1	8	1	U	138	53
E14.5	1	8	1	L	184	39
E14.5	1	8	2	U	125	55
E14.5	1	8	2	L	225	64
E14.5	1	9	1	U	166	64
E14.5	1	9	1	L	189	80
E14.5	1	9	2	U	70	29
E14.5	1	9	2	L	186	66

Age	Skin piece	Picture	Area (1, 2...)	Area (U/L)	N DAPI	n EDU
E14.5	2	1	1	U	69	31
E14.5	2	1	1	L	88	26
E14.5	2	1	2	U	96	24
E14.5	2	1	2	L	84	24
E14.5	2	2	1	U	76	36
E14.5	2	2	1	L	84	19
E14.5	2	2	2	U	88	35
E14.5	2	2	2	L	69	24
E14.5	2	3	1	U	150	53
E14.5	2	3	1	L	126	31
E14.5	2	3	2	U	87	29
E14.5	2	3	2	L	116	26
E14.5	2	4	1	U	99	34
E14.5	2	4	1	L	150	39
E14.5	2	4	2	U	117	49
E14.5	2	4	2	L	104	38
E14.5	2	5	1	U	118	35
E14.5	2	5	1	L	148	46
E14.5	2	5	2	U	66	27
E14.5	2	5	2	L	79	24
E14.5	2	6	1	U	99	32
E14.5	2	6	1	L	109	28
E14.5	2	6	2	U	81	33
E14.5	2	6	2	L	105	20
E14.5	2	7	1	U	116	49
E14.5	2	7	1	L	153	46
E14.5	2	7	2	U	59	22
E14.5	2	7	2	L	72	24
E14.5	2	8	1	U	89	40
E14.5	2	8	1	L	98	31
E14.5	2	8	2	U	54	20
E14.5	2	8	2	L	60	22
E14.5	2	9	1	U	149	61
E14.5	2	9	1	L	178	58
E14.5	2	9	2	U	70	31
E14.5	2	9	2	L	88	27

Age	Skin piece	Picture	Area (1, 2...)	Area (U/L)	N DAPI	n EDU
E15.5	1	1	1	U	56	10
E15.5	1	1	1	L	92	12
E15.5	1	1	2	U	74	19
E15.5	1	1	2	L	93	21
E15.5	1	2	1	U	103	25
E15.5	1	2	1	L	97	25
E15.5	1	2	2	U	71	21
E15.5	1	2	2	L	103	23
E15.5	1	3	1	U	72	22
E15.5	1	3	1	L	70	8
E15.5	1	3	2	U	60	25
E15.5	1	3	2	L	53	9
E15.5	1	4	1	U	84	20
E15.5	1	4	1	L	67	15
E15.5	1	4	2	U	84	14
E15.5	1	4	2	L	53	7
E15.5	1	5	1	U	58	23
E15.5	1	5	1	L	92	24
E15.5	1	5	2	U	46	24
E15.5	1	5	2	L	51	13
E15.5	1	6	1	U	118	27
E15.5	1	6	1	L	135	11
E15.5	1	6	2	U	85	16
E15.5	1	6	2	L	102	14
E15.5	1	7	1	U	74	23
E15.5	1	7	1	L	71	24
E15.5	1	7	2	U	117	40
E15.5	1	7	2	L	135	21

Age	Skin piece	Picture	Area (1, 2...)	Area (U/L)	N DAPI	n EDU
E15.5	2	1	1	U	143	51
E15.5	2	1	1	L	129	21
E15.5	2	1	2	U	91	33
E15.5	2	1	2	L	77	21
E15.5	2	2	1	U	89	25
E15.5	2	2	1	L	78	18
E15.5	2	2	2	U	92	32
E15.5	2	2	2	L	76	17
E15.5	2	3	1	U	103	33
E15.5	2	3	1	L	57	19
E15.5	2	3	2	U	67	30
E15.5	2	3	2	L	59	12
E15.5	2	4	1	U	78	19
E15.5	2	4	1	L	65	15
E15.5	2	4	2	U	95	36
E15.5	2	4	2	L	85	15
E15.5	2	5	1	U	66	26
E15.5	2	5	1	L	56	13
E15.5	2	5	2	U	71	14
E15.5	2	5	2	L	67	15
E15.5	2	6	1	U	54	26
E15.5	2	6	1	L	37	9
E15.5	2	6	2	U	43	23
E15.5	2	6	2	L	46	9
E15.5	2	7	1	U	52	15
E15.5	2	7	1	L	51	10
E15.5	2	7	2	U	191	66
E15.5	2	7	2	L	129	33

Age	Skin piece	Picture	Area (1, 2...)	Area (U/L)	N DAPI	n EDU
E16.5	1	1	1	U	82	14
E16.5	1	1	1	L	79	13
E16.5	1	1	2	U	75	14
E16.5	1	1	2	L	75	7
E16.5	1	2	1	U	82	22
E16.5	1	2	1	L	80	12
E16.5	1	2	2	U	99	30
E16.5	1	2	2	L	111	12
E16.5	1	3	1	U	82	24
E16.5	1	3	1	L	80	19
E16.5	1	3	2	U	102	47
E16.5	1	3	2	L	110	24
E16.5	1	4	1	U	106	27
E16.5	1	4	1	L	89	21
E16.5	1	4	2	U	44	11
E16.5	1	4	2	L	38	7
E16.5	1	4	3	U	36	11
E16.5	1	4	3	L	40	4
E16.5	1	5	1	U	72	21
E16.5	1	5	1	L	103	17
E16.5	1	5	2	U	112	34
E16.5	1	5	2	L	114	15

Age	Skin piece	Picture	Area (1, 2...)	Area (U/L)	N DAPI	n EDU
E16.5	2	1	1	U	54	10
E16.5	2	1	1	L	37	10
E16.5	2	1	2	U	69	22
E16.5	2	1	2	L	79	20
E16.5	2	2	1	U	61	25
E16.5	2	2	1	L	60	12
E16.5	2	2	2	U	40	7
E16.5	2	2	2	L	57	14
E16.5	2	3	1	U	74	17
E16.5	2	3	1	L	75	16
E16.5	2	3	2	U	33	9
E16.5	2	3	2	L	41	8
E16.5	2	3	3	U	34	15
E16.5	2	3	3	L	46	10
E16.5	2	4	1	U	114	48
E16.5	2	4	1	L	69	10
E16.5	2	4	2	U	72	20
E16.5	2	4	2	L	64	13
E16.5	2	5	1	U	66	20
E16.5	2	5	1	L	55	12
E16.5	2	5	2	U	47	20
E16.5	2	5	2	L	62	12
E16.5	2	6	1	U	41	11
E16.5	2	6	1	L	55	13
E16.5	2	6	2	U	32	8
E16.5	2	6	2	L	63	6

Appendix IV

Culture pictures of spheres from E14.5-E18.5

Below are pictures from each repeat of the spherical cell culture showing the replication in size of spheres between experiments.

E18.5

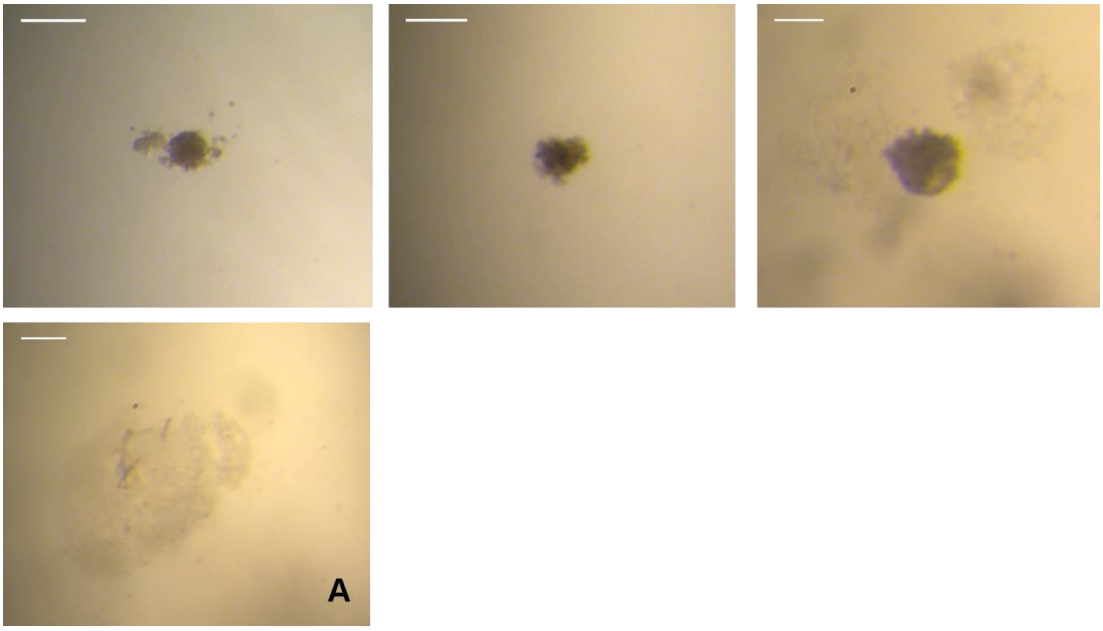

E17.5

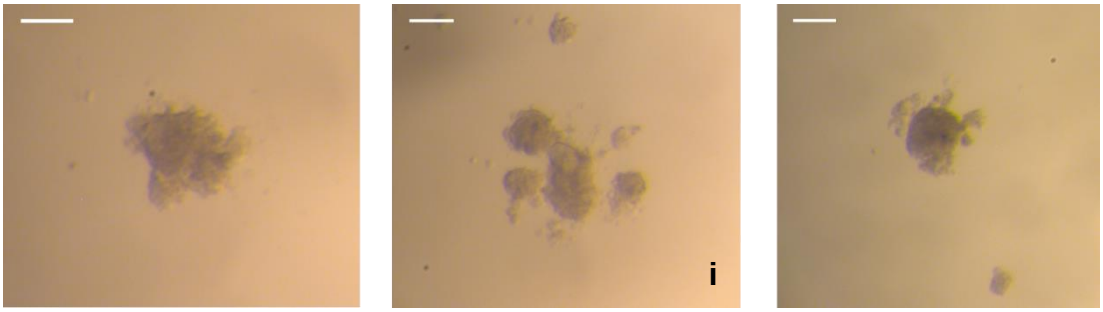

E16.5

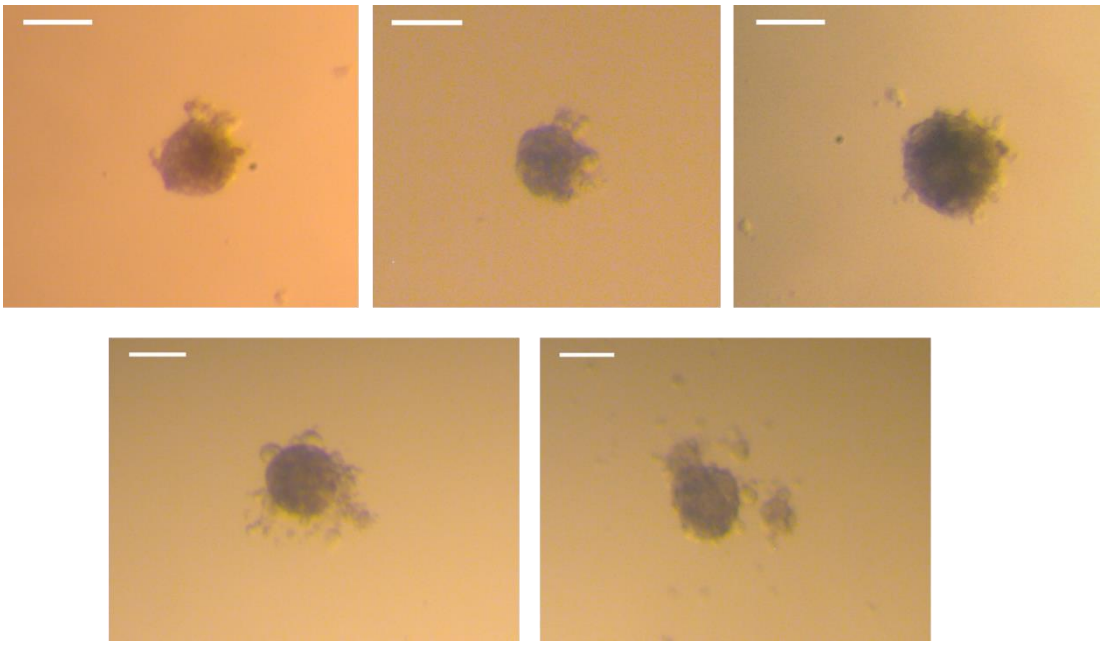

E14.5

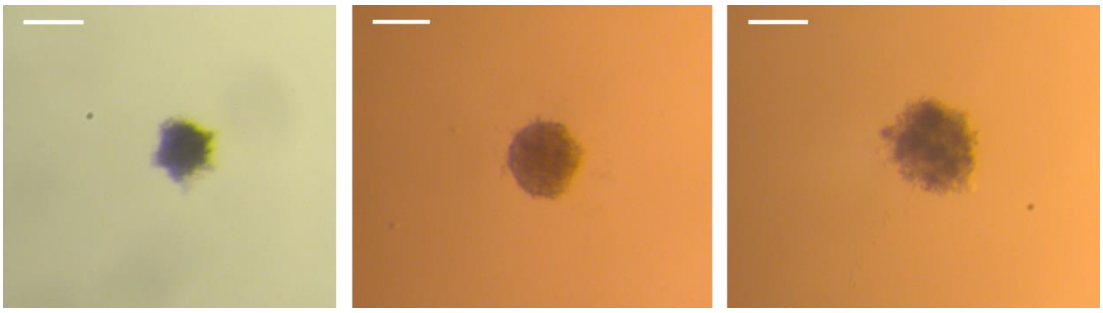

Culture pictures of E18.5, E17.5, E16.5, and E14.5 dermal cell spheres . The process of making spheres is highly reproducible with cells of from different ages and different experiments producing spheres of comparable sizes. Occasionally cells did not clump together in one sphere but created several smaller spheres close together (i). These were not used for further analysis. In one E18.5 experiment, Ficoll was used as a method of removing epidermal contamination. This, however, resulted in cells dying and therefore being unable to form spheres (A). Scale bars = 100μm